DEPARTMENT OF ELECTRONICS

UNIVERSITY OF SOUTHAMPTON

APPLICATION OF ESTIMATION TECHNIQUES TO PROBLEMS IN NUCLEAR MEDICINE

W.R. FITCH

OCTOBER, 1980.

A thesis submitted for the degree of

Doctor of Philosophy

CONTENTS

ABSTRACT

An online parametric method of System Identification accounting for Poisson noise inherent in the measurement of gamma radiation, is proposed for the identification of the parameters attributed to the main metabolistic flow systems of the human body.

The main metabolistic systems commonly examined using radioactive tracers are modelled, and it is shown how the Kalman-Snyder state estimation routines may be used to identify them. Simulations are used to show the efficiency of the algorithms.

A proposed semiconductor radiation detector which eliminates the need for a lead collimator is also described and some contributions made to outstanding computational difficulties.

ACKNOWLEDGEMENTS

The author would like to thank his supervisors Professor J.M. Nightingale and Dr. B.A. Carre for their continuous advice and encouragement during the project, and to members of staff and fellow students for their assistance.

He would also like to thank Dr. B. Goddard and Dr. J.S. Fleming of the Department of Nuclear Medicine, Southampton University Hospitals, Dr. J. Woodcock and Dr. R.B. Skidmore of the Ultrasonics Department, and Mr. G.E. Staddon and Mr. P.C. Jackson of the Isotopes Department, Avon Area Health Authority, who introduced current problems in metabolic flow determination, and enabled computing and other facilities to be made available. The time spent in discussion with them is much approciated.

The author would also like to thank Mrs. J. Bennett for her meticulous care taken in the preparation of the manuscript, and Mr. G. Garland for the preparation of many of the drawings.

PREFACE

The initial aim of this work was to apply estimation techniques specifically to a new radiation detection system based apon the Compton effect, which was being developed at Southampton University. Soon after this project was started, work on the Compton effect camera was transferred to the Medical Research Centre at Mill Hill, hence after development of imaging algorithms for the camera, the work was extended to cover general techniques for existing radiation detection systems, in conjunction with workers at Southampton University Hospitals.

The main contribution of the work consists of the adaption of state estimation techniques to identify rates of extraction or flow between organs of the body. The main metabolistic processes of the body have been described and modelled, and a method has been developed whereby using existing stochastic estimation techniques the metabolistic rates may be determined from measurements of radiation emitted from radioactive tracers for observable systems. The technique has been simulated, enabling the estimated rates to be compared with the true values, as well as those obtainable from deterministic techniques.

CHAPTER 1

SYSTEM IDENTIFICATION

Introduction

System Identification techniques have been developed in many fields, by engineers, bioengineers, statisticians and econometricians. Many of the techniques proposed have similarities to others, and indeed are special cases of more general ones. Survey papers and works of general interest analysing the methods are given in references (Ale), (Art), (Bal), (Bek), (Cue), (Eyk 1,2,3), (Lee), (Lie) and (Sag). To compare the methods an abstract framework is required such as that of Zadeh (Zad), who characterises the identification techniques by three quantities, the model, the input signal and the identification criterion. Each of these quantities will be analysed in turn, and it will thus be shown which identification techniques are of particular relevance to nuclear medical problems.

The model may be represented parametrically by state models such as:

$$\frac{dx}{dt} = f(x, u, \beta) \qquad (1.1)$$

$$y = g(x, u, \beta) \qquad (1.2)$$

where x is the state vector, u the input vector, y the output vector and β a parameter, or non-parametrically in the form of inpulse responses, transfer functions, covariance functions, spectral densities, Volterra series etc. Comparisons of the two representations may be found in the literature on time series analysis (Gre),(Jen), (Man), (Whi).

If the inputs to the system can be altered, and special signals applied the identification can in many cases be simplified. Impulse

functions, step functions and sinusoidal signals are of great value, the use of deterministic signals being discussed in references (Bos), (Cum), and (Wel). Coloured or white noise and pseudo random binary noise is also of use and this is discussed in (Nik) and (God). In biological systems the types of inputs that it is possible to apply are generally very limited and an identification technique needs to be chosen which is suitable to the particular circumstances, or which requires no special input.

The criterion which assesses the performance of the identification technique is normally expressed as a functional of an error such as:

$$V(y, y_m) = \int_0^T e^2(t)\, dt \qquad (1.3)$$

where y is the process output, y_m the model output and e is the error, all being functions defined on (0,T).

The error can be an output error

$$e = y - y_m = y - M(u) \qquad (1.4)$$

where M(u) denotes the output of the model where the input is u, an input error

$$e = u - u_m = u - M^{-1}(y) \qquad (1.5)$$

where $u_m = M^{-1}(y)$ decides the input of the model which produces the output y, or it may be defined in a more general fashion (Eyk 4), (Pot):

$$e = M_2^{-1}(y) - M_1(u) \qquad (1.6)$$

The notations M_1^{-1} and M_2^{-1} represent invertible models. The concept of invertibility is discussed in (Bro), (Sai) and (Sil).

In the problems of identification considered in this thesis, using nuclear medical techniques boluses of radioactive tracer are injected

into the circulatory system. We thus have an initial known step input. It is of interest to determine the extraction efficiency of each organ which removes the particular tracer from the blood. These terms may be made to appear explicitly in a parametric model and causes the parametric approach to be of particular interest. In our case it also has other advantages.

Measurements may be taken periodically of the radiactive intensity in different organs. Our identification problem may thus be expressed that we wish to identify the system from a string of input - output data, the input being known as a step function at time $t = 0$ corresponding to the applied bolus. It is of great interest to develop techniques whereby the result of the identification develops recursively as the process develops, subresults being obtained as each input - output pair is used. as opposed to techniques which require all the data in the time interval $(0,T)$ to produce an answer. This avoids the necessity to repeat the whole identification process if the estimate is not of sufficient accuracy and the observation period has to be increased to $(0,T_1)$ where $T_1 > T$. If an algorithm is available to provide an up date using only the new measurement and an old update, the computation becomes much less and it becomes

feasable in principle to propose that the identification is repeated until a specifide parameter accuracy is obtained. Idenfification techniques which are recursive and do not require the use of the whole string of input - output data at each step are called on-line methods. If the parameters are truly time varying then they must be tracked in real time, this being denoted as real-time identification. Nearly all methods of real time identification yield algorithms of the form

$$E\ (N + 1) \ = \ E(N) + G(N)\ e(N)$$

where the estimate after N input - output pairs is given by E(N), e(N) is the generalised error, and G(N) is a gain factor which is of varying complexity.

The online and real time identification problems may in some circumstances be formulated as model tracking problems figure (1.1). The known input is simultaneously applied to the unknown system and a model which is to simulate the system. The difference between the two outputs is then used to adjust the model, and the procedure repeated. This formulation was first considered by Whitaker (Whi). Modern parametrical, as opposed to so called classical non parametrical estimation techniques fall into these categories, and allow the use of and systems disturbed by noise, though in the latter case problems associated with estimation, and stability and non uniqueness of the identification occur. For deterministic systems and observable stable systems have been designed using Liapunov techniques (Lio), (Par), (Sha) and Lions techniques have been extended to stochastic systems by

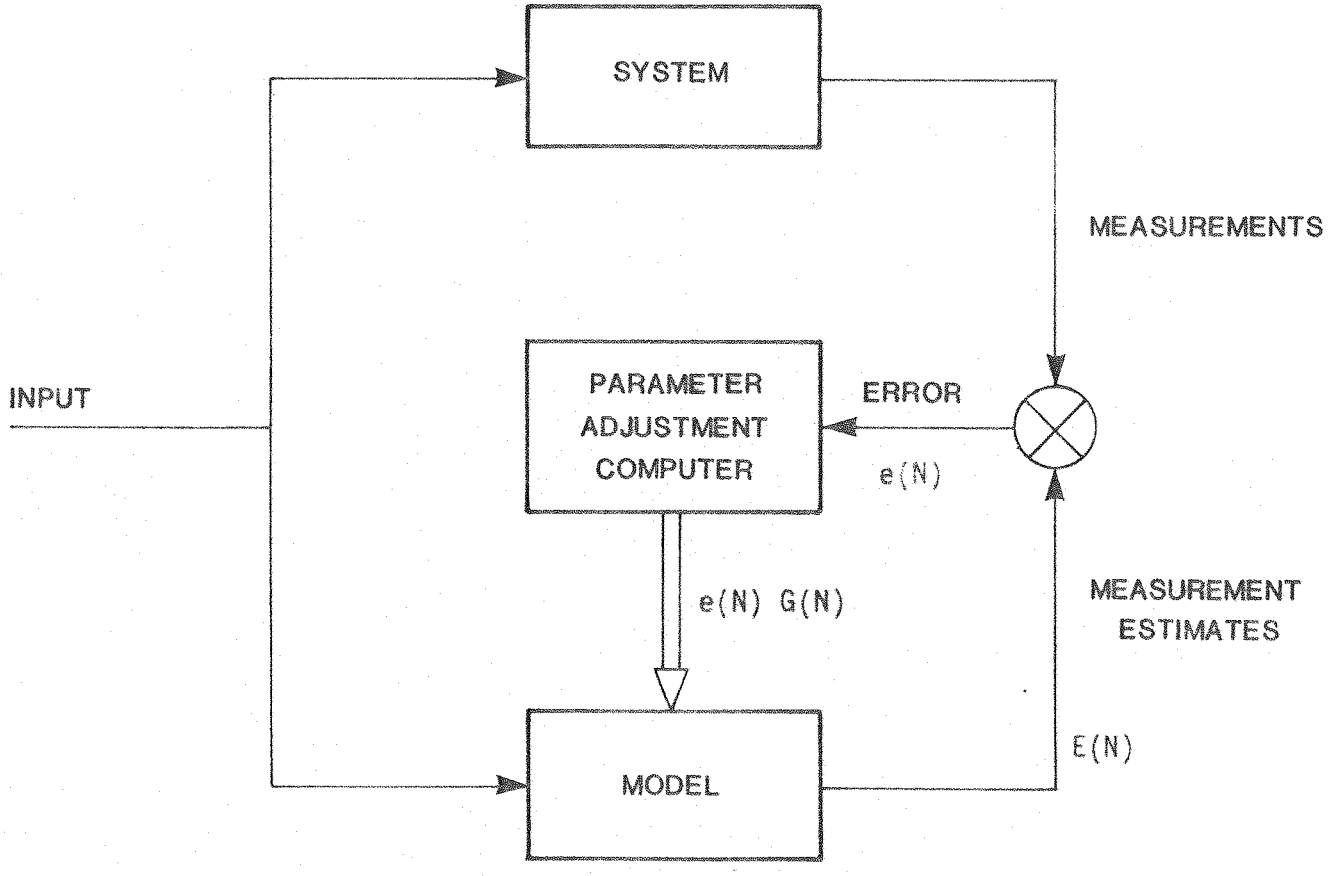

Figure 1.1 LEARNING MODEL SYSTEM IDENTIFICATION TECHNIQUE

Kushner (Kus 2). New stability tests have recently been developed by Popv (Pop) and Zames (Zam) which give indications of being of great use in the design of stable systems. Initial efforts in this direction have been applied by Landau (Lan) who has proposed a stable reference model system using the Popov criterion.

The following section describes a model tracking state estimation technique which allows for the presence of noise in both the system and measurements. This is of particular interest due to the gaussian noise present in many biological systems, and the poisson noise inherent in any measurement of radiation emitted from radioisotopes. It is then shown how this estimation technique may be used for system identification.

The theory used to develop the estimation equations is described in detail in the Appendices. In this chapter we outline the main steps in the development of the recursive algorithms and show the relationships between state estimation techniques and system identification.

State Estimation in the Presence of Noise

a) System Modelling

A main prerequisite of parameter estimation is to model the system adequately. Parametric time domain methods normally express the system in terms of differential or difference equations, differential equations forming continuous time models, difference equations describing discrete time processes. It may be shown that any set of differential equations of arbitrary order may be reduced to a vector differential equation of first order (see ref. (Oga) for ordinary differential equations, ref. (Tr) for partial differential equations). For a forced lumped parameter system with no inherent noise we have a first order system equation (1.1) which we repeat below:

$$\frac{dx}{dt} = f(x, u, \beta) \qquad (1.1a)$$

In general the system is driven by noise. If we consider the deterministic forcing function to be zero and denoting the noise by an additive (n x 1) vector dn we obtain, eliminating β by a change of variable

$$dx = f(x, t)\, dt + dn \tag{1.7}$$

Two useful types of noise processes are called the Wiener and Poisson processes, both described in Appendix B. In defining the processes it is shown that they are both Markov processes in that the present value of the noise depends solely apon the most recent past history, and are also independent increment processes in that events occurring in non-overlapping intervals are independent. These properties are important since they cause the system equation (1.7) to become mathematically tractable. The Wiener process is continuous, whereas the Poisson process is discontinuous. Most noise processes occurring in nature may be modelled by one or a combination of both of these processes.

Determination of the state x in equation (1.7) is called state or parameter estimation, while determination of the matrix A is called System Identification. State estimation techniques are well established. These are first derived, and it is shown how in some cases they may be used for System Identification as well.

b) Derivation of State Estimation Equations

A full derivation of the estimations equations for a system, state equation (1.7),observed by measurements consisting of poisson processes with a vector rate λ (x, t) is given in Appendices B and C. Since the system is driven by noise the transition matrix which fully describes deterministic systems no longer is sufficient to describe

the time evolution of the system. The probability density function $p\ (u,\ t|x(s))$, described and evaluated in Appendix C may be used for this purpose. An equation may be found which is satisfied by this function such that given only the apriori knowledge, the most probable state after a period of time may be found. This equation, the Fokker Planck equation may then be modified to take account of measurements which would improve the knowledge of the state.

The result, derived in Appendix C is repeated below

Let $x(t)$ be an $(n \times 1)$ vector Markov process generated by the state equation

$$dx(t) = f\ (x,t)\ dt + dn_g(t)$$

where dn_g is additive gaussian noise, and let $dN(t)$ be an $(m \times 1)$ vector Poisson step process with an $(m \times 1)$ rate parameter $\lambda\ (x(t),\ t)$.

Let $\lambda_i\ (x(t),\ t)$ be the i^{th} component of $\lambda\ (x(t),\ t)$

Let $p_x\ (u,\ t|O_{t_o,\ t\ +\ dt})$ be the conditional probability density function of the process $x(t)$ given $O_{t_o,\ t\ +\ dt}$, the minimal σ field generated by the process $N(s)$, $s \varepsilon [t_o,\ t\ +\ dt)$. Then to order dt

$$\partial p = L^{+}(p)\ dt + q\ (dN,\ dt,\ u)\ p \tag{1.9}$$

where

$$q\ (dN,\ dt,\ u) =$$

$$\sum_{i=1}^{m} (\lambda_i\ (u,\ t) - E\ \{\lambda_i\ (x,\ t)\})\ (E\ \{\lambda_i\ (x,\ t)\})^{-1}$$

$$(dN_i(t) - E\ \{\lambda_i\ (x,\ t)\}\ dt) \tag{1.9a}$$

where

$$E\ \{\lambda_i\ (x,\ t)\} = \int \lambda_i\ (u,\ t)\ p_x\ (u,\ t|O_{t_o,\ t})\ du \tag{1.9b}$$

and where $L^{+}(\cdot)$ is the Forward Fokker - Planck operator defined by

$$L^{+}(\cdot) = -\sum_{i=1}^{n} \frac{\partial}{\partial u_i} (f_i \cdot) + \tfrac{1}{2} \sum_{i=1}^{n} \sum_{j=1}^{n} Q_{ij} \frac{\partial^2(\cdot)}{\partial u_i \partial u_j} \tag{1.9c}$$

$$Q(t)\, dt = E\{dn_g(t)\, dn_g^{T}(t)\} \tag{1.9d}$$

The partial differential equation may be used to derive an expression for the state estimate $\hat{x}$. This is done by multiplying throughout by the state and integrating to yield

$$d\hat{x} = E\{f(x, t)\} + \sum_{i=1}^{m} E\{(x - \hat{x})\, \lambda^{T}(x)\}\, \gamma_i \{\hat{\lambda}^{T} \gamma_i\}^{-1} \{dN - \hat{\lambda}(t)\, dt\}^{T} \gamma_i \tag{1.10}$$

where

$$\hat{x} = E\{x \mid O_{t_o,\, t}\} \tag{1.10a}$$

$$\hat{\lambda} = E\{\lambda \mid O_{t_o,\, t}\} \tag{1.10b}$$

γ_i is a zero vector save for a 1 in the i^{th} position.

This equation is, save for limited cases, analytically intractable, but can be approximated by expanding $f(x)$ and $\lambda(x)$ about their optimum points. This produces two linked estimation equations. The result is summarised below:

Let $x(t)$ be an $(n \times 1)$ vector Markov process governed by

$$dx(t) = f(x, t)\, dt + dn_g(t) \tag{1.11}$$

and let $dN(t)$ be an $(m \times 1)$ vector Poisson step process with a $(m \times 1)$ vector rate parameter $\lambda(x(t), t)$. The first order linearised estimate s is given by the solution to the equations

$$ds = f(s)\, dt + \sum_{i=1}^{m} R(t) \frac{\partial \lambda}{\partial s}^{T} \gamma_i \left(\lambda^{T}(s)\, \gamma_i\right)^{-1} (dN(t) - \lambda(s)\, dt)\, \gamma_i \tag{1.12a}$$

$$dR = \frac{\partial f}{\partial s} R\, dt + \frac{R\, \partial f}{\partial s}^{T} dt + Q(t)\, dt +$$

$$\sum_{i=1}^{m} R(t) \frac{\partial^2 \ell n \lambda}{\partial s^2} R(t)\, \gamma_i^{T}\, dN(t) - \sum_{i=1}^{n} R(t) \frac{\partial^2 \lambda}{\partial s^2} R(t)\, dt \qquad (1.12b)$$

These continuous equations are of a suitable form to be used directly in a computer program by taking dt to be some small time interval such that not more than one collision occurs per time interval. The form that the equations take in this case is derived in Chapter 4. The equations are initialised using apriori knowledge of the values of the state. Suppose for example that the i^{th} element s_i of the initial state is known to lie anywhere between values b and a. If we may assume an equal likelihood of the initial state being anywhere between these points then Appendix F gives an initial covarance of $(b-a)^2/12$ which may be inserted for the initial value of R_{ii}. Off diagonals are put to zero with the assumption of zero correlation between the initial values of the states. The initial value of the state is taken as the mean of b and a.

Solution of the System Identification Problem by means of State Estimation

In the previous sections we have considered a system consisting of a Markov process x(t) generated by the equation

$$dx(t) = Ax\, dt + dn_g(t) \qquad (1.13)$$

Where dn_g denotes additive Gaussian noise.

In the previous section we have shown how, given measurements, disturbed by poisson noise, which depend in the state variable x in a manner to give an observable system (Med 2), (Pol), (Oga), (Ath 2), then the state variable may be determined using equation (1.12).

We now consider the case of system identification where we wish to determine the terms of the matrix A in equation (1.13)

A method commonly proposed is to write a new state equation by augmentation of the state x(t) with the unknown terms of the matrix A, refs (Sag), (Eyk 1) hence allowing the determination of both the state x(t) and system A. This approach has the disadvantage that the dimension of the system is made large, the estimation problem becomes non-linear and often it is impossible to determine all the variables from the measurements available.

An alternative approach may be adopted provided the system parameters, that is the elements of the matrix A may be assumed to be constant throughout the observation period, and secondly provided it is not required to find an estimate of the state vector x. In the cases of organ extraction rate determination to be considered both assumptions are valid. The mean flow rates are constant and best estimates of the intensity of isotope in each organ throughout the measurement period are not required, it being satisfactory to obtain estimates of the extraction efficiencies and related parameters alone.

The first stage is to derive a new state vector r, from which the matrix A may be derived, and to express the measurements in terms of this new vector. It is then possible to estimate this new vector using the state estimation routines, and then from the best estimate at the end of the estimation to form the best estimate of the matrix A. For blood flow rate estimation a possible new state vector consists of the vector of flow rates, and for this case the major problem becomes expressing the mean measurement rates in terms of the new state vector, the flow rates.

Measurements are taken of the intensities of different organs, hence the measurement rates can easily be written in terms of the intensities $x(t)$, $\lambda\,(x(t),\, t)$.

We may restate the problem in order to give a general method. Given a process x(t) generated by the equation

$$dx(t) = Ax\,dt + dn_g \tag{1.14}$$

With constant system matrix A, observed by measurements with an (m x 1) poisson rate vector λ (x(t), t) which depends apon the state of the system, derive a new system that generates a process r(t) from which the matrix A may be derived, having a system equation

$$dr(t) = dn_g' \tag{1.15}$$

observed by measurements with an (p x 1) poisson rate vector λ' (r(t), t) which depends upon the new state vector r.

The deterministic part of equations (1.14), (1.15) must be the same i.e. the vector r(t) in equation (1.15) gives the time evolution of x(t) and the value of the matrix A in equation (1.14). It would be convenient if equations (1.14) and equations (1.15) described identical noise systems, however the Gaussian noise in equation (1.14) cannot be represented exactly by the additive noise in equation (1.15). The representation of the system noise by an additive Wiener process dn_g in equation (1.14) affecting the intensities x(t) is as good approximation to the actual physical system. The system noise can also be adequately represented be additive Wiener process dn_g' affecting the rate vectors r(t) as shown in equation (1.15). To derive the new measurement vector $\lambda'(r(t),t)$ from the measurement vector $\lambda(x(t),t)$ we need the analytic relationship between x(t) and r(t). This may be achieved by solving the deterministic part of the equation (1.14), namely

$$dx(t) = Ax\,dt \tag{1.16}$$

We start with the assumption that the elements of A are given in terms of a vector r. i.e. we have

$$A = A(r) \quad \text{or} \quad a_{ij} = a_{ij}(r)$$

where a_{ij} is the ij^{th} term of matrix A.

We outline the solution of a system of dimension 2 which may be extended to higher dimensional systems.

Consider the (2 x 2) matrix equation.

$$\frac{\partial}{\partial t}\begin{bmatrix} x_1 \\ x_2 \end{bmatrix} = \begin{bmatrix} a_{11} & a_{12} \\ a_{21} & a_{22} \end{bmatrix}\begin{bmatrix} x_1 \\ x_2 \end{bmatrix} \tag{1.17}$$

$$dx = Ax\,dt \tag{1.18}$$

Full details of the solution of this equation are given in Appendix E. The vector x is changed by stages to produce a diagonal system matrix, giving:

$$\frac{\partial}{\partial t}\begin{bmatrix} f_1(x_1,x_2) \\ f_2(x_1,x_2) \end{bmatrix} = \begin{bmatrix} b_1(a) & 0 \\ 0 & b_2(a) \end{bmatrix}\begin{bmatrix} f_1(x_1,x_2) \\ f_2(x_1,x_2) \end{bmatrix} \tag{1.19}$$

Letting $\rho_1 = f_1(x)$, $\rho_2 = f_2(x)$, $\rho = f(x)$ (1.20)

we obtain

$$\frac{\partial}{\partial t}\begin{bmatrix} \rho_1 \\ \rho_2 \end{bmatrix} = \begin{bmatrix} b_1 & 0 \\ 0 & b_2 \end{bmatrix}\begin{bmatrix} \rho_1 \\ \rho_2 \end{bmatrix} \tag{1.21}$$

$$\dot{\rho} = B\rho \tag{1.22}$$

$$\begin{bmatrix} \rho_1 \\ \rho_2 \end{bmatrix} = \begin{bmatrix} \rho_1(0)\exp b_1 t \\ \rho_2(0)\exp b_2 t \end{bmatrix} \tag{1.23}$$

$$\rho = \exp Bt\,\rho(0) \tag{1.24}$$

With the known initial conditions of the state vector x, namely $x_1(0)$, $x_2(0)$ we may derive $\rho_1(0)$ and $\rho_2(0)$ using

$$\rho_1(0) = f_1(x_1(0), x_2(0)), \quad \rho_2(0) = f_2(x_1(0), x_2(0))$$

and hence obtain from equation (1.24) an analytic expression for ρ in terms of B and t. By reversal of the steps taken to derive equation (1.19) the inverse expression for x in terms of ρ can be obtained. The detailed steps for the equation of dimension 2 is given in Appendix D. To give the overall philosophy and to give the precise analytic expressions slightly different terminology is used.

Let the transformation matrices D and D^{-1} be defined by the equations

$$x = D\rho \tag{1.25}$$

$$\rho = D^{-1}x \tag{1.26}$$

replacing equation (1.20).

Consider the system equation

$$\dot{x} = Ax \tag{1.27}$$

Substitution of equation (1.22) gives

$$D\dot{\rho} = AD\rho \tag{1.28}$$

$$\therefore \quad \dot{\rho} = D^{-1} AD\rho \tag{1.29}$$

solving this equation we obtain

$$\rho = \exp(D^{-1} ADt)\, \rho(0)$$

$$\therefore \quad x = D \exp(D^{-1} ADt)\, D^{-1} x(0) \tag{1.30}$$

where D^{-1} AD is diagonal and x may be easily evaluated.

Since D, D^{-1} and A all depend solely upon the vector r, equation (1.30) gives the required analytic expression for x:

$$x = x(r).$$

The system is observed by measurements with a (m x 1) poisson rate vector λ (x(t), t), which is dependent upon the state of the system. By the use of equation (1.30) we obtain

$$\lambda\ (x(t),\ t) \ = \ \lambda\ (x(r,\ t),\ t) \ = \ \lambda_1\ (r,t)$$

The system identification problem has thus been transformed to the State Estimation problem:
Given the process r(t) generated by

$$dr(t) \ = dn_g'$$

Observed by measurements with an (m x 1) poisson rate vector λ_1 (r(t), t) estimate the state vector r(t).

We see that this problem may be solved directly by the methods described in the previous section. The implementation of the equations is described in detail in Chapter 4.

Conclusion

Various techniques of System Identification have been reviewed and it has been shown that an on-line parameter identification technique is desirable. Such a technique exists for stochastic systems, but only for state identification. The development of the continuous time estimation equations has been outlined, and it has been shown how under certain conditions, satisfied by the conditions of the nuclear medical problems posed, these state estimation equations may be used for system identification.

CHAPTER 2

DETECTION OF ISOTOPE RADIATION INTENSITY

Introduction

Over the past eighty years X-rays, and lately gamma-rays, have been used increasingly in the field of patient diagnosis. The X-ray technique requires an external source to be positioned to one side of the patient. The transmitted rays are detected on the other, the information being commonly displayed as an exposed photographic plate, or in the case of the 'E.M.I.-scanner' (Pat 1) and related instruments, as a computer reconstruction of a three dimensional object, normally displayed in the form of adjacent slices.

The ability to detect gamma rays has made it possible to position sources at regions of interest. Isotopes may be incorporated in chemicals occurring in or having properties similar to those occurring naturally in the body. Detection of these gamma ray emitting isotopes can give direct functional studies of the metabolism of the body.

The gamma ray sources emit radiation in all directions. To create an image some directional information must be known. Gamma rays cannot be focussed hence normal imaging techniques are not applicable, and other methods must be used. This is generally achieved by the use of a lead collimator, the lead being considered opaque to the incoming rays. The most elementary form is the gamma ray scanner. This has a detector head consisting of a scintillator or semiconductor with a converging lead collimator, Figure (2.1), focussed at a single point. The system views only this point at any time, and is swept mechanically

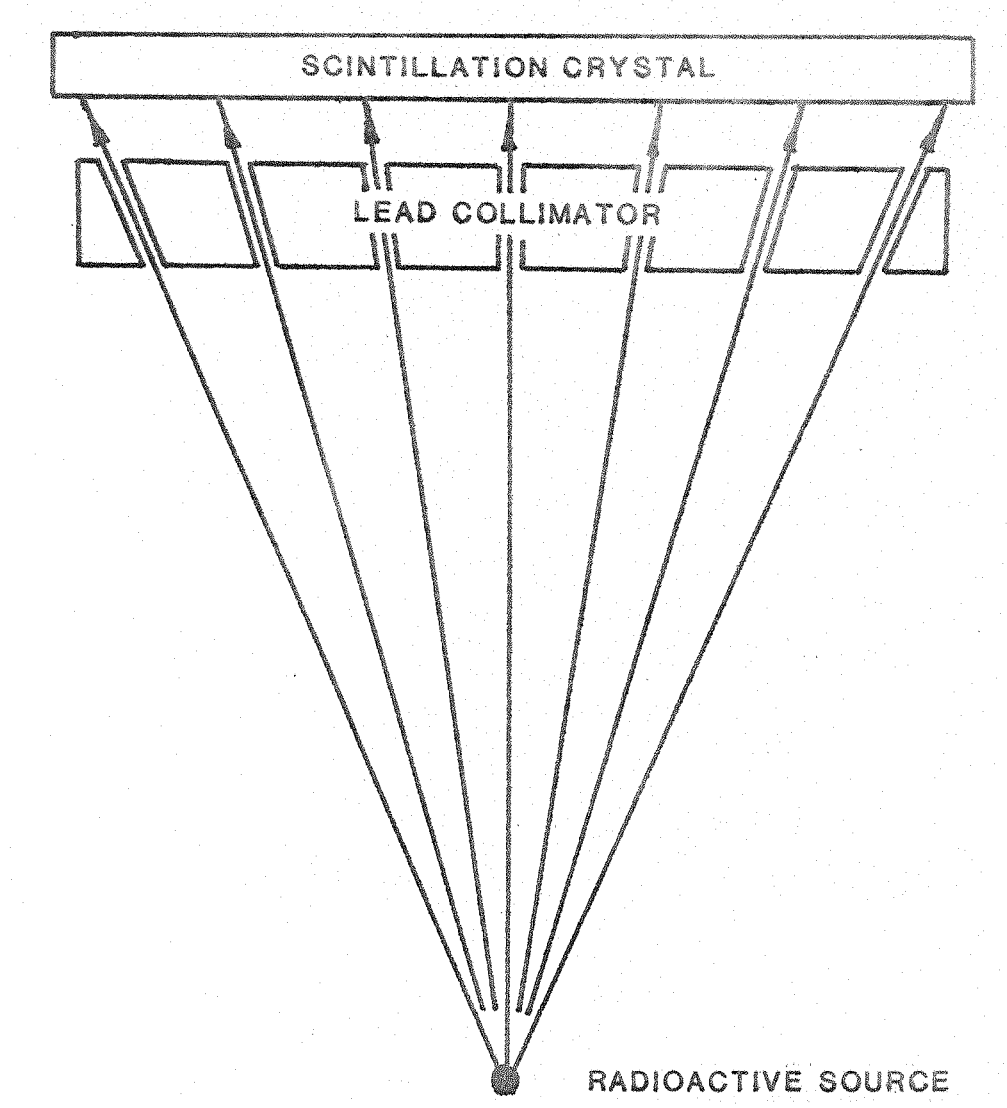

FIG 2.1 HEAD OF A GAMMA RAY SCANNER WITH CONVERGING COLLIMATOR

over the region of interest. The process is slow since each point is viewed only for a short period of time, and production of an image can take up to thirty minutes.

In 1956 Anger introduced a multichannel collimator camera which is now in a similar, but technically more advanced form, gradually becoming standard equipment for scanning in many centres, (Ang. 1). It consists of a multichannel lead collimator, coupled to a sodium iodide scintillation crystal viewed by an array of photomultiplier tubes, figure (2.2). The light flashes produced in the crystal are detected by the photomultiplier tubes, an electric network driven by the differing outputs of each tube determining the position of each flash.

Alternatives to this system have been investigated over the last twenty years. Image intensifiers were introduced in 1964 to image low intensity sources, (Ter), but have since been used to image all types of sources. A wire spark gas chamber with a digitised readout was described by Kaufman et. al. in 1971, (Kau). This is a compact instrument capable of covering large areas with higher resolution and lower cost, but with a slower counting rate than the Anger camera. A multiwire proportional chamber was constructed in the same year, (Sch). Liquid Xenon detectors with a higher stopping power than gas chambers have also been constructed by Zaklad et. al. in 1972, (Zak). Semiconductor detectors have been developed by Detko, (Det), Parker, (Par), and Hofker, (Hof), and a survey made in the report by Hofker in 1971. Many early methods of detection have been surveyed by Anger, (Ang. 2), and a later survey of detection systems given by Moody in 1970, (Moo).

All the preceeding detection systems have used lead collimators.

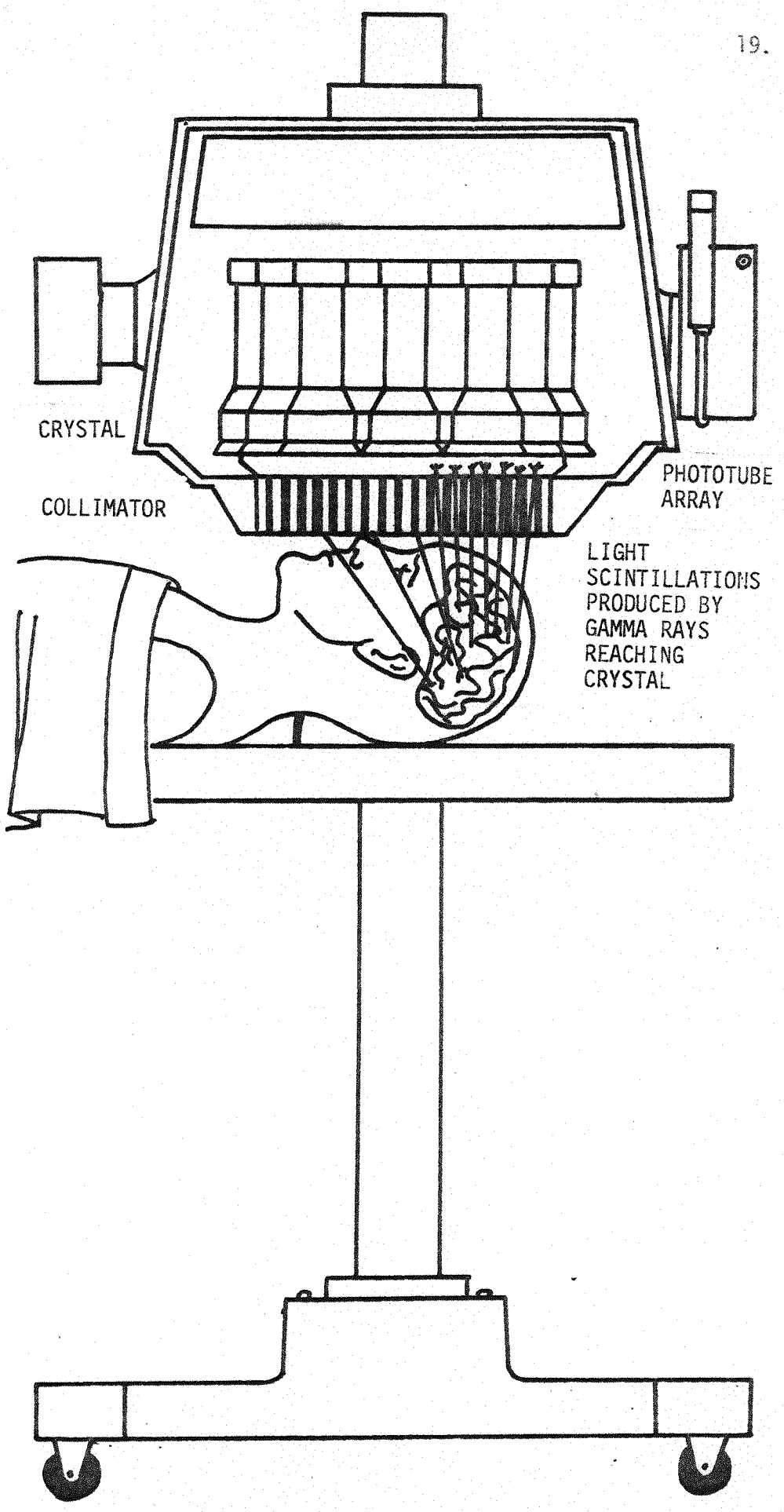

FIG 2.2 THE ANGER SCINTILLATION CAMERA

In the following section the disadvantages of the collimator system are outlined, and it is shown how these disadvantages may be overcome by use of special properties of the Compton effect. The resulting instrument denoted 'the Compton effect camera' is described in the theses of Everett, (Eve), Doshi, (Dos) and Fleming, (Fle). A preliminary report (Eve. 1) gives further details of the potentialities of the system. Due to the many potentialities of the system we outline the method, and show how some computing problems which arise in the production of the image may be overcome.

The Compton Effect Gamma Ray Camera

A disadvantage of conventional methods of detection of gamma radiation utilising collimators is that only a small fraction of the total radiation is emitted parallel to the collimator holes. This means that comparitively large does need to be administered. Lesser doses can be administered if the collimator holes are increased, but this leads to lower resolution. Improvements in manufacturing technique now have little effect since the theoretical limits of resolution are close to being achieved.

A method of detection of the position of radioactive isotopes eliminating this drawback was proposed by Todd, (Tod). It requires no collimator, but uses the properties of the Compton Effect (Appendix A) to determine the position of isotopes. The Compton Effect is observed when photons, having the energies associated with commonly used isotopes pass through some liquids, gasses and semiconductors. When used as a detector semiconductors have many advantages, noteable being the far greater stopping power, and a semiconductor detector forms the basis of the proposed camera. A problem inherent in the method is that the derivation of the image from the detector measurements requires

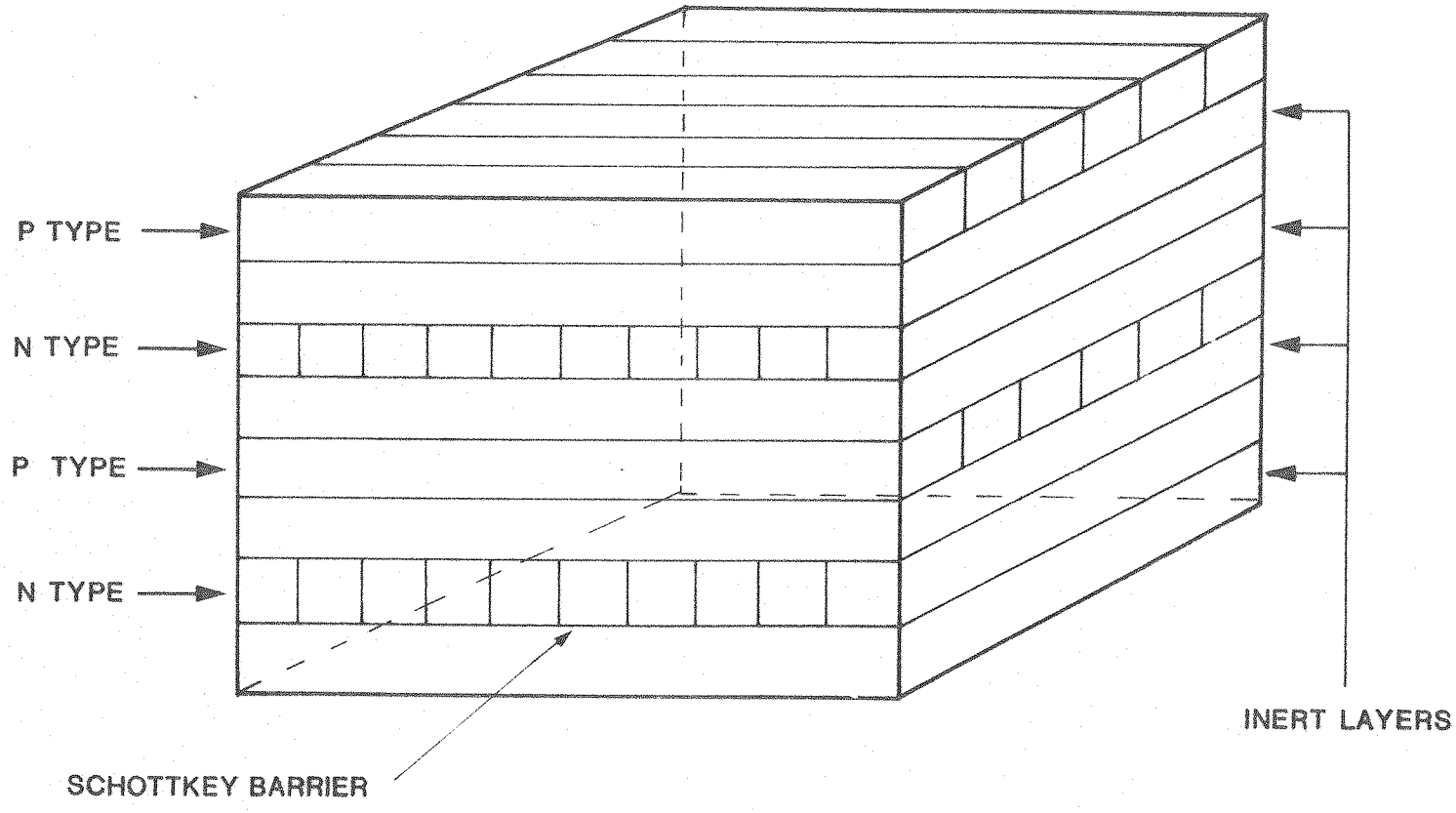

FIG 2.3 CONFIGURATION OF THE COMPTON EFFECT GAMMA CAMERA

a large amount of computation, but due to the potential advantage of the method, the Compton Camera is described, and it is shown how sharp images may be produced with minimal computation.

The Structure of the Camera

The camera contains a semiconductor detector through which radiation emanating from the source passes. Any Compton collisions occurring in the detector cause the gamma ray photons to be deflected, and in doing so produce free electrons which produce electrical signals whose magnitude may be amplified and hence measured. The position at which the free electron is produced gives the position of the collision, the magnitude of the energy aquired by the electron enables the angle of deflection of the photon to be determined.

To determine the position of the Compton collisions the detector is divided vertically, using lithium drifting techniques, into a multiple sandwich of p and n type doped semiconductors, separated by inert layers, Figure (2.3). An electron liberated by a collision is attracted towards the nearest p type layer, and the hole produced by the same process travels towards the nearest n type layer. The pulses observed when the electrons and holes reach the p and n type layers respectively give the vertical height of the collision.

To determine the position of the collision in the horizontal plane the p and n type layers are divided further into orthogonal strips by Schottkey barriers which have dead spaces of only 1μm. Pulses are only produced on one strip in the p layer, and one in the n layer at any time, thus giving the position in the horizontal plane. The energy of the pulse may be determined by use of a pulse shaping amplifier via a ferrite decoder transformer (Eve).

Mode of Operation of the Camera

There are several steps from the determination of measurements in the camera detector to the production of a useable image. Here we show how the collision angle may be determined from the measurements of the energy liberated by the electron, how posssible locii of the photon may be determined, and how from this limited knowledge an image may be produced.

a) Determination of the Deflection Angle of a Photon at its first collision in the Defector

Consider a three stage Compton Effect collision of a gamma-photon in a semiconductor, Figure (2.4). The photon is emitted when a photon in the radioactive source falls from one energy level to another. The photon may have one of several initial energies depending apon the actual energy transitions performed. Let the initial energy of the photon be denoted by E_1.

With reference to Figure (2.4) let the energy liberated at the first and second collisions be ΔE_A and ΔE_B respectively. Denoting the the energy of the photon incident at the second and third collision parts by E_2 and E_3 respectively

$$E_2 = E_1 - \Delta E_A \tag{2.1}$$

$$E_3 = E_2 - \Delta E_B \tag{2.2}$$

Assuming a possible value for E_1 and by measurement of ΔE_A and ΔE_B, see (Eve) for details, we can calculate E_2 and E_3. We denote these provisional values by E_2^* and E_3^*.

From Appendix A the relationship between the deflection angle ψ_2 at the second collision point and the wavelengths before and

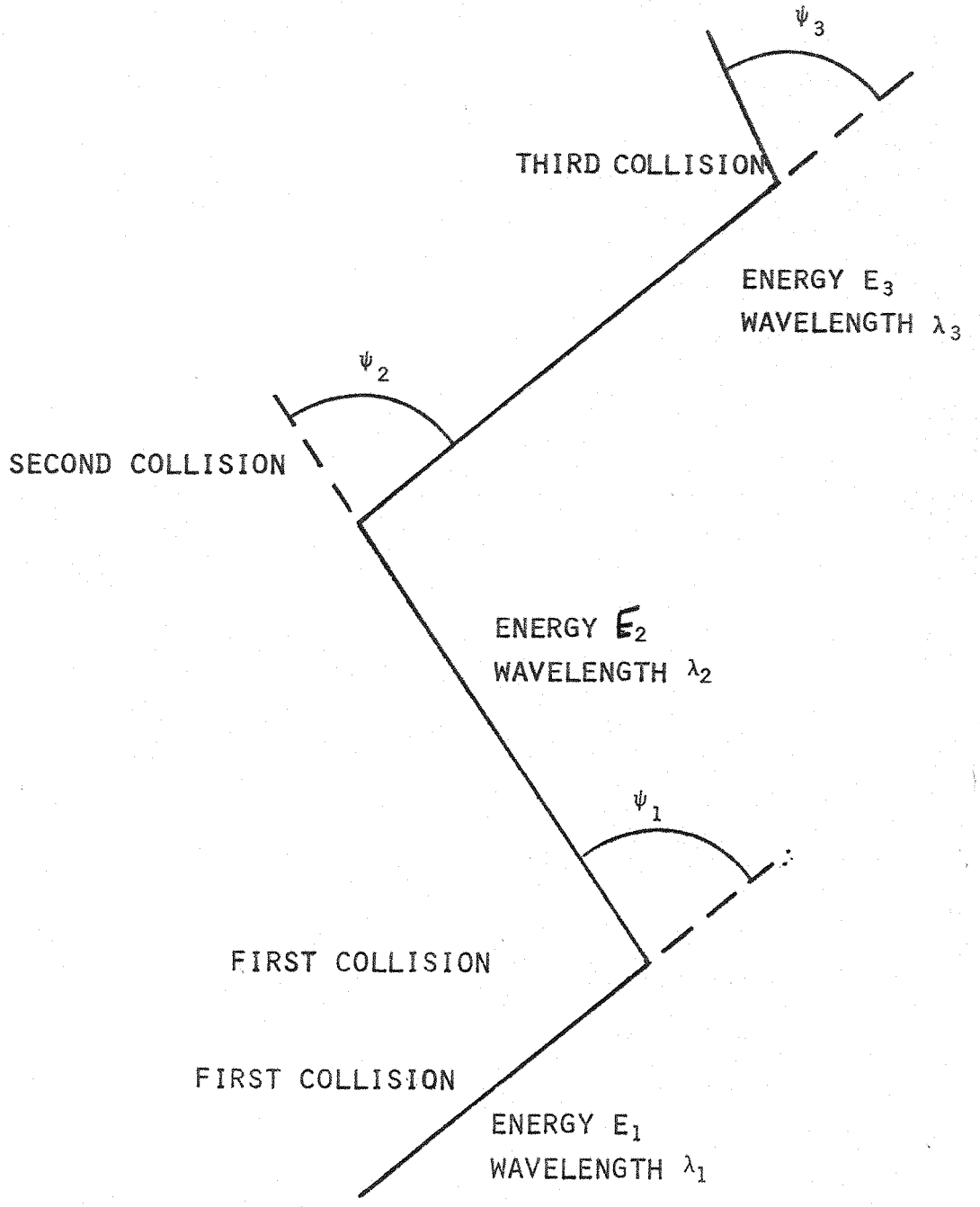

FIGURE 2.4 THREE STAGE COMPTON COLLISION PROCESS

after the second collision, λ_2 and λ_3 respectively are given by

$$\lambda_3 - \lambda_2 = \frac{h}{m_0 c}(1 - \cos \psi_2)$$

Estimates of λ_2 and λ_3 may be calculated from the estimates E_2^* and E_3^* by use of the formulae

$$\lambda_2^* = \frac{hc}{E_2^*} \qquad \lambda_3^* = \frac{hc}{E_3^*}$$

A provisional value of the angle ψ_2, denoted by ψ_2^* is thus obtained corresponding to the assumed value of E_1, the initial photon energy.

The position of the collisions of the photons may be determined by noting at which orthogonal strips the energy pulses occur. ψ_2 may be determined from the position of the collisions, hence it may be determined whether the calculated value of ψ_2, namely ψ_2^*, is correct. If it is incorrect different values for E_1 are assumed until the value for E_1 gives a satisfactory value for ψ_2^*. At this point our found value of E_1 may be used to determine the angle ψ_1 using the equation

$$\lambda_1 = hc/E_1 \qquad \lambda_2 = hc/E_2$$

$$\lambda_2 - \lambda_1 = h(1-\cos \psi_1)/m_0 c$$

Note that if E_1 is known apriori by the use of a mono-energetic radioactive tracer, then no check of ψ_2^* and ψ_2 is required, and only two collisions are necessary. We determine ψ_1 from the equations

$$\lambda_2 - \lambda_1 = \frac{h}{m_0 c}(1-\cos \psi_1)$$

The above procedure has enabled a limited amount of knowledge of the position of the isotope radiation to be determined. We know the co-ordinates of the first and second collision points and the deflection angle of the photon at the first collision, we hence deduce that the photon source lies somewhere on the surface of a cone, semiangle ψ_1, apex the first collision point, with the axis passing through both collision points, Figure (2.5).

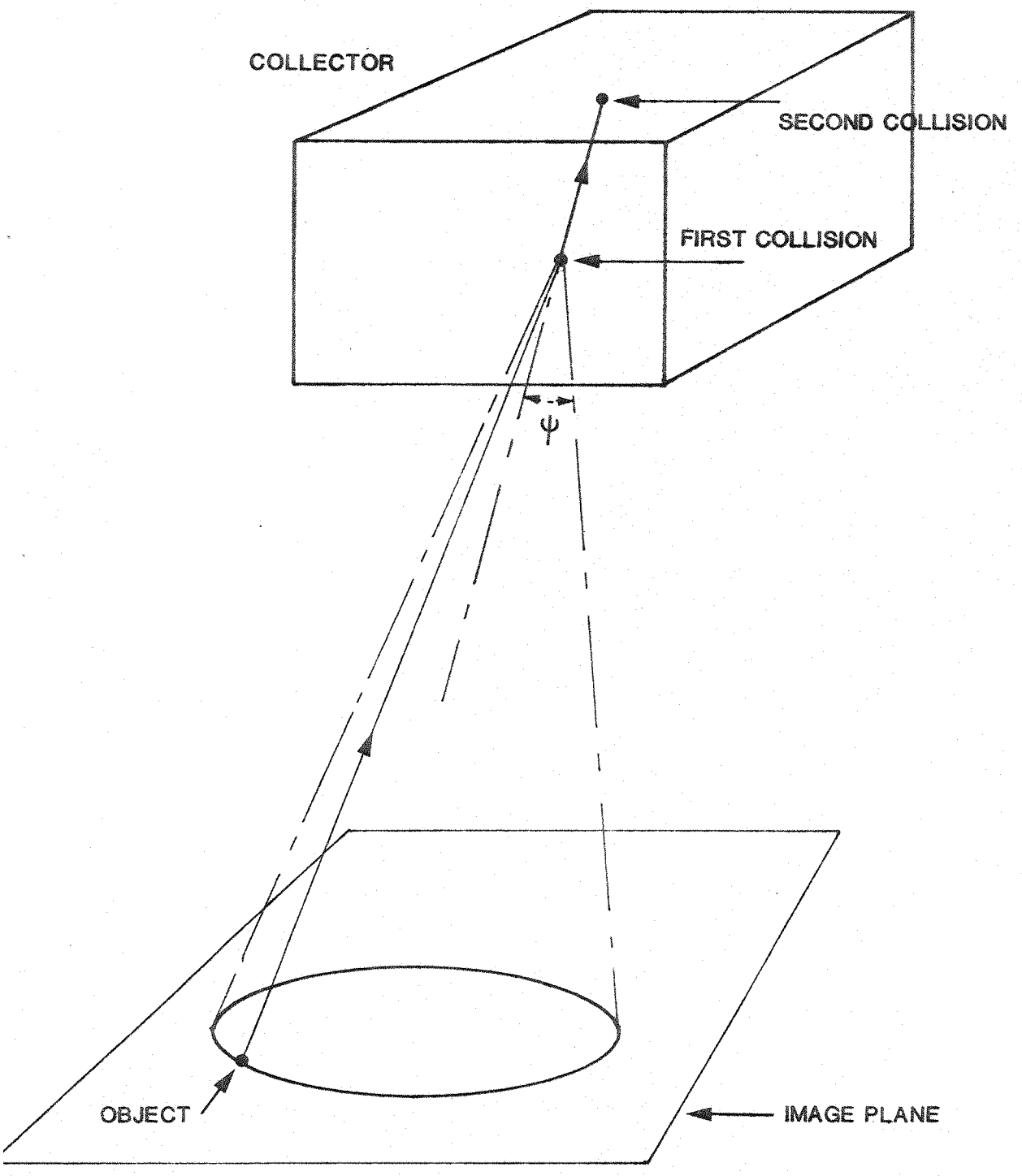

FIG 2.5 TWO STAGE COLLISION PROCESS

This information is sufficient to produce an image of the radioactive source.

b) Determination of the position of the source in the image plane (production of an image).

A body emitting radiation may be considered to consist of a set of point sources. If the position and intensity of each point source is known, then an image of the object may be produced. If the response of the measuring system to a point source is good, the corresponding image of the total object will be correspondingly sharp. In the following section we show how a point source may be imaged.

Consider a point source emitting several photons, Figure (2.6). If the measurement is assumed perfect then the cones will intersect at the source point. With imperfect measurements the cones will pass through a sphere, centre the point source, of radius ε, where the magnitude of ε is dependent apon the measurement errors, Figure (2.7a).

If we consider horizontal planes passing above, through and below the object, Figure (2.7b), then the cones will be represented on the plane by conic sections, which on the planes above and below the object will appear to be randomly distributed, but on the plane passing through the object will all pass within distance ε from the object. To build up an image a rectangular grid is imposed on each plane, the size of the grid being made compatible to ε, which may be calculated by studying the measurement errors (Eve). The square containing the source will be intersected by all the cones. If we give each square a count value representing the number of cones intersecting it, then the source position will be represented by a square with a high count value. The counts in the other grid squares will be ideally zero, but in practice will be finite, but smaller, the magnitude of the

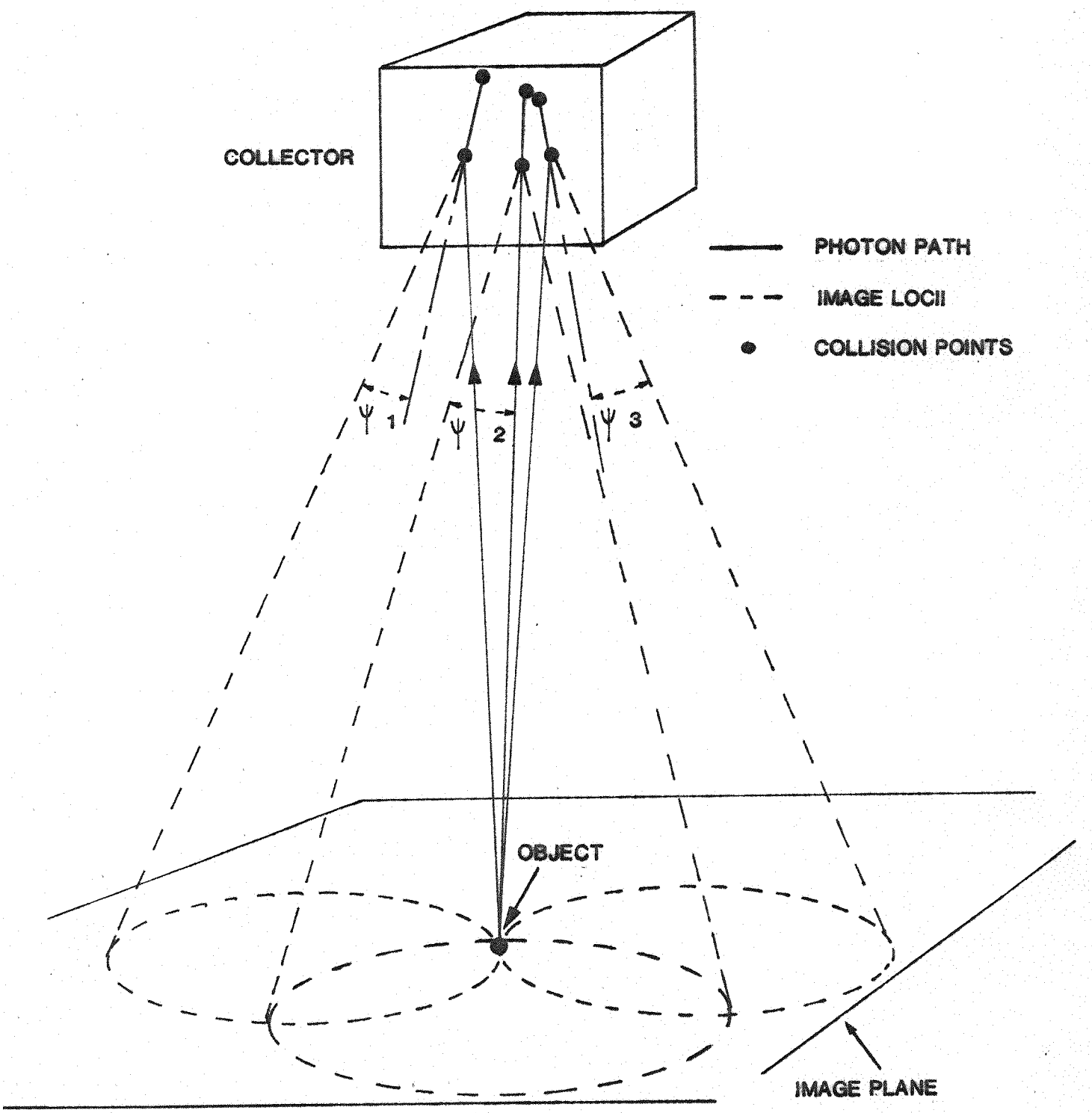

FIG 2.6 PRODUCTION OF NON - PROCESSED IMAGE USING THREE COLLISIONS

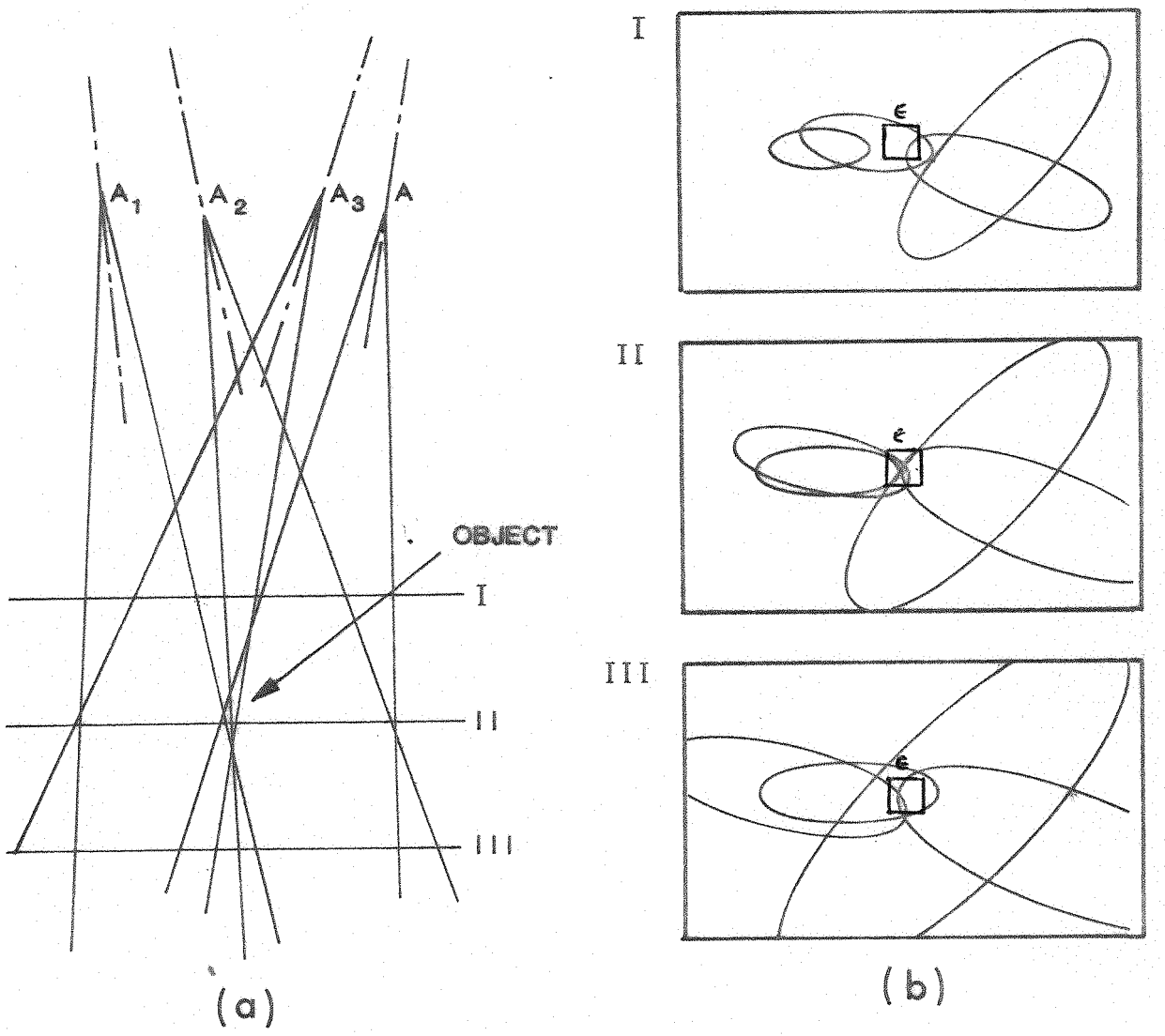

FIG 2.7 PRODUCTION OF POSSIBLE IMAGE LOCII
ABOVE, BELOW AND IN THE PLANE CONTAINING THE OBJECT

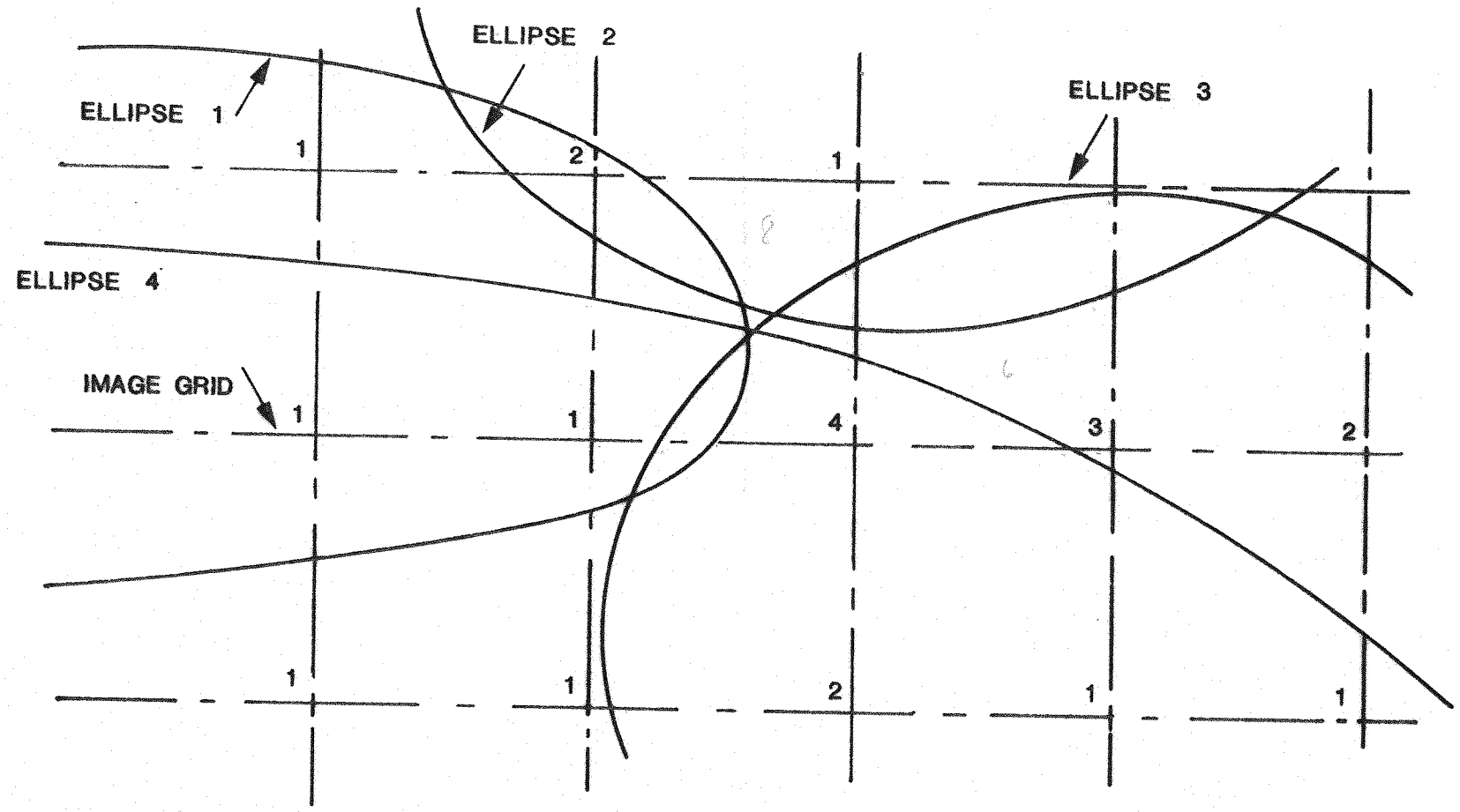

FIG 2.8 PRODUCTION OF POINT SPREAD FUNCTION

count decreasing in magnitude as the distance from the object increases. The quality of the image is normally expressed in terms of the point spread functions, the response of the imaging device to a point source. Here we make some assumptions to obtain an approximate expression for the point spread function.

c) Determination of the Approximate Point Spread Fuction

If we consider the region in the image plane surrounding the object, the conic sections produced by the intersection of the cones with the image plane will generally produce curves of small curvature, passing within distance ε of the object, figure (2.8). We may consider, as a first approximation, the conic sections to be straight lines passing through the object as in figure (2.9).

Consider a strip at radius R, of width ΔR, from the object. The intensity will be given by the number of counts divided by the area. i.e.

$$\text{Intensity at Radius } R = \frac{\text{No of counts in strip}}{\text{Total area of strip}}$$

$$= \frac{2\,(\text{No of lines})}{2\pi R \qquad \Delta R} = \frac{n}{\pi R \quad \Delta R}$$

$$\propto \frac{Q}{\pi R \quad \Delta R}$$

where n is the number of cones resulting from a source of intensity Q. The point spread function is shown in Figure (2.10).

It may be seen that the tail of the point spread function is proportional to $1/R$. This tail may to a large extent be eliminated by utilising the fact that it is built up of a set of conic sections This allows a form of apriori processing to be performed.

IDEALISED IMAGE

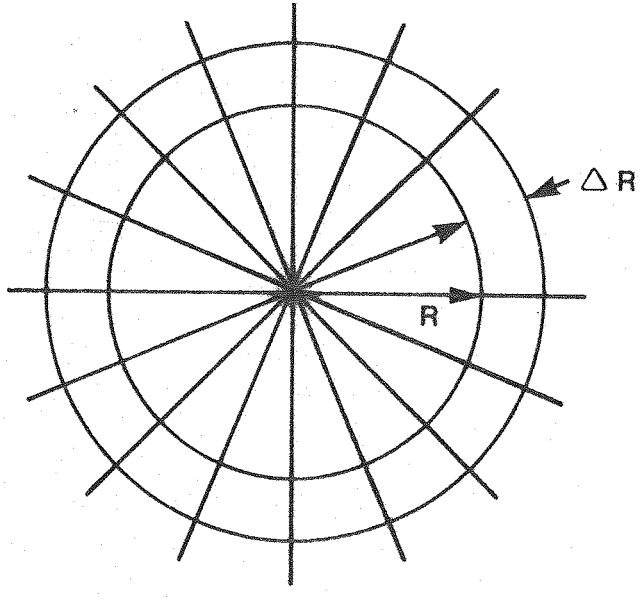

INTENSITY AT RADIUS R

$$= \frac{\text{INTENSITY IN STRIP WIDTH } \triangle R}{\text{TOTAL AREA OF STRIP}}$$

$$= \frac{2 * (\text{NO OF LINES})}{2 \pi R * \triangle R}$$

$$= \frac{Q}{\pi R \triangle R}$$

FIG 2.9 CALCULATION OF THE POINT SPREAD FUNCTION

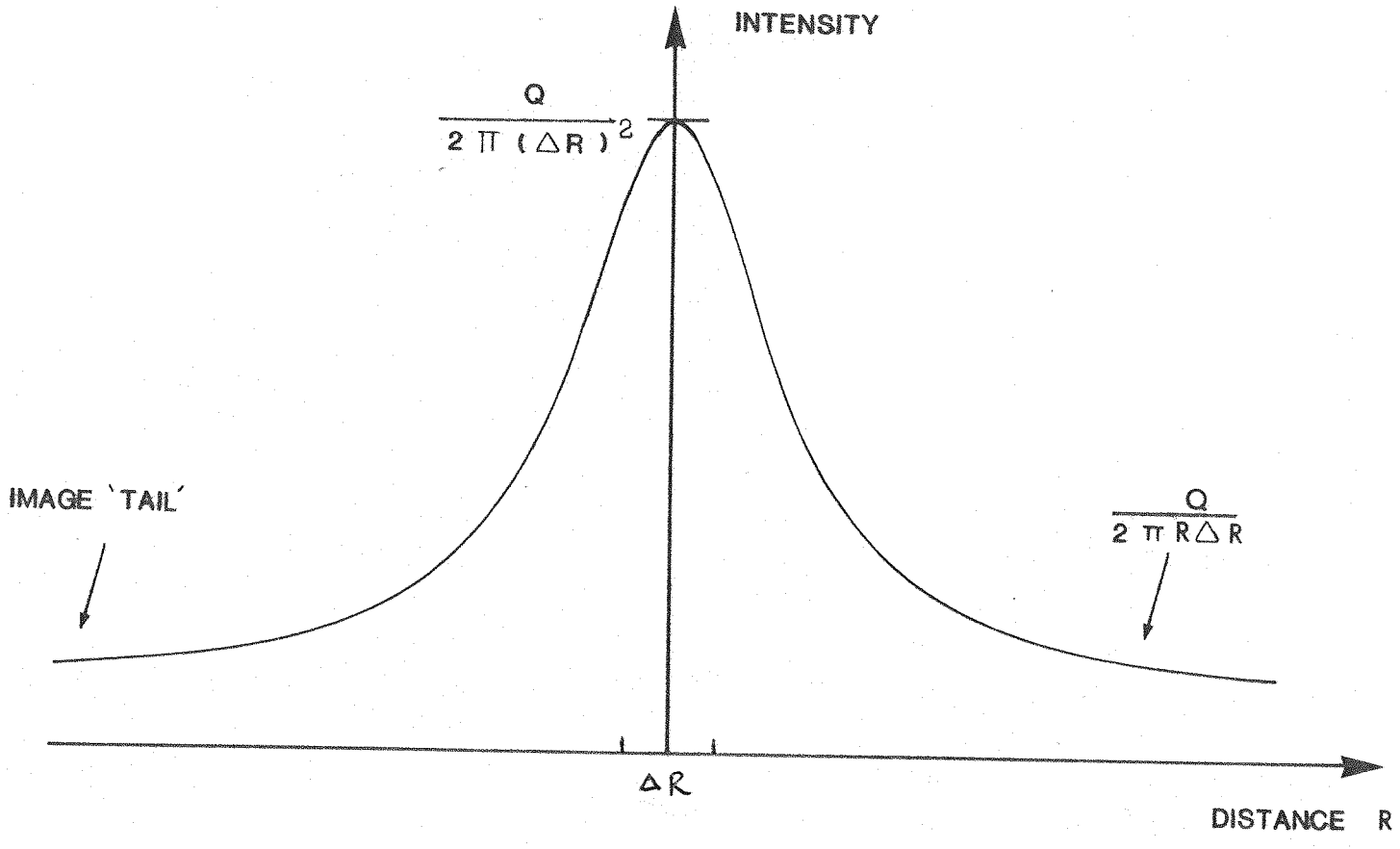

FIG 2.10 POINT SPREAD FUNCTION OF POINT SOURCE

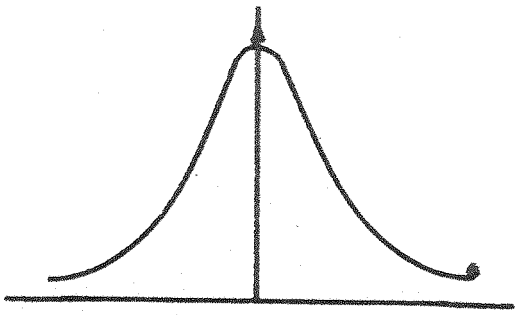

FIG 2.11 : FOCUSSED

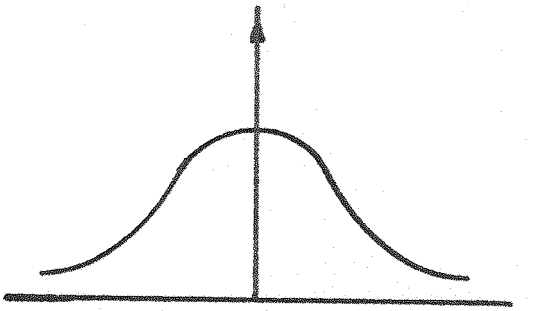

FIG 2.12 : DEFOCUSSED

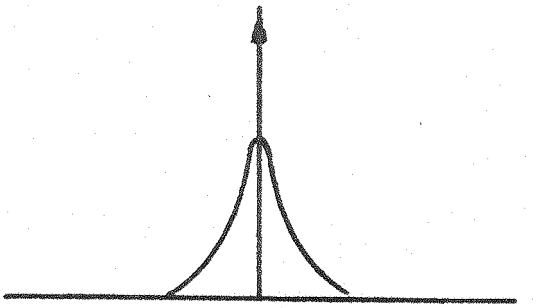

FIG 2.13 : PROCESSED

POINT SPREAD FUNCTIONS OF POINT SOURCES

Apriori Processing of the Image of the Compton Effect Camera

Consider the image of a point source. If many conic sections make up the image the plot of the density of ellipse lines against the distance r will be of the form shown in figure (2.11). A non-focussed image would have a density distribution as shown in figure (2.12). This defocussed image has a smaller intensity near the object, but has the same 'tail' as the focussed image. If we could subtract the contribution of the defocussed image from that of the focussed image, then we would obtain the distribution of figure (2.13) which has a smaller variance, and no tail, and which would produce a sharp total image.

To produce the defocussed image we may use the fact that the image is built up of many conic sections, and plot for each cone, the intersection with the image plane of a similar cone, of identical semiangle ψ but whose apex lies a small distance δ from the apex of the original cone, figure (2.14). Encoraging preliminary results have been obtained, (Dos).

Three Dimensional Imaging

It has been noted that we may produce images on planes at various distances from the detector, figure (2.7). We noted that only in the plane passing through the object do the cones pass through the object to within the errors set by the measurement accuracies of the instrument, resulting in the images produced above and below the object plane being defocussed. Considering the apriori processing technique which subtracts a defocussed version of the image from the original, in planes above and below the object the defocussed images will cancel, while only in the plane containing the object will one image be focussed and the

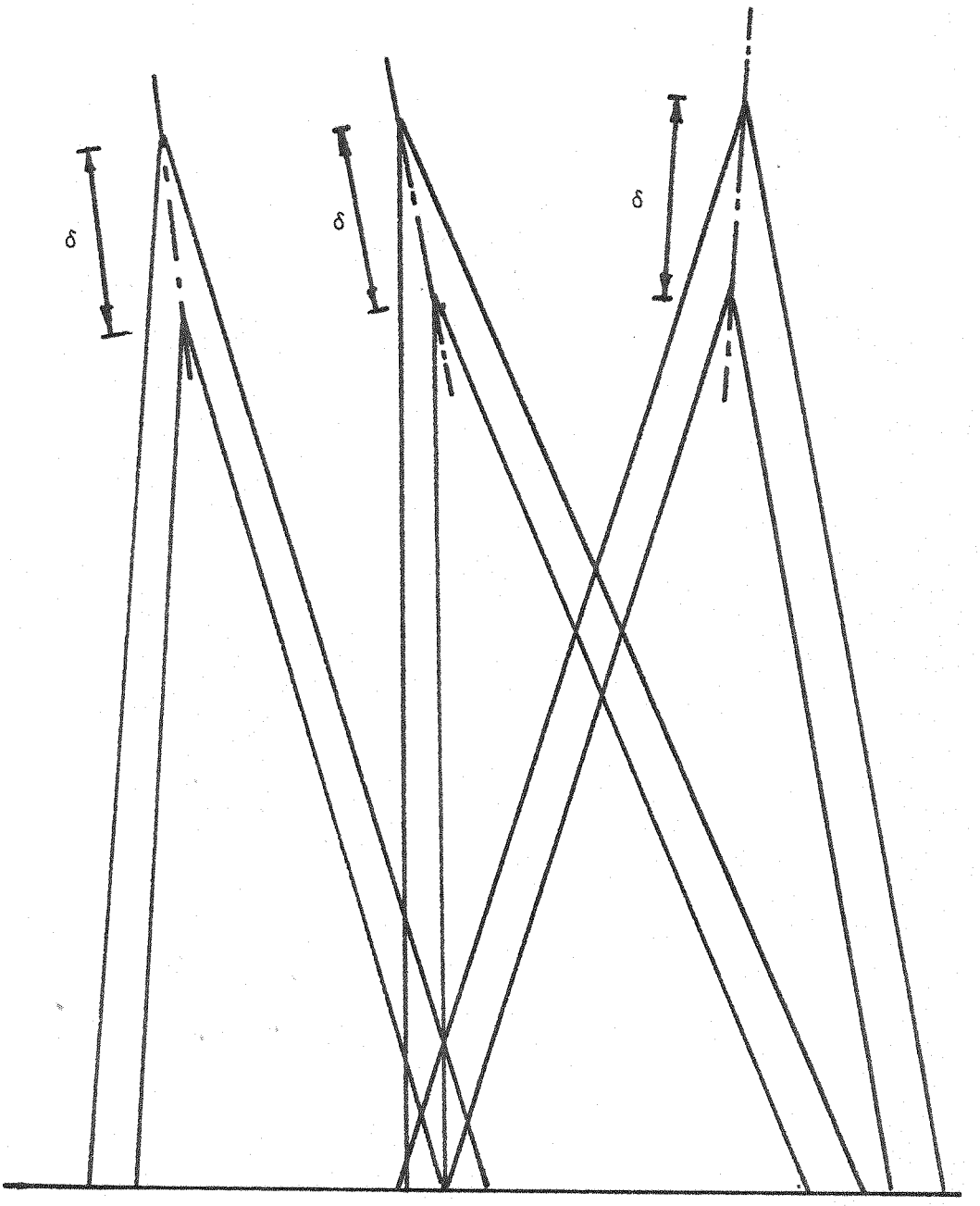

FIG 2.14 PRODUCTION OF DEFOCUSSED AND FOCUSSED IMAGES FOR APRIORI PROCESSING

other defocussed resulting in a sharp image point. A sharp response will thus be produced on the plane containing the object, but not on planes above or below the object.

By the use of this technique images may be produced on planes at various distances from the collimator giving a three-dimensional image. The spatial resolution in the vertical direction will be related however to the extent to which the miss distance of the cones change with distance from the detector. If the aperture of the collector is small and the distance from the collector to the object is large then the three dimensional resolution will be poor.

Solution of Some of the Problems involved in the computation of the image of the Compton Effect Camera

To obtain the image the intersection of cones with an image plane must be plotted. This intersection will always be a conic section, either a hyperbola, parabola, ellipse or circle. To produce a camera with a quick response time fast algorithms to produce their cones must be used.

Method of Plotting Conics

Doshi used three methods to plot the conic sections (Dos).

1) A contrubution to a cell was made if the solution to the equation of the conic in the image plane

$$a_1 x^2 + 2a_{12} xy + a_{22}y^2 + 2a_{13} x + 2a_{23}y + a_{33} = 0$$

lay in that cell when the value of y was fixed so as to correspond to a line passing through that cell and parallel to the axis, Figure (2.15). The value of y takes all values over the image plane, complex values of x denoting that the conic does not pass through a row of cells through which the line passes. The method does not give contributions to

all squares through which the ellipse passes, and there is anisotropy in the plotted conic section.

2) With reference to Figure (2.16) a point is plotted on the conic every value of $d\phi$ varying ϕ from ϕ_{min} to ϕ_{max}, ϕ_{max} being determined as the maximum value of ϕ at which the source is likely to occur. The probability that a collision occurred at each point was evaluated, and the contributions at each point so weighted.

3) The most likely point was found and this alone plotted. All of these methods, except 3 which was found to be inadequate were too complex for a practical system, and hence an effective method was looked for which would plot all the grid elements intersected by the elipse, since if the point which contained the image was not plotted, any other points plotted would in fact simple be noise in the image.

We consider two ellipse plotting methods, firstly a fairly efficient method of implementing a variation of method (2) and secondly a method which attempts to cut down the number of multiplications so as to reduce the computation time.

Method 1

We first derive the equations for the parameters of the ellipse which needs to be done once only for each ellipse.

With reference to Figure (2.17) we see that

$$p = \tfrac{1}{2}h\,(\tan(\theta+\psi) - \tan(\theta-\psi))$$

$$\alpha = \tan^{-1}\left(\frac{h}{p}\right) = \tan^{-1}\left\{\frac{2}{\tan(\theta+\psi) - \tan(\theta-\psi)}\right\}$$

$$a = h\,(\tan(\theta+\psi) - \tan(\theta-\psi))$$

$$\ell = h \sec\theta$$

$$r = \ell \tan\psi = y_\alpha$$

$$x_\alpha = h\tan\theta - (h\tan(\theta-\psi) + a/2)$$

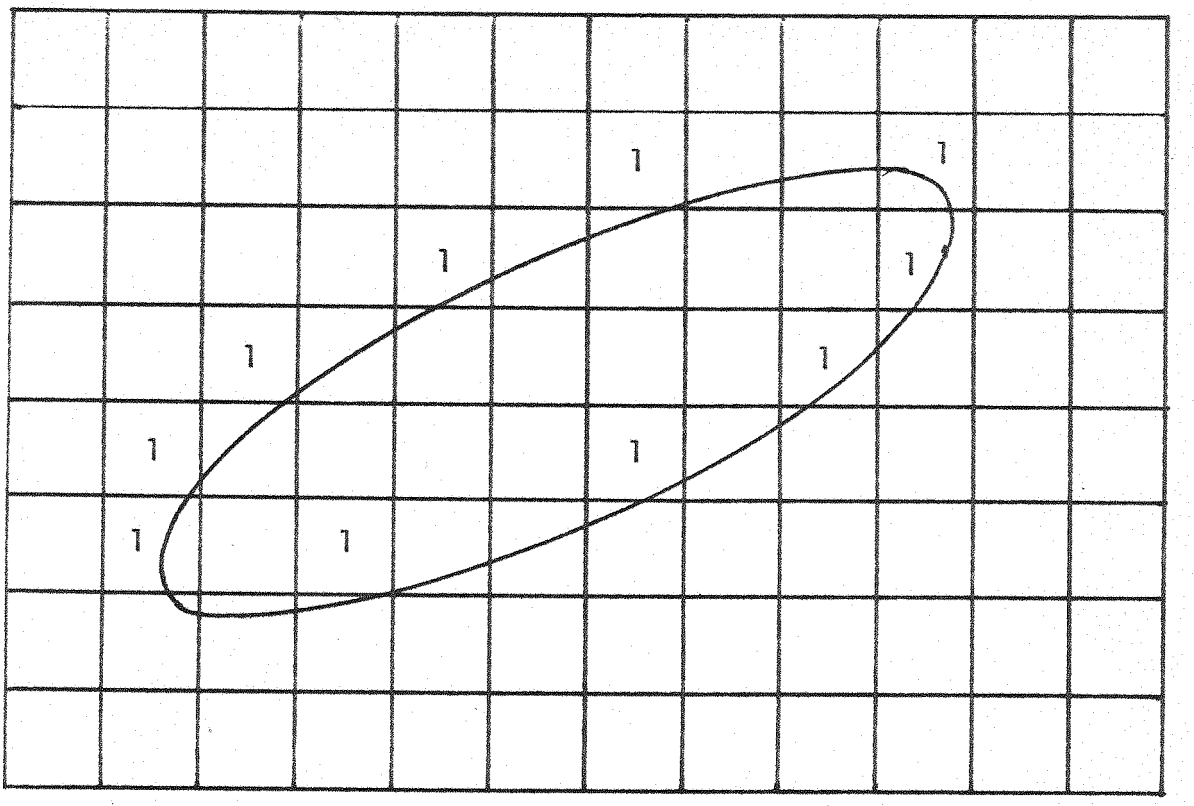

FIGURE 2.15 ANISOTROPY OF AN ELLIPSE PRODUCED WHEN METHOD 1 IS USED FOR PLOTTING

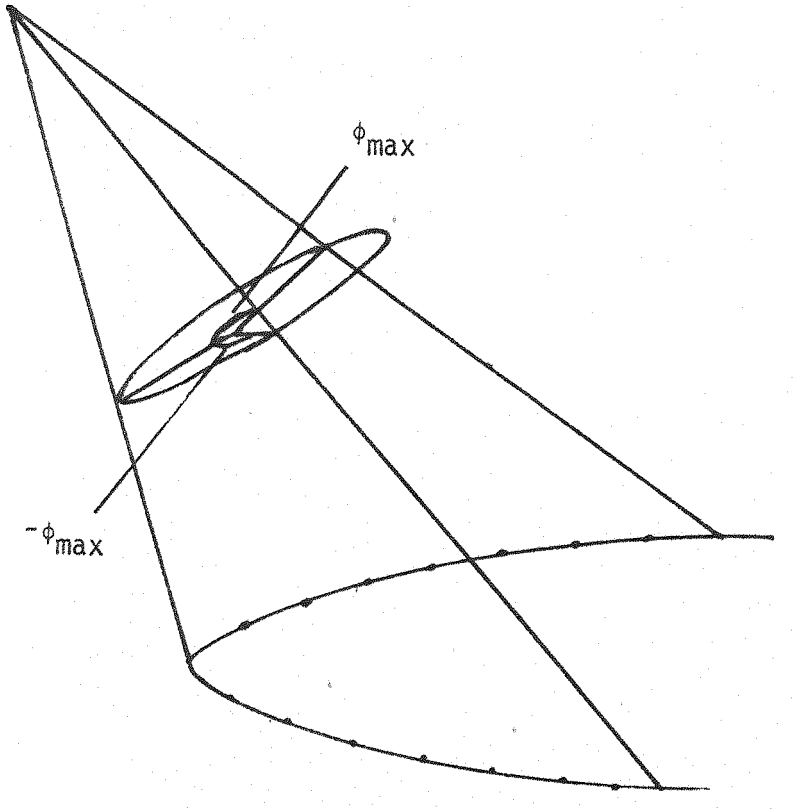

FIGURE 2.16 VARYING ϕ TO PRODUCE THE CONIC POINTS

With reference to figure (2.18) we see that

$$b = \frac{a\, y_\alpha}{\sqrt{(a-x_\alpha)\ (a+x_\alpha)}}$$

Where we have used the standard equation of the ellipse

$$\frac{x^2}{a^2} + \frac{y^2}{b^2} = 1 \quad b^2 = \frac{a^2}{a^2-x^2}\, y^2$$

Consider the projection of a circle radius b onto a plane at angle α to the circle. This will be the desired ellipse. With reference to figure (2.19).

$$\begin{aligned} R &= \sqrt{c^2 + d^2} \\ &= \sqrt{[h^2 \sec^2\alpha + b^2 \sin^2\phi]} \\ &= \sqrt{[b^2 \cos^2\phi \sec^2\alpha + b^2 \sin^2\phi]} \\ &= b\sqrt{[\cos^2\phi \sec^2\alpha + \sin^2\phi]} \end{aligned}$$

Hence we may vary ϕ from $-\phi_{max}$ to ϕ_{max} to produce points on the ellipse. If $\phi_{max} = \pi$ then the whole ellipse is produced. ϕ may be expressed in terms of β to give points equispaced in β.

Method 2 Approximate method of Image Formation

Consider the equation of an ellipse, major axis the x axis, then we have:

$$\frac{x^2}{a^2} + \frac{y^2}{b^2} = 1 \quad \text{or } y^2 = -k\, x^2 + b^2 \ , \ k \triangleq \frac{b^2}{a^2}$$

With reference to figure (2.20) we start at x = a, y = 0 and plot in the direction of the arrow.

If we can obtain the points on the ellipse for x varying from a to zero in unit steps, then this will be sufficient since the unit

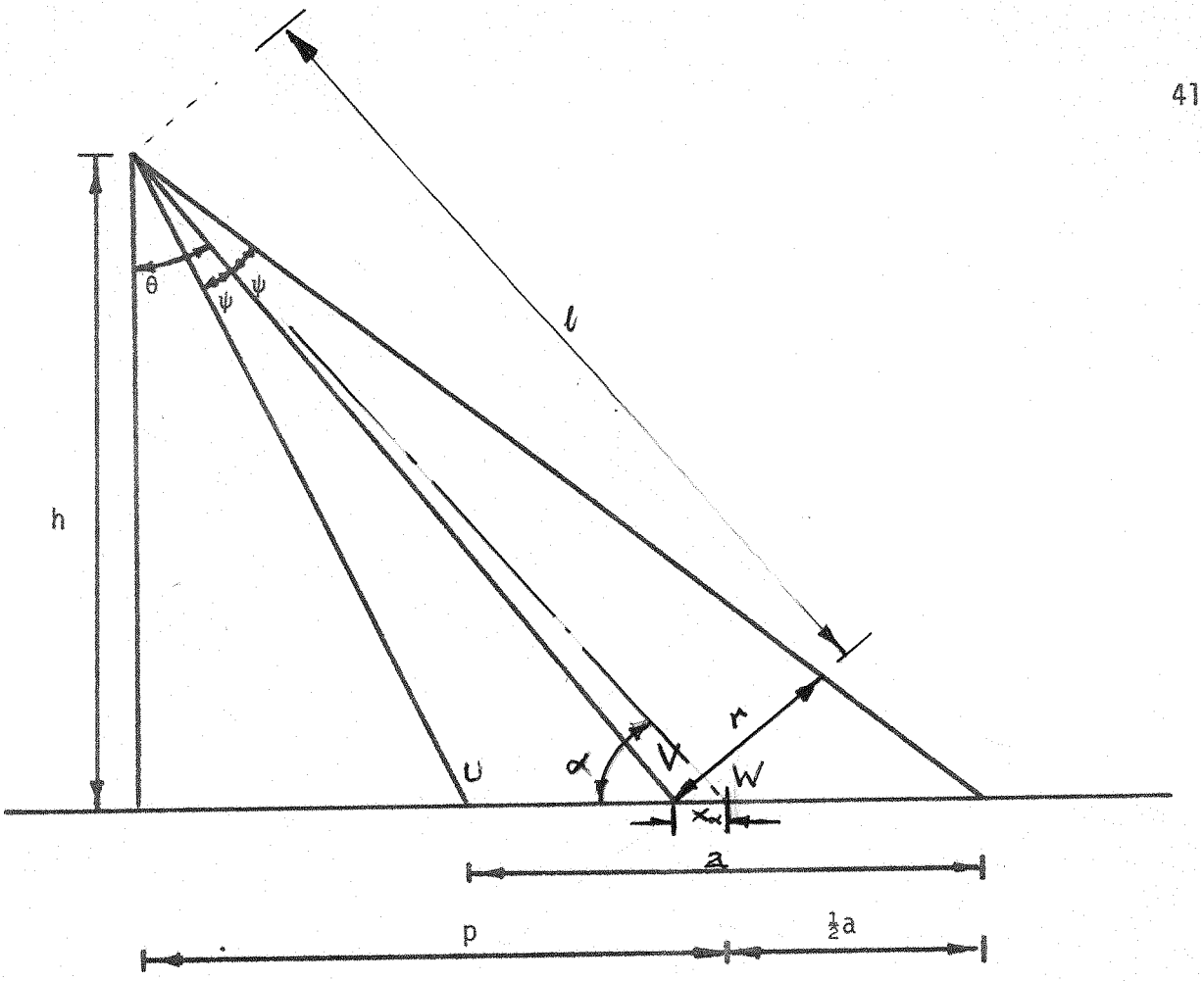

FIGURE 2.17 MAJOR PARAMETERS OF THE CONE

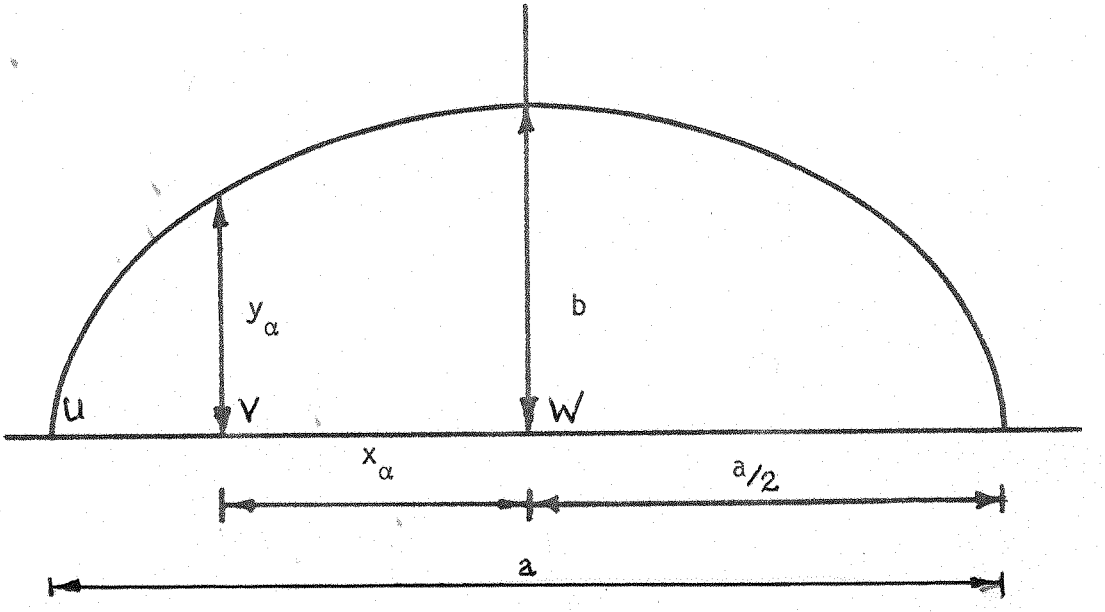

FIGURE 2.18 MAJOR PARAMETERS OF THE ELLIPSE

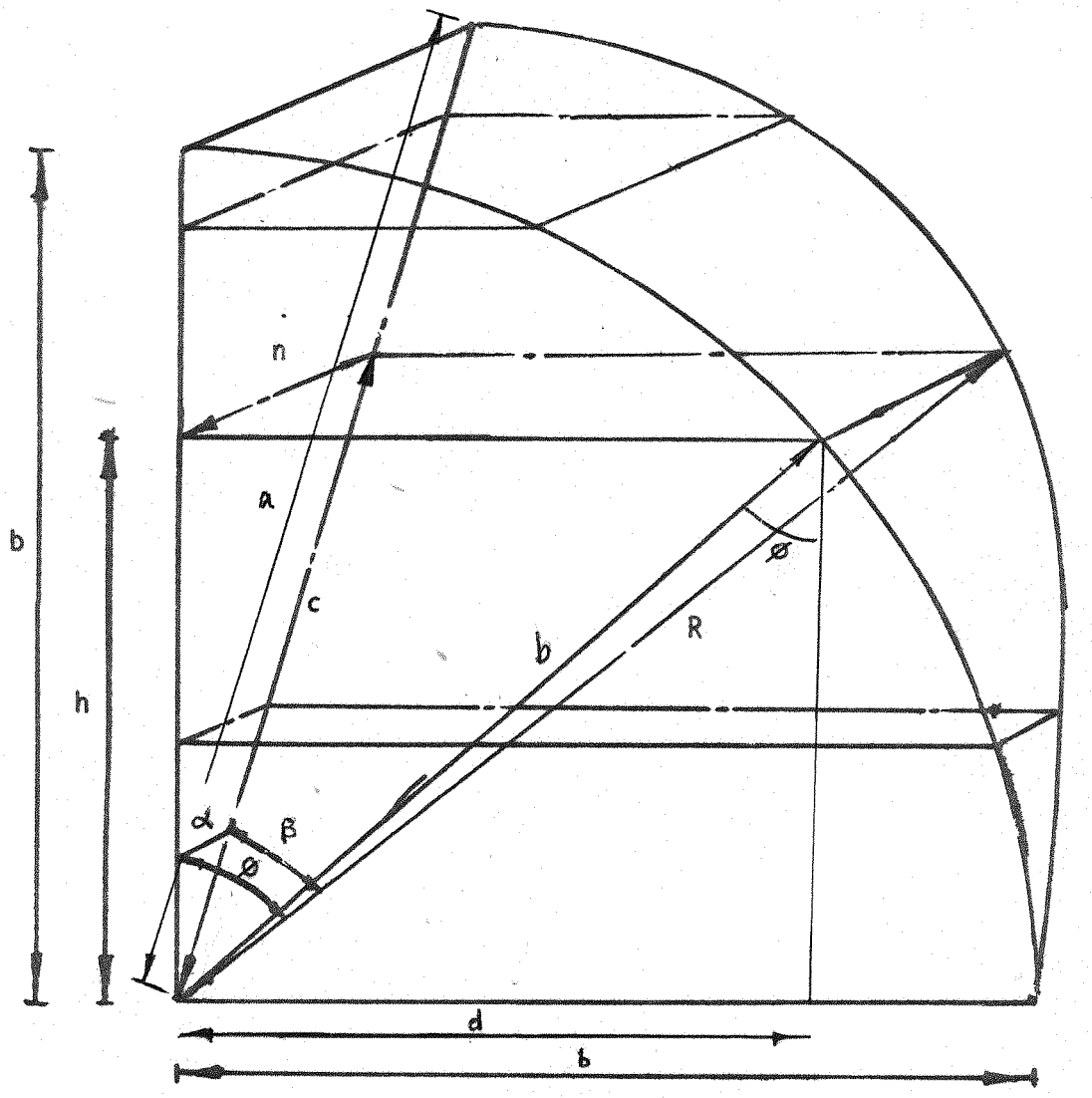

FIGURE 2.19 PARAMETERS USED IN THE CALCULATION OF THE EFFECTIVE RADIUS OF AN ELLIPSE

of measurement can be adjusted to give the required accuracy.

Consider a general point on the curve (i, y_i) where i is an integer and is the present value of x, and y_i is the value of y corresponding to x = i.

The next value of i will be i-1

The next value of i^2 will be $(i-1)^2 = i^2 - (2i-1)$

Noting that $y_i^2 = -ki^2 + b^2$, we see that the next value of y^2, namely y_{i-1}^2 will be given by

$$\begin{aligned} y_{i-1}^2 &= -k\,(i-1)^2 + b^2 \\ &= -k\,(i^2 - (2i-1)) + b^2 \\ &= -k\,i^2 + b^2 + k(2i-1) \\ &= y_i^2 + k(2i-1) \end{aligned}$$

This recursive equation can be made the basis of an approximate ellipse plotting routine. At any point the next value of i may be found by decreasing i by 1. The next value of y^2 namely y_{i-1}^2 may be found from the current value of y^2, namely y_i^2, i and k. This may be done using a square root routine, but this exact solution is unnecessary and an approximation may be used by obtaining j as the nearest integer. The routine shown in figure (2.21) (which would be implemented in machine code to acrue the speed advantage gives the required value of y.

We note that as the arc from x = a to x = 0 is traversed y and hence y^2 increases. The squares of the integers, starting from zero are taken by means of simple addition and shift operations using the formula $(a+1)^2 = a^2 + (2a + 1)$, and their squared values compared to those of y_{i-1}^2. The value of y_{i-1} corresponding to y_{i-1}^2 is taken to be the integer whose squared value just exceeds y_{i-1}^2.

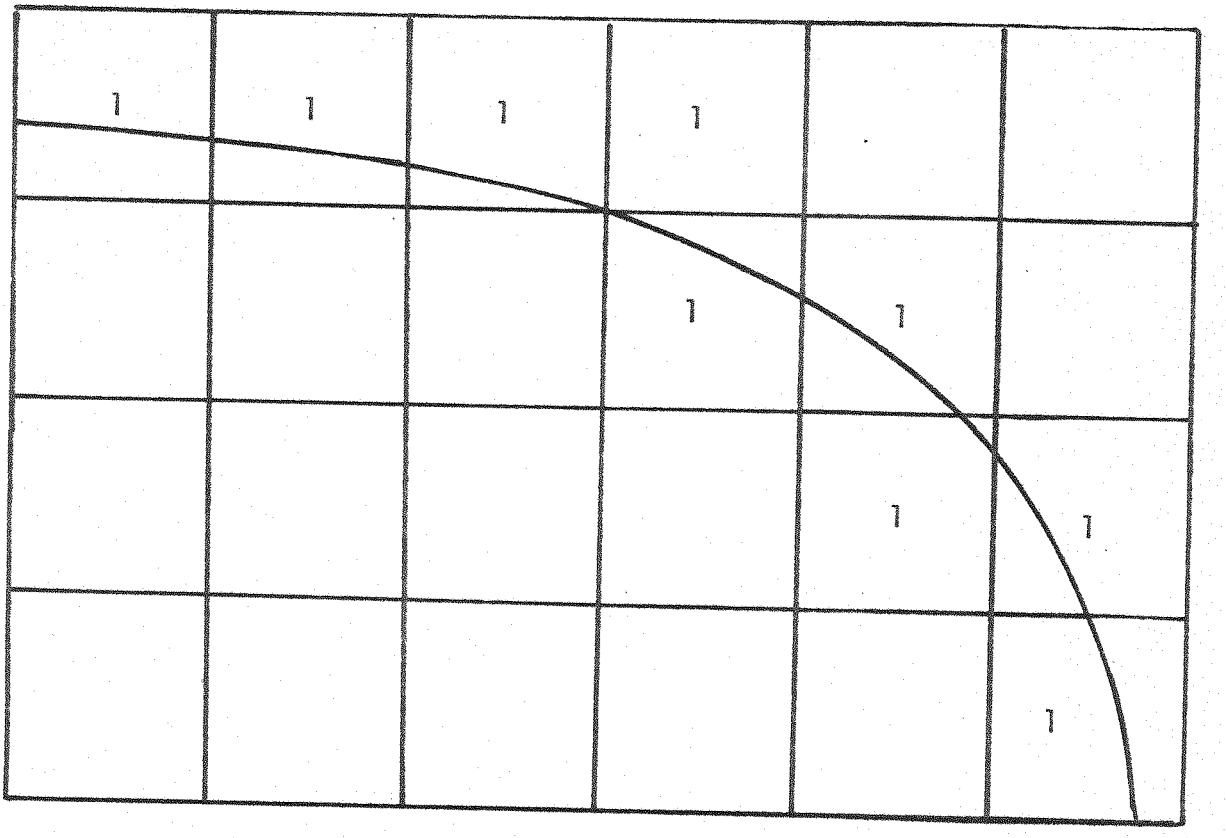

FIGURE 2.20 PLOTTING AN ELLIPSE BY THE APPROXIMATE METHOD, XAXIS PARALLEL TO MAJOR AXIS

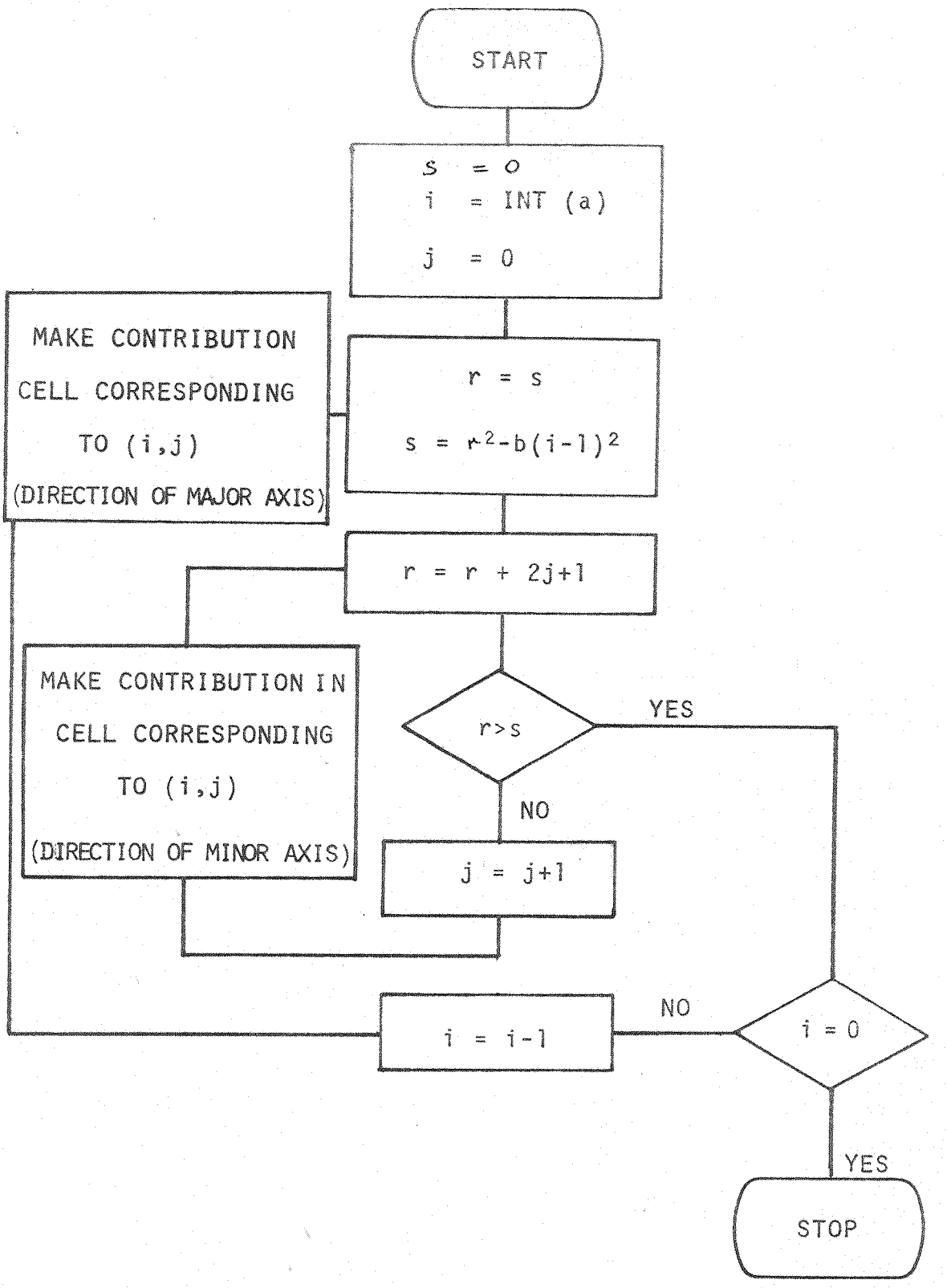

FIGURE 2.21 FLOW CHART TO PLOT ELLIPSE USING APPROXIMATE SQUARE ROOT METHOD

This algorithm may be modified to give a very efficient method of plotting ellipses aligned in any arbitrary position. A contribution in the direction of the minor axis is given every time the inner loop of figure (2.21) is traversed, and a contribution in the direction of the major axis is produced every time the outer loop is traversed.

The contribution in the image grid directions corresponding to contributions parallel to the major and minor axes are easily found using the rotation matrix

$$\begin{bmatrix} \alpha \\ \beta \end{bmatrix} = \begin{bmatrix} \cos\theta & \sin\theta \\ -\sin\theta & \cos\theta \end{bmatrix} \begin{bmatrix} u \\ v \end{bmatrix}$$

where α,β are the contributions in the image grid directions, u,v are unit lengths in the x and y directions corresponding to the major and minor axes of the ellipse, and θ is the angle between the grid side and the major axis.

An example of ellipse plotting using this method is shown in figures (2.22) and (2.23). It can be seen that by varying the ratio of the grid size to the step length that it can be made certain that a contribution will be made in every grid square through which the ellipse passes. Other conic sections hyperbolas and parabolas may be plotted using slight modifications to the above algorithm, these modifications have been analysed,(Fit),but since the ellipse is the most common conic section to occur due to the predominance of Compton collisions with small deflection angles ψ_1, and arguably the best scheme for a practical camera would be to disregard those collisions resulting in hyperbolas or parabolas in the image plane, the resulting algorithms are not presented here.

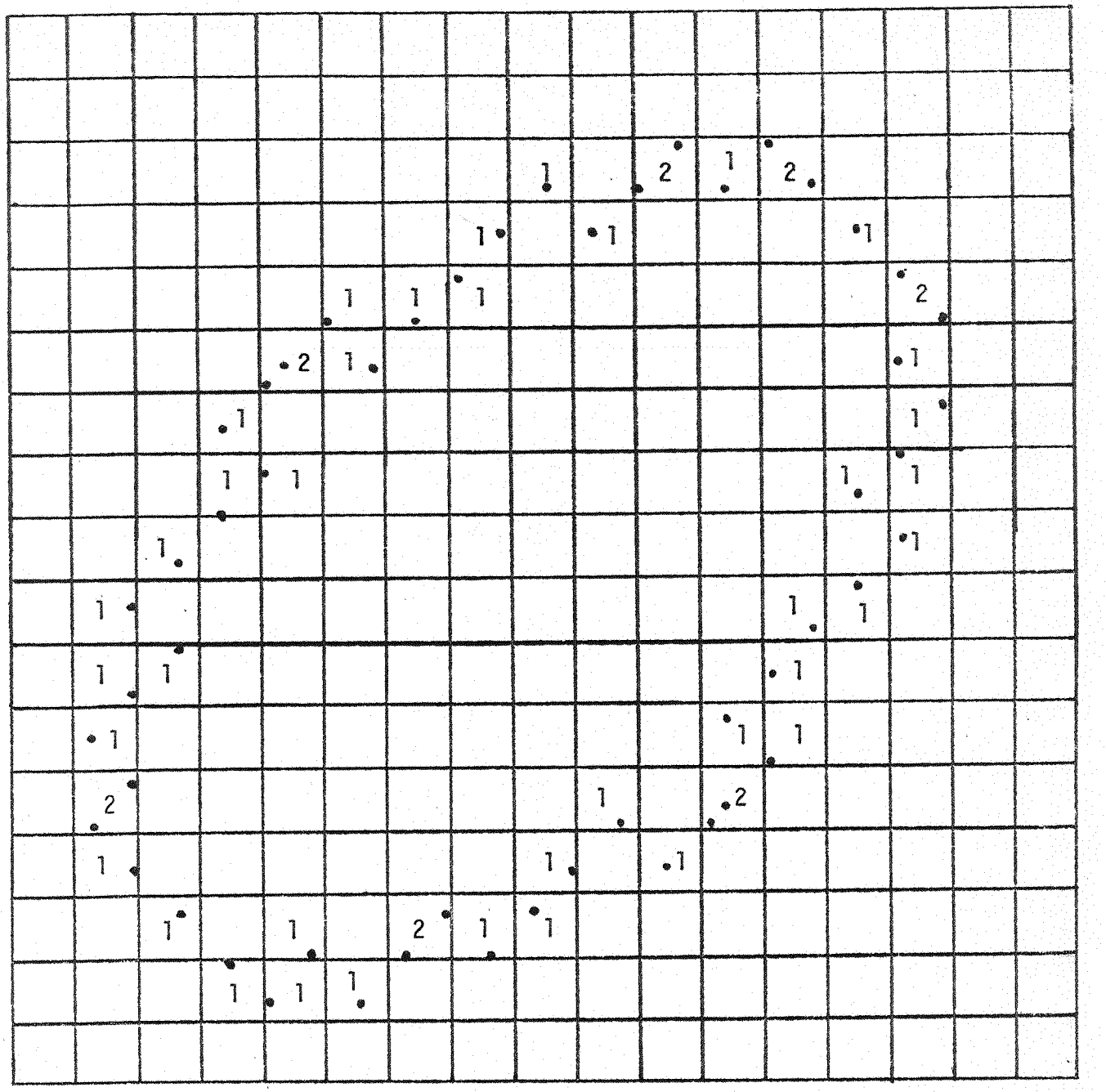

FIGURE 2.22 COPY OF COMPUTER PRINTOUT OF TYPICAL ELLIPSE PLOTTED BY APPROXIMATE METHOD. RATIO OF GRID SIZE TO STEP LENGTH IS 1. NUMBERS REPRESENT NUMBER OF POINTS PER GRID SQUARE

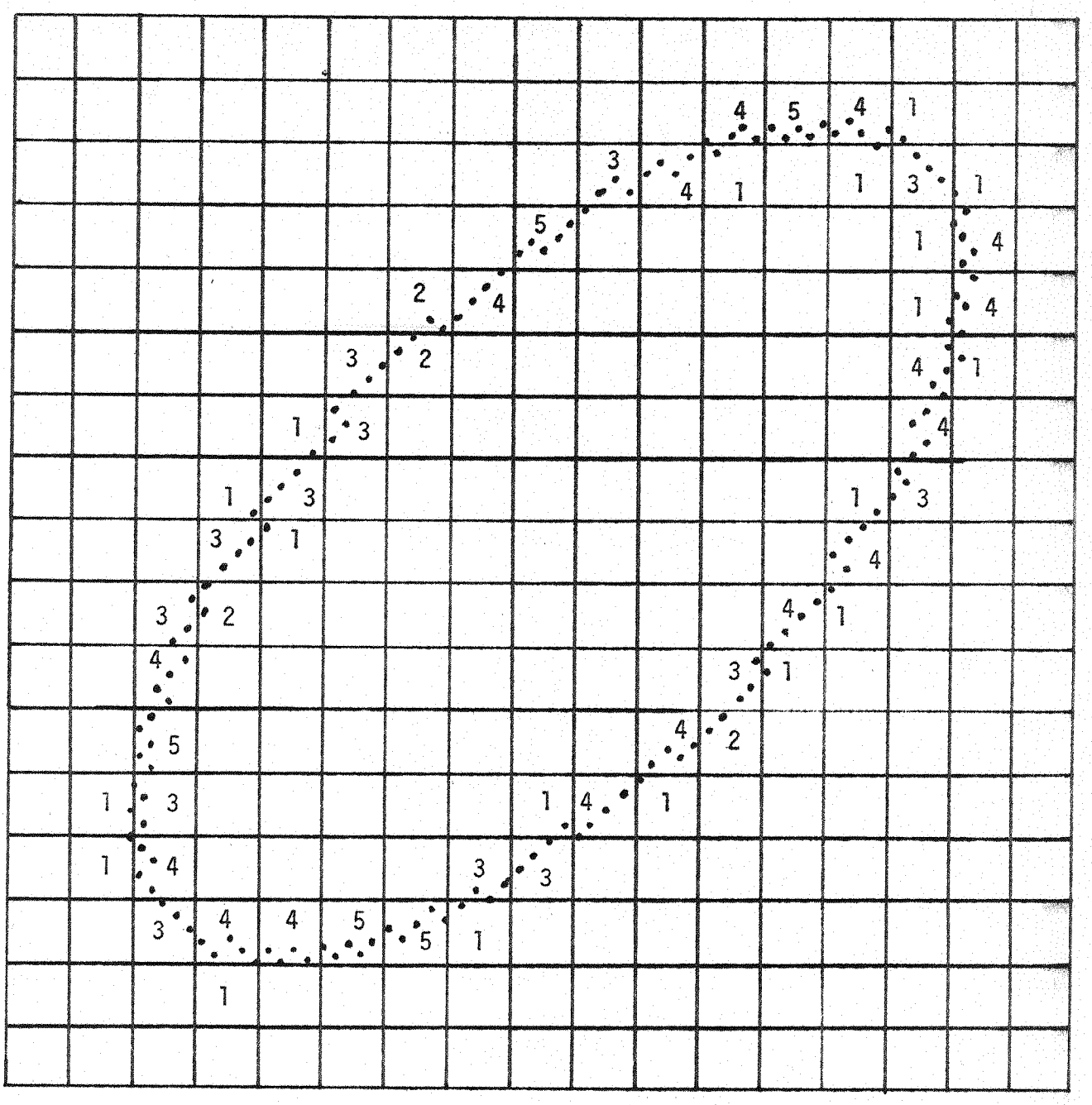

FIGURE 2.23 COPY OF COMPUTER PRINTOUT OF TYPICAL ELLIPSE PLOTTED BY APPROXIMATE METHOD. RATIO OF GRID SIZE TO STEP LENGTH 3 NUMBERS REPRESENT NUMBER OF POINTS PER GRID SQUARE.

Conclusion

Various methods of detection of radiation have been surveyed and one method relying upon the Compton Effect, a process which occurs readily with radiation in the energy range produced by most important isotopes, has been singled out as having special potentialities. These are response to very low quantities of radioactive tracer, dispensing with the large cumbersome lead collimator present in most other detector systems, and also some degree of 3.D resolution.

The computational problems preculiar to this system have been outlined, and algorithms proposed which would go some way to enabling images to be produced in times compatible with other systems.

CHAPTER 3

THE IDENTIFICATION OF THE EXTRACTION EFFICIENCIES OF ORGANS OF THE BODY USING RADIOACTIVE TRACERS

Introduction

Radioactive tracers are commonly used to visualise the liver and spleen, the kidneys, and the biliary system. Radioactive compounds are used which emulate the action of naturally occurring substance. These may be visualised either by 'static' or 'dynamic' images, a static image being the totalised image of all radiation emanating from the object for the duration of the scan, dynamic scans being a set of scans taken from the same orientation, the latter enabling changes in emission rate to be observed. Static scans are usual except in the case of the kidneys where the use of dynamic scans enable a measure of the mean transit time between the kidneys and bladder to be computed.

It is of interest to obtain a measure of the extraction efficencies of each organ. In this chapter present techniques are outlined, and it is shown how estimation techniques can be used to improve the reliability of the results, and in some cases obtain results unobtainable by deterministic methods.

Liver Spleen and Bone Marrow System

Introduction

The liver spleen and bone marrow all contain reticuloendothelial cells which extract particles lying especially in the range 10 - 100 nm. Over the past thirty years various methods have been employed to determine estimates of the rates at which these particles are extracted. Radio-

colloid methods have tended to oust chemical methods, and we will concentrate on the determination of estimates of radiocolloid clearance. This was first attempted using blood clearance curves (Dob 1), (Pla). In 1952 Dobson et al (Dob 2) used serial blood sampling and ^{32}P labelled chromic phosphate. More recently external counting techniques have been used (Chr). Colloidal radiogold ^{198}Au was used in 1954 by Vetter et al (Vet) and ^{131}I labelled human serum alubim in 1958 by Biozzi (Bio). $^{99}Tc^{m}$ sulphur colloid, the method being first described by Mundschenk et al (Mun) in 1971, is now used widely in conjunction with Anger type nuclear cameras.

Modelling of the factors influencing the colloid clearance is complicated since the rate is dependent upon both the hepatic blood flow and the extraction efficiency of the colloid (Bra). The colloidal clearance rate is useful only as an indication of liver blood flow, and parameters more indicative of actual flow rates are required, however the parameter has been shown to be of use in the detection of cirrhosis where values are considerably reduced (Tap). A model showing the contributing effects of blood flow and extraction efficiency the liver, spleen and bone marrow has been developed by Miller et al (Mil) and corroborates this evidence. The colloidal clearance rate was found to be useful in the detection of cirrhosis, but not useful as an indicator of non-cirrhotic liver disease, nor of secondary tumours of the liver, the clearance rate in these cases being indistinguishable from normal.

Attempts to estimate the extraction rates of the liver and spleen as opposed to the hepatic clearance rate have been made by Karren et al (Kar) and DeNardo et al (DeN). These are of especial interest since increased uptake of the spleen relative to the liver determined by

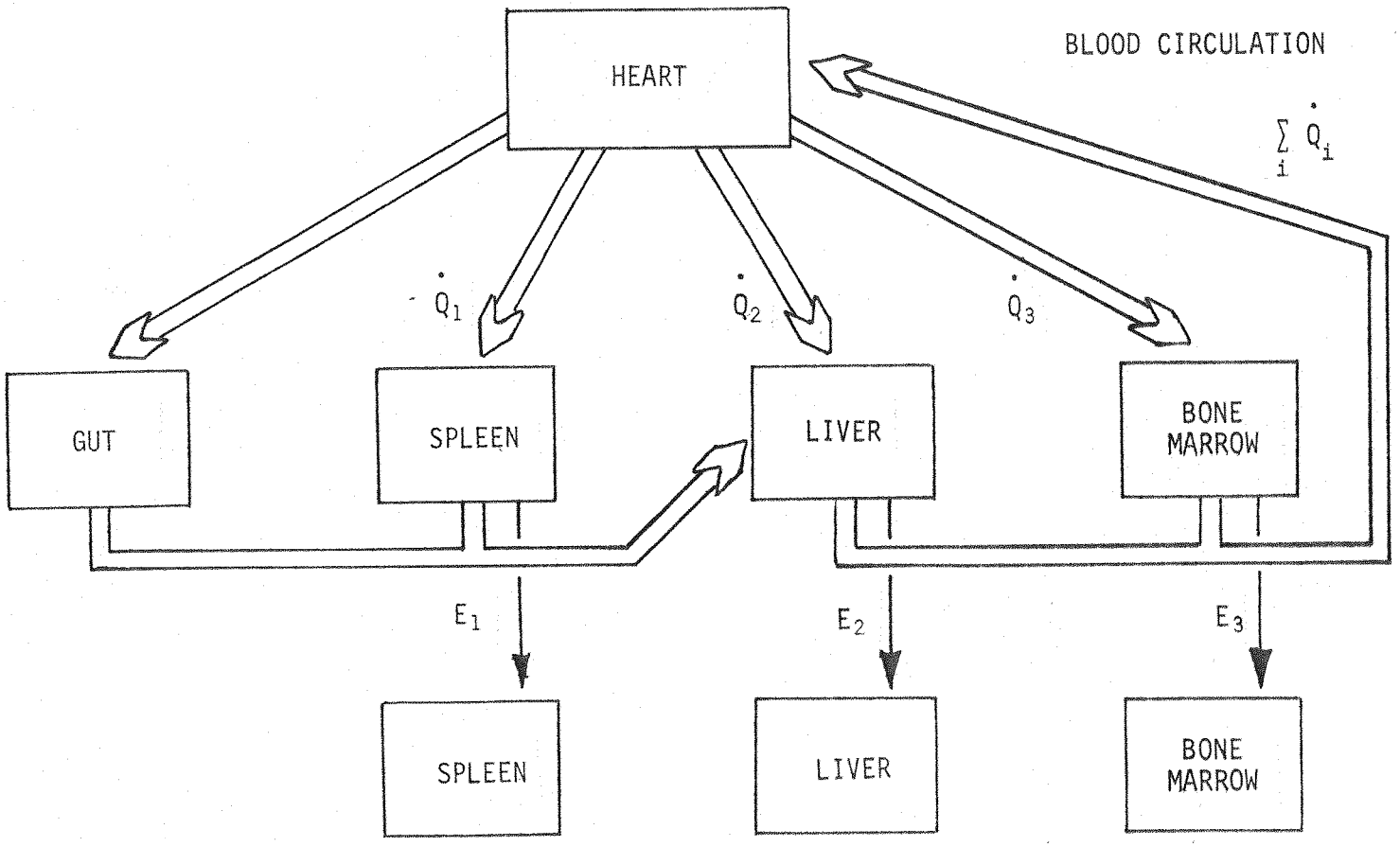

FIG 3.1. EXTRACTION OF $^{99}Tc^{m}$ - SULPHUR COLLOID BY LIVER, SPLEEN AND BONE MARROW

visual inspection of the scan has been correlated with cirrhosis, carcinoma, anemia and diabetes mellitus (Wil), while decreased splenic uptake has been correlated with reticuloendothelial and hematopoietic neoplasia (Wil), (Bek). Karen et al applied the exponential fit routines of Miller et al to determine the extraction rates for the rat, While De Nardo et al used a parameter estimation technique utilising a Gauss Newton iterative process. The latter produced measurements of the hepatic, extrahepatic and splenic rates, which it was claimed, allowed the differential diagnosis of cirrhosis and hepatitis. In neither of these latter cases did the model take account of the partial clearance of colloid in the portal vein by the spleen.

In the following section the model of Miller et al is developed to give expressions for the intensities of radio colloid in the liver and spleen in terms of the relavent extraction efficiencies and blood flows. It is shown how the extraction efficiencies may be determined from the results of a dynamic liver scan using the deterministic method of Karen et al, and how the Snyder Filter may be used to determine an estimate of these efficiencies with improved accuracy.

Mathematical Model

Colloid injected into a venous return, commonly in the arm, will be transported around the body as indicated in block diagram form in Figure 3.1. A small fraction is extracted by the bone marrow. Studies on rats have indicated that the smallness of this fraction is not due to low blood flow, which contrarily is thought to be quite large, but due to the low extraction efficiency of the bone marrow. The main extraction takes place in the liver which is supplied both by a direct feed, the hepatic artery and also via either the spleen or the gut.

Further extraction takes place in the spleen which reduces the concentration of colloid in the portal vein.

Let the volume flows to the Gut, Spleen and Bone Marrow be denoted $\dot{Q}_0$, $\dot{Q}_1$ and $\dot{Q}_3$ respectively, and the direct supply to the liver through the hepatic artery $\dot{Q}_2$

Let the extraction rates of the colloid to the spleen, liver and bone marrow be E_1, E_2 and E_3 respectively.

The quantity of colloid extracted at any moment from an organ is related to the concentration of the colloid and the extraction rate by the equation

$$\frac{dq}{dt} = -EC \quad \text{or} \quad \frac{dq}{dt} = \frac{-Eq}{v} \qquad 3.1$$

Where

q = quantity of colloid in blood

E = the extraction rate

C = the concentration of the colloid

V = the volume of blood in the organ

If an organ of blood volume V is supplied with a blood flow $\dot{Q}$, then the extraction of colloid causes a reduction in the concentration of colloid in the blood leaving the organ.

Equating colloid entering and leaving the organ we obtain

Colloid entering in blood supply = Colloid extracted by R.E. cells + colloid leaving via blood supply

$$dq_{in} = dq_{ext} + dq_{out}$$

$$\dot{Q}\, C_{in}\, dt = E\, C_{in}\, dt + \dot{Q}\, C_{out}\, dt$$

$$Cin\, [\dot{Q}-E] = \dot{Q}\, C_{out}$$

$$C_{out} = C_{in}\, [1-E/\dot{Q}] \qquad 3.2$$

If two blood flows of colloid concentration C_1, C_2 and volume flow $\dot{Q}_1$, $\dot{Q}_2$ combine then the resultant flow will have colloid concentration C_3 given by

$$C_3(\dot{Q}_1 + \dot{Q}_2) = C_1 \dot{Q}_1 + C_2 \dot{Q}_2$$

$$C_3 = (C_1 \dot{Q}_1 + C_2 \dot{Q}_2)/(\dot{Q}_1 + \dot{Q}_2) \qquad 3.3$$

With these preliminary statements the equations governing the extraction of colloid as shown in Figure 3.1 may be written by inspection.

Let the concentration of colloid in the blood entering the spleen be C_0 and that leaving the spleen be C_1. Let the extraction efficiency of the spleen be E_1 and the flow in the portal vein $\dot{Q}_1$ then the concentration leaving the spleen is given by

$$C_1 = C_0 [1-E_1/\dot{Q}_1] \qquad 3.4$$

The concentration of the colloid entering the liver C_2 is given by the resultant concentration of the direct feed through the hepatic artery and the feeds via the gut and spleen. It is given by the expression

$$C_2 = \frac{C_1 \dot{Q}_1 + C_0 (\dot{Q}_0 + \dot{Q}_2)}{\dot{Q}_0 + \dot{Q}_1 + \dot{Q}_2} \qquad 3.5$$

We see that the extraction equations giving the changes in concentration in the blood, spleen, liver and bone namely $\dot{q}_0$ $\dot{q}_1$ $\dot{q}_2$ and $\dot{q}_3$ are given by

$$\frac{dq_0}{dt} = -[E_1 C_0 + E_2 C_2 + E_3 C_0]$$

$$\frac{dq_1}{dt} = E_1 C_0$$

$$\frac{dq_2}{dt} = E_2 C_2$$

$$\frac{dq_3}{dt} = E_3 C_o \qquad 3.6$$

to solve these equations we use the relationships between the concentrations and intensities to give a set of equations solely in terms of the intensities. We use the relationships.

$$C_2 = \frac{C_o\{[1-E_1/\dot{Q}_1]\dot{Q}_1 + \dot{Q}_o + \dot{Q}_1\}}{\dot{Q}_o + \dot{Q}_1 + \dot{Q}_2}$$

$$= \frac{C_o\{2\dot{Q}_1 + \dot{Q}_o - E_1\}}{\dot{Q}_o + \dot{Q}_1 + \dot{Q}_2} \qquad 3.7$$

and

$$C_o = q_o/V_o \qquad 3.8$$

where V_o is the total blood volume.

Hence

$$\frac{dq_o}{dt} = \frac{-q_o}{V_o}\left[E_1 + E_3 + E_2\{2Q_1 + \dot{Q}_o - E_1\}/\dot{Q}_o + \dot{Q}_1 + \dot{Q}_2\right]$$

$$\frac{dq_1}{dt} = E\, q_o/V_o$$

$$\frac{dq}{dt} = E_2\, q_o\left[2\dot{Q}_1 + \dot{Q}_o - E\right] / \left[\dot{Q}_o + \dot{Q}_1\, \dot{Q}_2\right] V_o$$

$$\frac{dq_3}{dt} = E_3\, q_o/V_o \qquad 3.9$$

This may be written in matrix form:

$$\frac{d}{dt}\begin{bmatrix} q_0 \\ q_1 \\ q_2 \\ q_3 \end{bmatrix} = \begin{bmatrix} -(R_1 + R_2 + R_3) & & & \\ R_1 & 0 & & \\ R_2 & & 0 & \\ R_3 & & & 0 \end{bmatrix} \begin{bmatrix} q_0 \\ q_1 \\ q_2 \\ q_3 \end{bmatrix} \qquad 3.10$$

where

$$R_1 = E_1/V_0 \qquad 3.11$$

$$R_2 = \frac{E_2 \, |2\dot{Q}_1 + \dot{Q}_0 - E_1|}{(\dot{Q}_0 + \dot{Q}_1 + \dot{Q}_2)\, V_0} \qquad 3.12$$

$$R_3 = E_3/V_0 \qquad 3.13$$

This matrix equation may be converted to diagonal form

$$\frac{d}{dt}\begin{bmatrix} q_0 \\ q_1 - \frac{R_1}{R} q_0 \\ q_2 - \frac{R_2}{R} q_0 \\ q_3 - \frac{R_3}{R} q_0 \end{bmatrix} = \begin{bmatrix} -(R_1 + R_2 + R_3) & & & \\ & 0 & & \\ & & 0 & \\ & & & 0 \end{bmatrix} \begin{bmatrix} q_0 \\ q_1 - \frac{R_1}{R} q_0 \\ q_2 - \frac{R_2}{R} q \\ q_3 - \frac{R_3}{R} q \end{bmatrix} \qquad 3.14$$

where $$R = R_1 + R_2 + R_3 \qquad 3.15$$

The solution to this can be seen to be

$$q_0 = \exp(-Rt)\, q(0) \qquad 3.16$$

$$q_1 = \frac{R_1}{R} q_0 = \text{const} = q_1(0) + \frac{R_1}{R} q_0$$

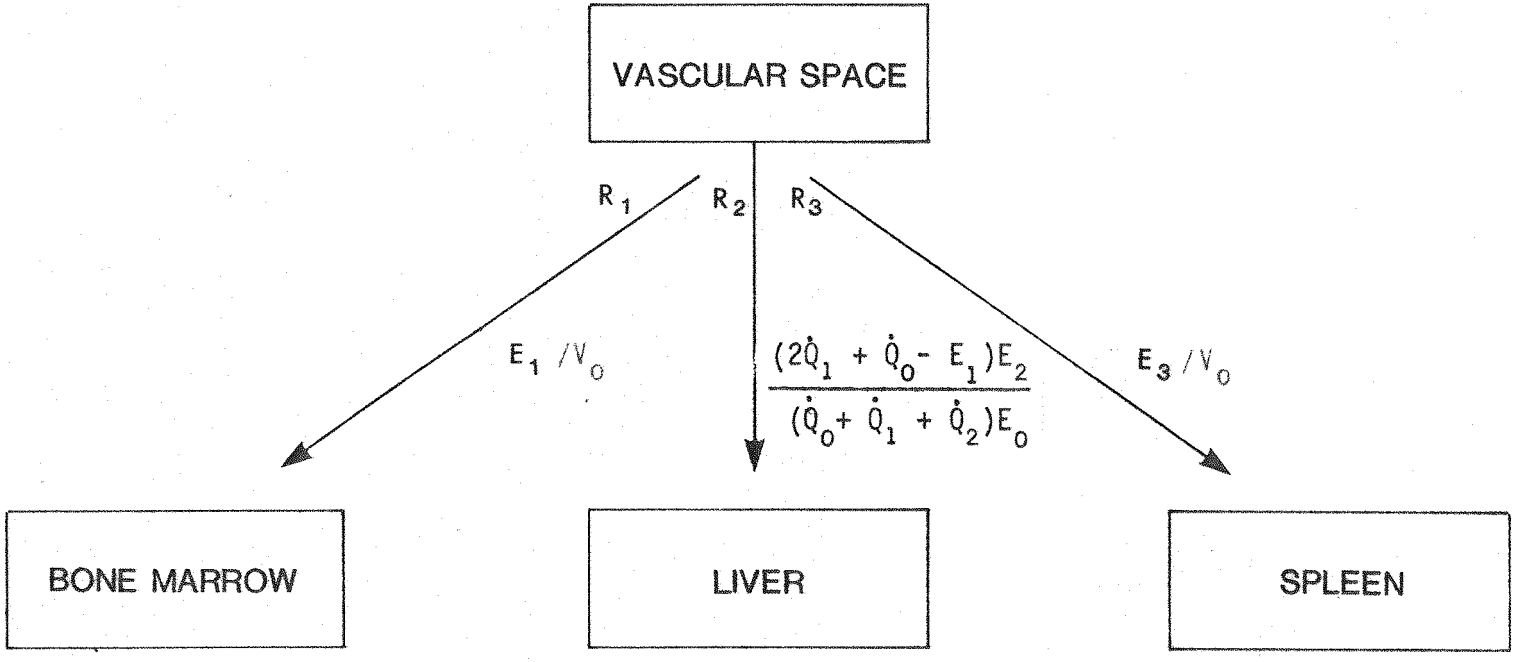

FIGURE 3.3 R_2 INCLUDES CONTRIBUTION FROM GUT AND SPLEEN.

EFFECTIVE EXTRACTION OF $^{99}Tc^{m}$ COLLOID TO LIVER, SPLEEN AND BONE MARROW

$$\therefore \quad q_1 = \frac{R_1}{R} [q_0(0) - q_0]$$

$$q_1 = \frac{R_1}{R} [1 - \exp(-Rt)] q_0(0) \qquad 3.17$$

and similarly

$$q_2 = \frac{R_2}{R} [1 - \exp(-Rt)] q_0(0) \qquad 3.18$$

$$q_3 = \frac{R_3}{R} [1 - \exp(-Rt)] q_0(0). \qquad 3.19$$

where we have used the initial conditions

$$q_1(0) = q_2(0) = q_3(0) = 0 \qquad 3.20$$

We see that the spleen liver and bone marrow have extraction curves of the form shown in Figure 4.5 and that we may postulate a flow model Figure 3.3 with overall extraction rates R_1, R_2, R_3.

Extraction curves obtained from a dynamic scan taken for 20 minutes, using $^{99}Tc^m$ labelled with liocoll are given in Chapter 4. Curves are shown only of the liver and spleen.

It is seen that the liver spleen and bone marrow curves all rise exponentially with the same time constant, $\frac{1}{R}$, and reach plateau values proportional to the extraction rates.

We now outline the method of Karen et al (Kar) to show how using the model of Miller et al (Mil) we may determine the extraction rates.

Determination of Extraction Rates using exponential fitting techniques

An Anger camera is positioned so that the liver and spleen are in the field of view, a posterior view is suitable for this, and gives good spatial separation on the resultant image. $^{99}Tc^m$ labelled sulphur colloid, or better milli-microspheres the particles of the latter having a more uniform size, are injected and a dynamic scan

started immediately and images taken for fifteen to twenty minutes with frames being taken every fifteen seconds.

At the end of the scan a totalised image can be created, regions of interest defined, and time activity curves displayed using standard programs supplied by manufactures of nuclear medicine data systems (Link, Dec, MDS. etc). Time constants and plateaux of the liver and spleen curves may then be obtained using standard exponential fit and averaging techniques. A listing of a FORTRAN program to be run in conjunction with data produced by the MED program of a Link data system. Dyanne computer system is given in Appendix F. The program gives directly the total extraction rate and calculates the liver and spleen extraction rates, R_1 and R_2 by simple division.

We may now use equations 3.11, 3.12 and 3.13 to determine the extraction rates E_1, E_2 and E_3. We note that in 3.11 and 3.13 the extraction rate, or clearance as it is more normally expressed is obtained by multiplying the rate constant by the dilution volume.

Clearance = Rate constant . Volume

As the time volume of the blood is unknown the method of DeNardo (DeN) may be used by incorporation of a factor of 100 into the rate constants to express the clearance in units of ml/mm per 100ml of dilution, and to express the dilution volume in units of 100 ml.

This gives values for

$$E_1 \quad , \quad \frac{E_2\,[2\dot{Q}_1 + \dot{Q}_o - E_1]}{\dot{Q}_o + \dot{Q}_1 + \dot{Q}_2} \quad \text{and } E_3$$

To obtain a value for E_2 assumptions of the blood flows $\dot{Q}_o$, $\dot{Q}_1$, $\dot{Q}_2$ must be made in the absence of further measurements. Cowles et al (Cow)

---

† Fortran Coding supplied by John Fleming of Southampton University Hospital.

quote a flow of 841 ml/min/m^2 for flow to splanchnic tissue and a flow of 595 ml/min/m^2 to the bone marrow

ie. $\dot{Q}_0 + \dot{Q}_1 = 841$ ml/min/m^2

$Q_3 = 595$ ml/min/m^2

The mean rest portal vein blood flow measured by local thermal dilution was reported as 500 ml/min (Cot) which using figures of 1.8 m^2 surface area of man gives portal vein flow of 277 ml/min/m^2. We may thus write

$\dot{Q}_1 = 277$ ml/min/m^2

The total liver flow has been reported as 1500 ml/min/m^2 (Map), hence we have the expression

$\dot{Q}_0 + \dot{Q}_1 + \dot{Q}_2 = 1500$ ml/min/m^2

Any actual patient will not have the above values especially if suffering from a disease such as cirrhosis which affects the blood flow to the organs. The above values are also suspect since they are derived from the results of different workers in the field. We therefore round the figures to ones conve nently near the correct ones and make

$\dot{Q}_0 = 500$ ml/min/m^2

$\dot{Q}_1 = 500$ ml/min/m^2

$\dot{Q}_3 = 500$ ml/min/m^2

$\dot{Q}_4 = 500$ ml/min/m^2

Any differences in the flow values used to those occurring in the patient will be reflected in the extraction rates contained by the algorithm.

The values above may be multiplied by

100/{Blood Volume . Body Surface Area}

to obtain limb of ml/min/100 ml dilution.

To give

$$Q_o = \frac{500 \times 1.8}{5400} = .6 \text{ ml/min/100 ml dilution}$$

Similarly

$$\dot{Q}_1 = \dot{Q}_2 = \dot{Q}_3 = \dot{Q}_4 = .6 \text{ ml/min/100 ml dilution}$$

Substituting these values in the expression for the second extraction rate we obtain

$$R_2 = \frac{E_2 [2\dot{Q}_1 + \dot{Q}_o - E_1]}{\dot{Q}_o + \dot{Q}_1 + \dot{Q}_2} = \frac{E_2 [1.8 - E_1]}{1.8}$$

and hence with the above assumed values E_2 may be determined by the substitution of the first estimated extraction rate $R_1 = E_1$ into the above expression.

Application of the Snyder Filter to give estimates of the flow rates with improved accuracy.

The results of the previous section enable the state and measurement equations for the Snyder Filter to be written by inspection

The rates R_1 to R_3 are constants hence satisfying the state equation

$$\frac{d}{dt} R_1 = \frac{d}{dt} R_2 = \frac{d}{dt} R_3 = 0 \qquad 3.21$$

If measurements are taken of the liver and spleen intensities, poisson rates will be

$$\lambda_1 = \frac{R_1}{R} [1 - \exp Rt] q_o(0) \qquad 3.22$$

$$\lambda_2 = \frac{R_2}{R} [1 - \exp Rt] q_o(0) \qquad 3.23$$

If measurement of the uptake of radiocolloid into the bone is recorded then we have a third measurement

$$\lambda_3 = \alpha \frac{R_3}{R} \left[1 - \exp Rt\right] q_0(0) \qquad 3.24$$

where α is the ratio of the observed bone mass to the total bone mass. This latter measurement is required only if the clearance rate to the bones is required.

These equations are in the form required for the application of the filtering equations, equation (1.12). Comparisions are made of the results obtained by this and the exponential curve fit method in the next chapter.

Practically two methods could be used to obtain the required data, either the data could be stored on magnetic disk, regions of interest formed after the recording and offline processing. Alternatively a method similar to that of DeNardo could be performed. Two radiocolloids are used, one traced with $^{99}Tc^m$ and the other with ^{198}Au one to position the camera and define the regions of interest, the second to determine the extraction rates the latter technique allowing the possibility of on-line processing. Disadvantages exist with both techniques, the first requiring large amounts of data storage, since the data would need to be recorded in a serial or 'LIST' mode in which each count is recorded together with its x and y position and the required information of the number of collisions in each time interval given by time markers. The first method would also increase the time before the result could be obtained. The second method would increase the radioactive dose and would be more cumbersome to administer since two isotopes would need to be administered at different times.

The Kidney Bladder System

Introduction

Renal scintigraphy and the determination of quantitative measurements describing the performance of the kidneys are both of great value in the evaluation and follow up of patients with renal disease. The most common quantitative renal measurement is the glomerular filtration rate (G.F.R). A common procedure to determine this is to inject ^{51}Cr-chromate and then to use the blood clearance curves obtained from blood samples taken over three hours. The Chromate during this time does not stay in the vascular space, but flows into, and remains in dynamic equilibrium with, the extravascular space.

A two compartmental system was proposed by Sapirstein et al (Sap) who analysed the system for a dog and used the disappearance curve of creatnine to verify his results. Chantler et al (Cha) compared the glomerular filtration obtained using the results of Sapirstein but using inulin in man with that using ^{51}Cr - chromate using the same method. They also compared the results with those obtained using an analysis using only one compartment, and tailored correction factors, the 'single injection, single exponential' method.

With the advent of $^{99}Tc^{m}$ labelled DTPA, useful for renal scintigraphy Hilson et al (Hil) compared the results using this and ^{51}Cr chromate using Chantlers single exponential method. The results agreed with high correlation, and enabled a dynamic scan and an estimation of glomerular filtration rate to be performed with only one injection of one isotope.

It is necessary in some instances to distinguish between the action of the left and right kidneys. At present very few quantitative

techniques exist for this, qualitative examination of the scans being the norm. To distinguish between the effect of both kidneys more complicated models are required to model the transport of the isotope. Arnold et al (Arn) reported the perfusion of seventeen compounds which have been used in kidney studies, of which three technetium products were recommended, are in common use and are of relevance to this study:

1) Sn-DTPA : This is cleared rapidly by glomerular filtration without tubular resorbtion. It promptly appears in the urine and pelvocalyceal system. Only a small fraction retained in the cortex, (Hiramatsu 1970 (Hir)).

2) GH : A sizeable fraction is promptly excreted to the urine. 6% is retained by each kidney, largely by the cortex, and located intercellularly (Kazem et al (Ka)). Visualisation of delayed images is excellent.

3) DMSA : Urinary excretion is extremely slow. It is excellent for delayed images of parenchyme. It oxidises spontaneously and must be used within six hours of preparation. It has similar characteristics to mercury labelled chloromerodine (Lin et al (Li), Hirst et al (His)).

It can be seen that there are two main mechanisms that of DTPA and that of DMSA, GH being cleared by a mixture of the two. DMSA is cleared by glomerular filtration and is fixed mainly in the cortex, whereas DTPA after clearance by glomerular filtration passes directly to the bladder along drainage tubes. We now analyse these systems and show how the unknown parameters may be determined.

Mathematical Modelling

1. DMSA

A block diagram of the route taken by DMSA is given in Figure 3.4. Using equation 3.1 governing extraction of isotope by a colloid we may directly write the matrix equation describing the time evolution of the intensities in each compartment.

Let the intensity of isotope in the vascular space, extravascular space, left kidney and right kidney by q_0, q_1, q_2 and q_3 respectively and the extraction or clearance rates as shown in Figure 3.4 (r_0, r_1, r_2 and r_3). Then

$$\frac{d}{dt}\begin{bmatrix} q_0 \\ q_1 \\ q_2 \\ q_3 \end{bmatrix} = \begin{bmatrix} -(r_0 + r_2 + r_3)/V_0 & r_1/V_0 & & \\ r_0/V_0 & -r_1/V_1 & & \\ r_2/V_0 & & 0 & \\ r_3/V_0 & & & 0 \end{bmatrix} \begin{bmatrix} q_0 \\ q_1 \\ q_2 \\ q_3 \end{bmatrix} \qquad 3.25$$

Using the method described in Appendix D we may diagonalise this equation to obtain analytical expressions for the intensities in each compartment.

$$\frac{d}{dt}\begin{bmatrix} q_0/r_1V_0 \\ q_1/\varepsilon \\ q_2 \\ q_3 \end{bmatrix} = \begin{bmatrix} \alpha & \varepsilon & & \\ \varepsilon & \beta & & \\ r_1r_2 & & 0 & \\ r_1r_3 & & & 0 \end{bmatrix} \begin{bmatrix} q_0/r_1V_0 \\ q_1/\varepsilon \\ q_2 \\ q_3 \end{bmatrix} \qquad 3.26$$

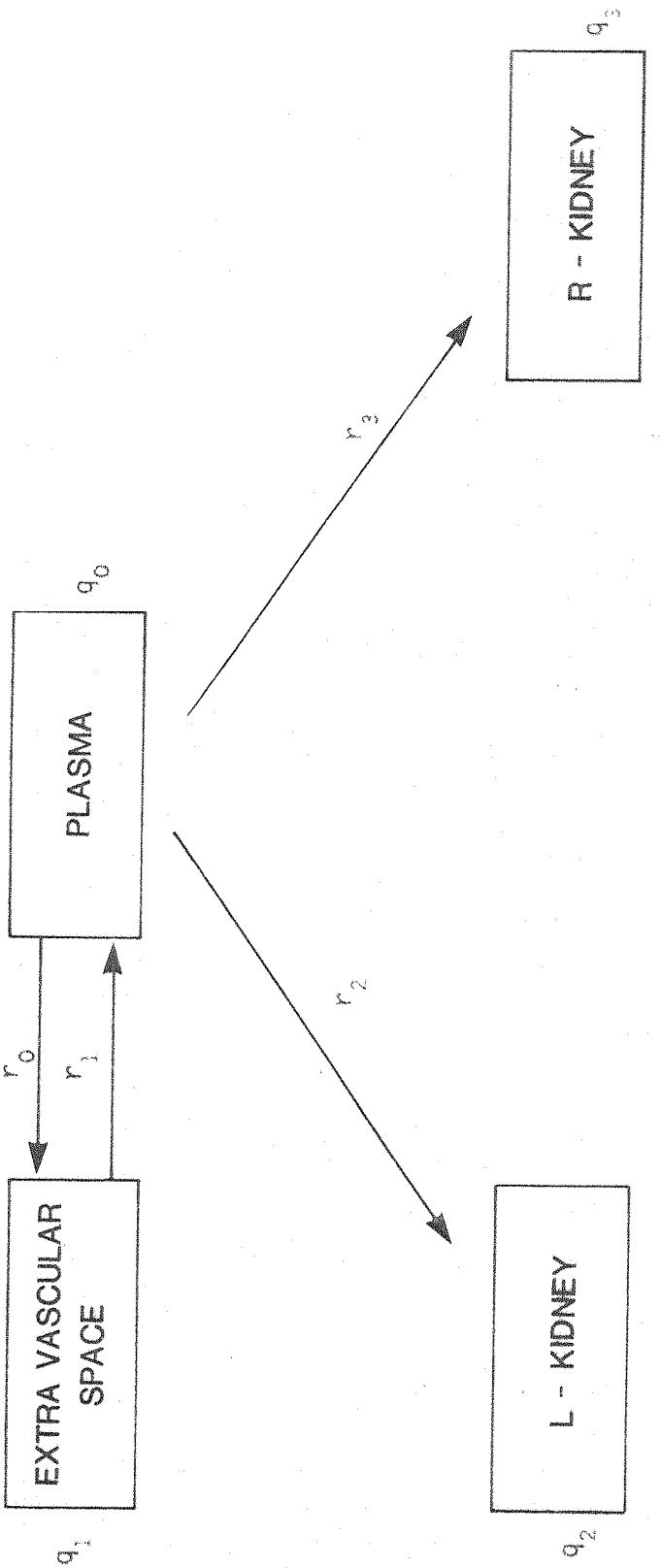

FIGURE 3.4 ROUTE OF $^{99}Tc^m$ LABELLED DMSA THROUGH BODY

where

$$\alpha = -(r_o + r_2 + r_3)\, V_o$$

$$\varepsilon = \sqrt{[r_o\, r_1\, V_o\, V_1]}$$

let

$$Q_o = {}^{q_o}/_{r_1 V_o} + dQ_1 \qquad 3.27$$

$$Q_1 = {}^{q_1}/_{\varepsilon} + cq_o/r_1 V_o \qquad 3.28$$

Then, again with reference to Appendix D:

$$\frac{d}{dt}\begin{bmatrix} Q_o \\ Q_1 \\ q_2 \\ q_3 \end{bmatrix} = \begin{bmatrix} \lambda_1 & & & \\ & \lambda_2 & & \\ r_1 r_2 & -d & 0 & \\ r_1 r_3 & -d & & 0 \end{bmatrix} \begin{bmatrix} Q_o \\ Q_1 \\ q_2 \\ q_3 \end{bmatrix} \qquad 3.29$$

where

$$\lambda_1 = \alpha - c\varepsilon$$

$$\lambda_2 = r_1 + c\varepsilon$$

$$c = \frac{\alpha + r_1 + \sqrt{[(r_1 + \alpha)^2 + 4\varepsilon]}}{2\varepsilon}$$

$$\varepsilon = \sqrt{[r_o\, r_1]}$$

Subtraction of row equations gives

$$\frac{d}{dt}\begin{bmatrix} Q_o \\ Q_1 \\ Q_2 \\ Q_3 \end{bmatrix} = \begin{bmatrix} \lambda & & & \\ & \lambda_2 & & \\ & & 0 & \\ & & & 0 \end{bmatrix} \begin{bmatrix} Q_o \\ Q_1 \\ Q_2 \\ Q_3 \end{bmatrix} \qquad 3.30$$

where

$$Q_2 = q_2 - \frac{r_1 r_2}{\lambda_1} Q_o + \frac{d}{\lambda_2} Q_1 \qquad 3.31$$

$$Q_3 = q_3 - \frac{r_1 r_3}{\lambda_1} Q_o + \frac{d}{\lambda_2} Q_1 \qquad 3.32$$

The solution to this equation is

$$Q_o = \exp\left[- \lambda_1 t\right] + K_o$$

$$Q_1 = \exp\left[- \lambda_2 t\right] + K_1$$

$$Q_2 = \left\{q_2 - \frac{r_1 r_2}{\lambda_1} Q_o + \frac{d}{\lambda_2} Q \right\}\Big|_{t=0}$$

$$Q_3 = \left\{q_3 - \frac{r_1 r_3}{\lambda_1} Q_o + \frac{d}{\lambda_2} Q \right\}\Big|_{t=0} \qquad 3.33$$

Inserting the initial condition that at time t=0 a bolus injection of Q units of radioactive tracer are injected into compartment 1, the vascular space, then

$$q_o(0) = q_2(0) = q_3(0) = 0$$

$$q_1(0) = Q$$

$$Q_o(0) = d\,Q/\varepsilon$$

$$Q_1(0) = Q/\varepsilon$$

$$Q_2(0) = \frac{dQ}{\varepsilon}\left\{\frac{1}{\lambda_2} - \frac{r_1 r_2}{\lambda_1}\right\}$$

$$Q_3(0) = \frac{dQ}{\varepsilon}\left\{\frac{1}{\lambda_2} - \frac{r_1 r_3}{\lambda_1}\right\}$$

$$K_o = \frac{dQ}{\varepsilon} - 1$$

$$K_1 = Q/\varepsilon - 1$$

Hence

$$Q_0 = \exp[-\lambda_1 t] + \frac{dQ}{\varepsilon} - 1$$

$$Q_1 = \exp[-\lambda_2 t] + \frac{Q}{\varepsilon} - 1$$

$$Q_2 = \frac{dQ}{\varepsilon}\left\{\frac{1}{\lambda_2} - \frac{r_1 r_2}{\lambda_1}\right\}$$

$$Q_3 = \frac{dQ}{\varepsilon}\left\{\frac{1}{\lambda_2} - \frac{r_1 r_3}{\lambda_1}\right\} \qquad 3.34$$

from which we may determine q_0, q_1, q_2, q_3 from the relationships

$$q_0 = r_1 [Q_0 - dQ_1]$$

$$q_1 = \varepsilon [Q_1 - c [Q_0 - d Q_1]]$$

$$q_2 = Q_2 + \frac{r_1 r_2}{\lambda_1} Q_0 - \frac{d}{\lambda_2} Q_1$$

$$q_3 = Q_3 + \frac{r_1 r_3}{\lambda_1} Q_0 - \frac{d}{\lambda_2} Q_1 \qquad 3.35$$

Measurements may be made over the left and right kidneys. These will both have 'blood backgrounds' hence will be of the form

$$m_1 = q_2 + K_1 q_1$$

$$m_2 = q_3 + K_2 q_1 \qquad 3.36$$

where K_1 and K_2 can be assumed to be known. The measurements m_1 and m_2 are hence known functions of r_0, r_1, r_2 and r_3 and are thus in a suitable form for the implementation of the estimation equations 2.7.

2. DTPA

Block diagrams of the route taken by DTPA are given by figures 3.5 a,b. It difuses into and from the extra vascular space with rates r_0 and r_1 respectively and is extracted by the left and right kidneys with rates r_2 and r_3. The pharmacutical then takes time ΔT_2 and ΔT_3 to flow from the glomerulus of the right and left kidney respectively. Standard procedures now exist on most gamma camera computer systems to compute the mean transit time through the kidneys (the time for material to flow from points A to points B in Figure 3.5, ΔT_2, ΔT_3 respectively). Here we solve the system equations so that with the use of suitable measurements the filtration rates and the transit times may be estimated using the discrete form of equation 2.7

We see from the analysis in the previous section that q_0 and q_1, the intensities in the vascular and extravascular space,are given by the equation

$$\frac{d}{dt}\begin{bmatrix} q_0 \\ q_1 \end{bmatrix} = \begin{bmatrix} -(r_0 + r_2 + r_3)/V_0 & r_1/V_1 \\ r_0/V_0 & -r_1/V_1 \end{bmatrix} \begin{bmatrix} q_0 \\ q_1 \end{bmatrix} \qquad 3.37$$

we may also see by inspection of Figure 3.5 that

$$\dot{q}_{A_1}(t) = r_2 q_0(t) / V_0$$

$$\dot{q}_{A_2}(t) = r_3 q_0(t) / V_0 \qquad 3.38$$

$$q_{B_1}(t) = q_{A_1}(t - \delta t_1)$$

$$q_{B_2}(t) = q_{A_2}(t - \delta t_2) \qquad 3.39$$

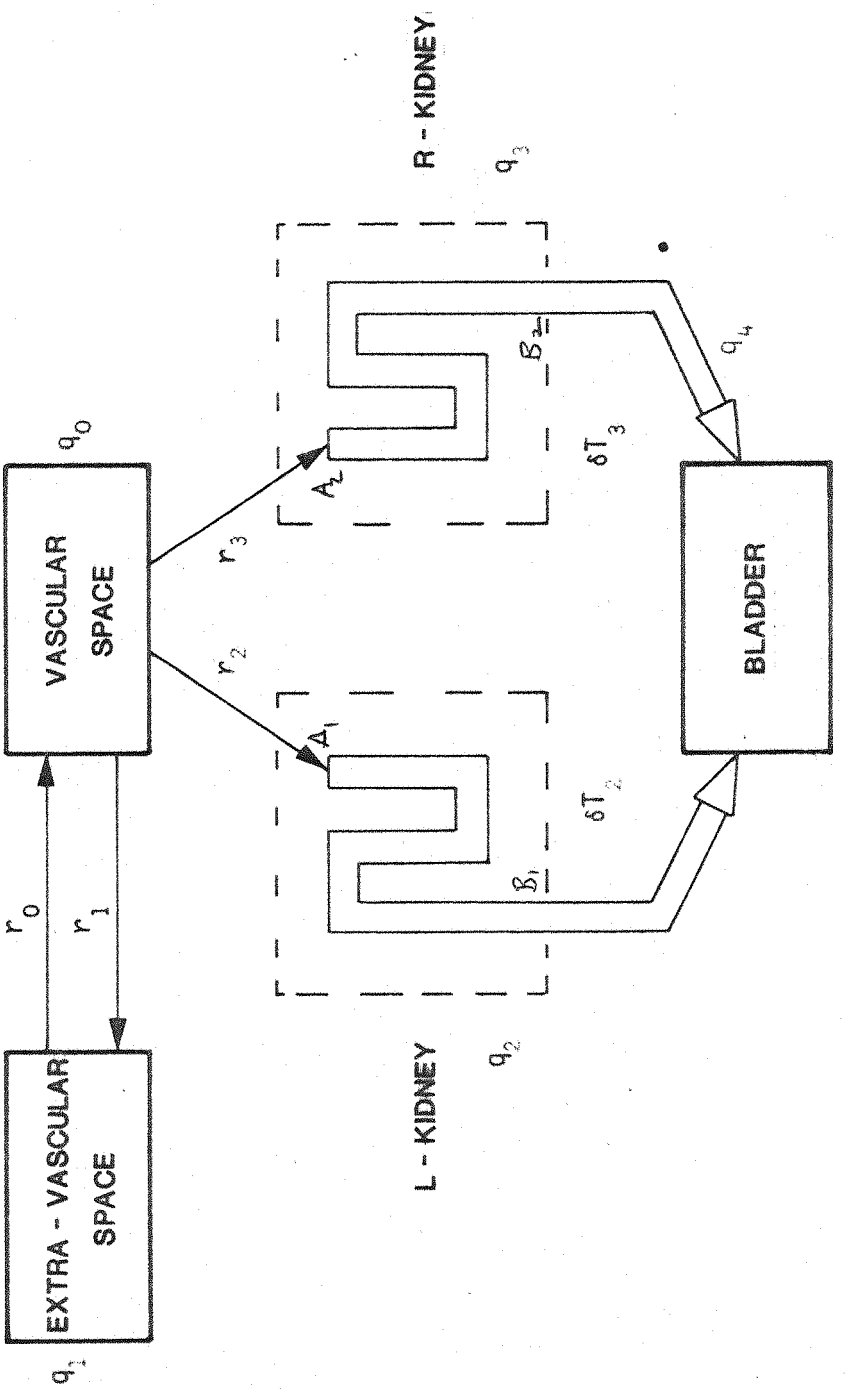

FIGURE 3.5a EXTRACTION AND FLOW OF $^{99}Tc^{m}$ LABELED D.T.P.A. IN THE URINARY SYSTEM

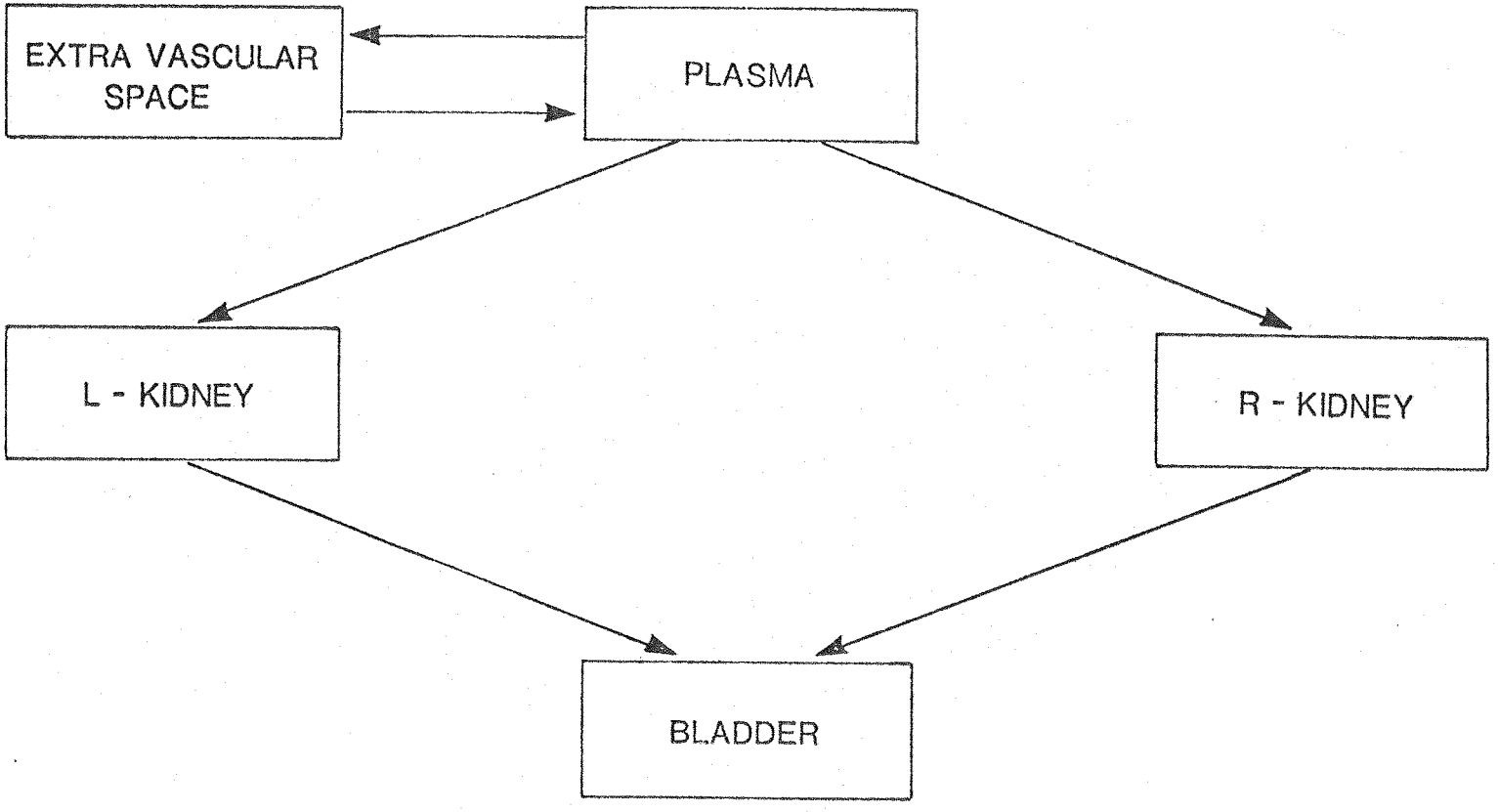

FIGURE 3.5b ROUTE OF $^{99}Tc^{m}$ LABELLED D.T.P.A. THROUGH BODY

Assuming that the transit time for B_1 and B_2 to the Bladder is negligible

$$Dq_4(t) = \dot{q}_{B_2}(t) + \dot{q}_{B_1}(t) \qquad 3.40$$

$$q_2 = \int_{t-\delta t_1}^{t} \dot{q}_{A_1}(t)\, dt \qquad 3.41a$$

$$q_3 = \int_{t-\delta t_2}^{t} \dot{q}_{A_2}(t)\, dt \qquad 3.41b$$

Measurements may be made of the intensities of the right and left kidneys and the bladder. The analytical expressions for these are now found:

From the analysis for DMSA we have, using the same change of variable to Q_o and Q_1

$$Q_o = \exp\left[-\lambda_1 t\right] + \frac{d\,Q}{\varepsilon} - 1$$

$$Q_1 = \exp\left[-\lambda_2 t\right] + \frac{d\,Q}{\varepsilon} - 1 \qquad 3.42$$

$$q_o = r_1 \left[Q_o - d\,Q_1\right]$$

$$q_1 = \varepsilon \left[Q_1 - c\left[Q_o + d\,Q_1\right]\right] \qquad 3.43$$

Where $\lambda_1, \lambda_2, c, d$ and ε have been defined in the previous section.

Using equations 3.38 and 3.41 we may derive the expressions for q_2 and q_3

$$q_2 = \int_{t-\delta t_1}^{t} \frac{r_1 r_2}{V_o} \left[Q_o - d\,Q_1\right] dt$$

$$= \frac{r_1 r_2}{V_o} \left\{ \int_{t-\delta t_1}^{t} Q_o \, dt - d \int_{t-\delta t_1}^{t} Q_1 \, dt \right\} \qquad 3.44$$

Now

$$\int Q_o \, dt = \int \left\{ \exp \lambda_1 t + \frac{dQ}{\varepsilon} - 1 \right\} dt$$

$$= \frac{\exp \lambda_1 t}{\lambda_1} + \frac{dQt}{\varepsilon} - t \qquad 3.45$$

and

$$\int Q_1 \, dt = \int \left\{ \exp \lambda_2 t + \frac{dQ}{\varepsilon} - 1 \right\} dt$$

$$= \frac{\exp \lambda_2 t}{\lambda_2} + \frac{dQ}{\varepsilon} - t \qquad 3.46$$

Hence

$$q_2 = \frac{r_1 r_2}{V_o} \left\{ \left[\frac{\exp \lambda_1 t - \exp \left[\lambda_1 - (t-\delta t_2)\right]}{\lambda_1} + \frac{dQ\delta t_2}{\varepsilon} + \delta t_2 \right] \right.$$

$$\left. - d \left[\frac{\exp \lambda_2 t - \exp \left[\lambda_2 (t - \delta t_2)\right]}{\lambda_2} + \frac{dQ\delta t_2}{\varepsilon} + \delta t_2 \right] \right\} \qquad 3.47$$

and q_3 is found by replacing δt_2 by δt_3 in the above expression for q_2 equation 3.47.

From equation 3.40 we obtain the expression for q_4

$$q_4 = \int_o^t \{ q_{B_1}(t) + q_{B_2}(t) \} \, dt$$

$$= \int_{\delta t_2}^{t} q_{A_2}(t) \, dt + \int_{\delta t_3}^{t} q_{A_3}(t) \, dt$$

$$= \sum_{i=2}^{3} \int_{\delta t_i}^{t} q_{A_i}(t) \, dt \qquad 3.48$$

Thus

$$q_4 = \sum_{i=2}^{3} \frac{r_i r_1}{V_o} \left\{ \int_{\delta t_i}^{t} Q_o \, dt - d \int_{\delta t_1}^{t} Q_1 \, dt \right\}$$

$$= \sum_{i=2}^{3} \frac{r_i r_1}{V_o} \left\{ \left[\frac{\exp[\lambda_1 t] - \exp[\lambda_1 \delta t_i]}{\lambda_1} + \frac{d\,Q\,(t - \delta t_i)}{\varepsilon} - t - \delta t_i \right] \right.$$

$$\left. - d \left[\frac{\exp[\lambda_2 t] - \exp[\lambda_2 \delta t_i]}{\lambda_2} + \frac{d\,Q\,(t - \delta t_i)}{\varepsilon} - t - \delta t_i \right] \right\} \qquad 3.49$$

We have now put the measurements in a form suitable for the application of the Snyder filter. Note that for these two cases no proof of the convergence nor the stability of the resultant filter has been given. Further work needs to be done in this direction, though introductory work in the dual problems of controllability and observability has been done by Bucy (Buc).

3. The Biliary System

Introduction

The main factors influencing the function of the hepato biliary system are the blood clearance, the liver blood flow, the hepatocellular uptake, metabolism and secretion into the bile, and the biliary transport. The traditional tracer used has been ^{131}I - Rose bengal, but more recently $^{99}Tc^m$ labelled compounds have been developed, the latter having the advantage of high photon flux rates, and low radiation dosage. Compounds which have been used in conjunction with a $^{99}Tc^m$ label have been derivatives of acetanilidoiminodiacetic acid, namely dimethyl-, diethyl-, ethoxy- and p-iodo-IDA see (Lob), (Har), and derivatives

of pyridoxal, namely py-glutamate, py-lucine and py-arginine, and also di-hydrothyoctic acid (DHT), and Mercapto isobutyric acid (MIBA).

Wistow et al (Wis) investigated the cumulative bile, and cumulative urinary excretion for up to three hours of all the above compounds in baboons. Diethyl IDA was found to have the fastest blood clearance, the best liver uptake, and lowest urinary excretion (Figure 3.6). We consider the use of diethyl-IDA, and outline the main factors affecting the kinetics of the tracer.

Mathematical Model and Kinetics of Diethyl IDA

$^{99}Tc^{m}$ Diethyl IDA has a high affinity for the normal human hepatocytes. It accumulates in the polygonal cells of the liver parenchyma with high extraction efficiency immediately following intravenous injection. After a short intrahepatic transit time it is excreted into the bile, without being conjugated in the process. The complex then appears rapidly in the larger bile ducts from where it passes into the intestinal tract, Figure (3.7). In the process a portion of the activity extracted by the liver is temporarily stored in the gall bladder. A second route of elimination, only observed to a significant extent when hepatic function is impaired is via the kidneys to the urinary bladder. Extrahepatic recirculation appears to be negligible in normal subjects. A block diagram of the path taken by the tracer is shown in Table (3.8). The modelling of the process is complicated by the action of the sphincter of Oddi at the junction of the bile duct and the duodenum. In the non fasting state the splincter of Oddi is contracted allowing no bile to pass into the duodenum. When a meal is eaten, the hormone cholecystokin causes the sphincter of Oddi to relax, the gall bladder to contract,

Compound	Blood Clearance (%)	Cumulative Biliary Extraction (%)	Cumulative Urinary Extraction (%)
Diethyl IDA	1	80	5
Dimethyl IDA	3	75	2
p - ethoxy - IDA	2	36	34
p - iodo IDA	4	62	15
Py glutamate	3	31	28
Py lucine	4	32	27
Py arginine	4	18	25
DHT	15	27	8
MIBA	12	24	16
Rose Bengal	2	67	2

Table 3.8 Baboon Data obtained three hours after injection (Wis)

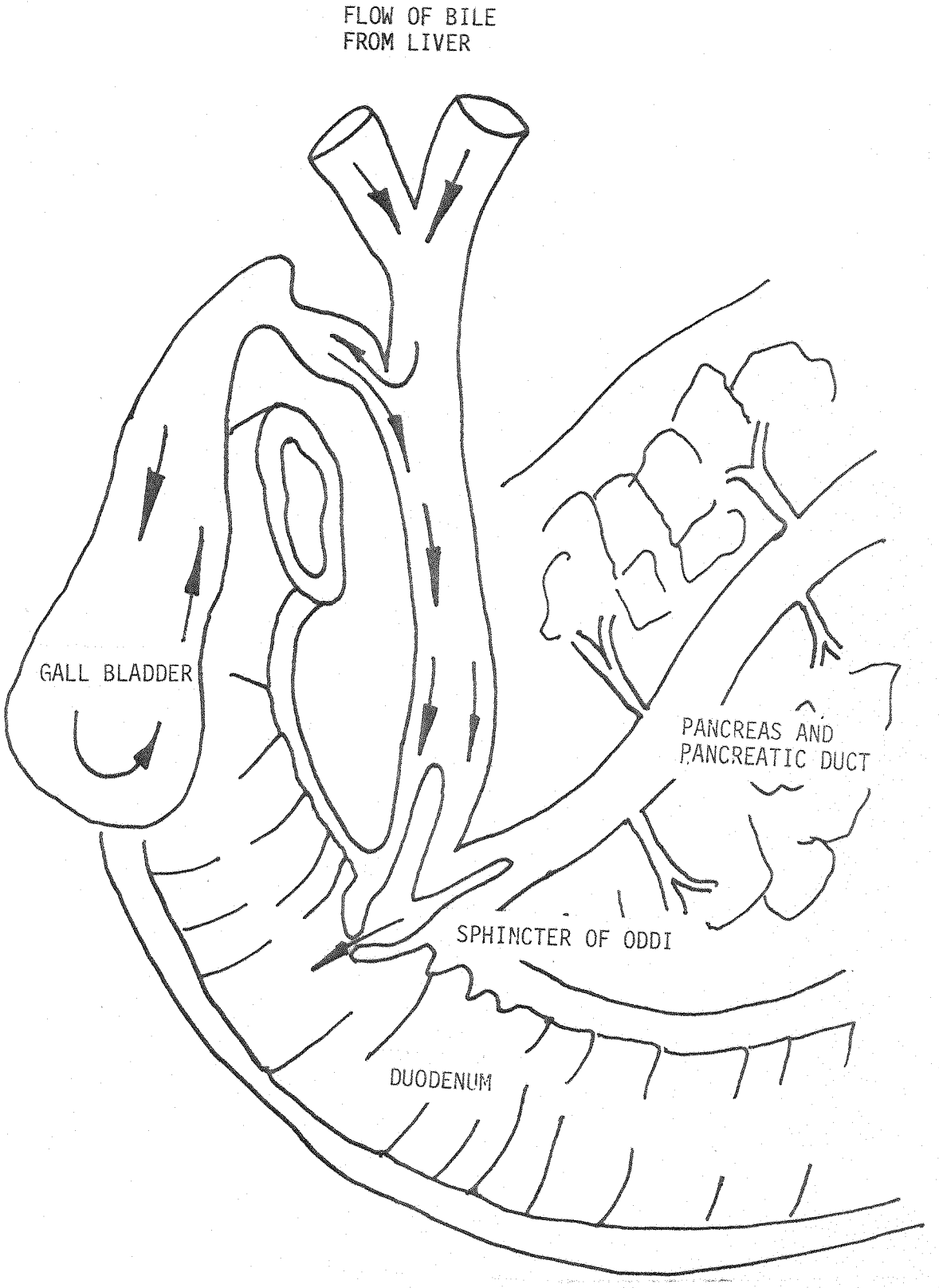

FIG 3.7 THE BILIARY SYSTEM: FLOW OF BILE FROM LIVER TO DUODENUM

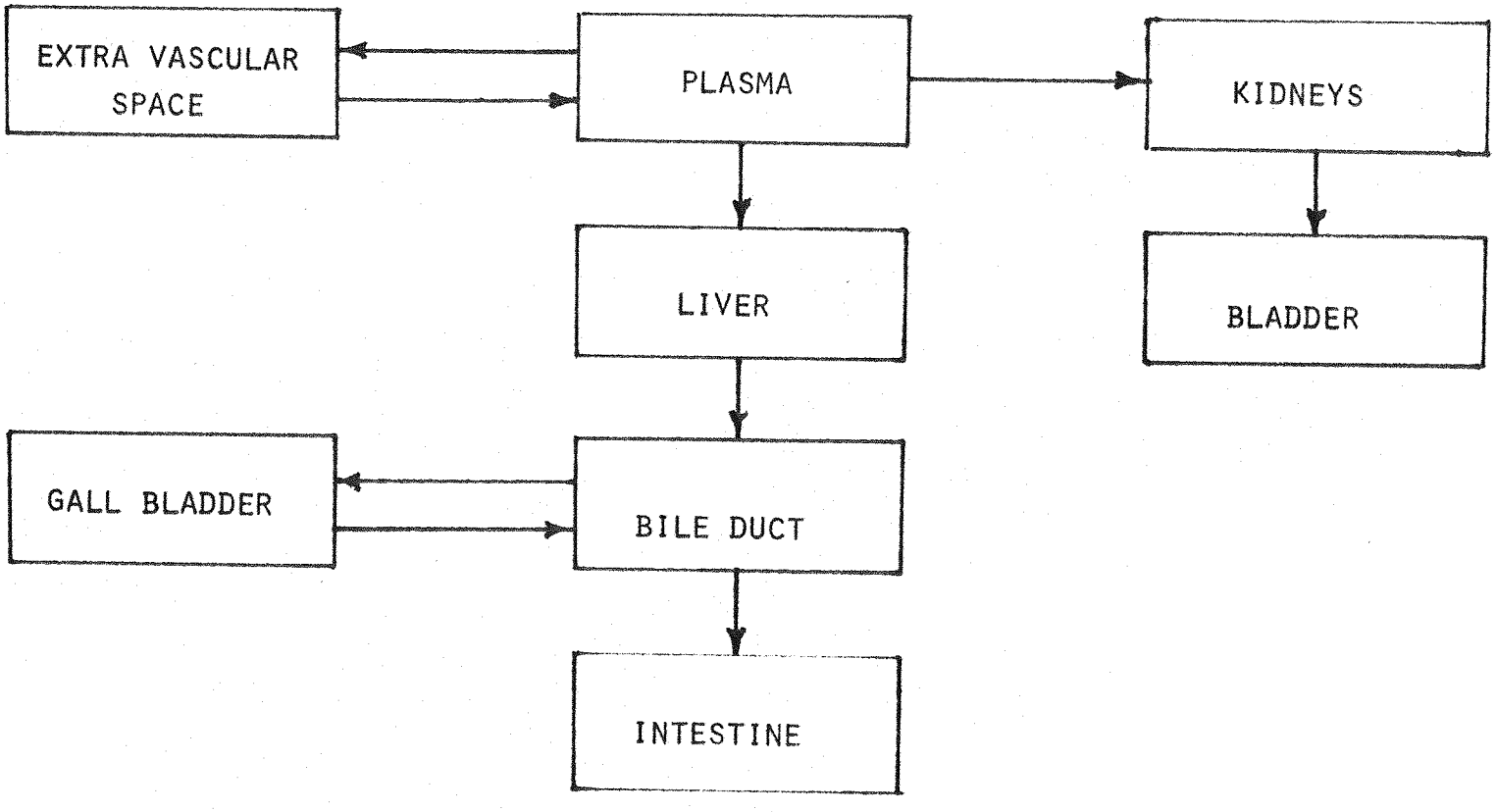

FIGURE 3.8 BLOCK DIAGRAM OF THE ROUTE TAKEN BY $^{99}Tc^{m}$ LABELLED ETHYL - IDA

and bile to flow freely into the duodenum. The activity is more marked if a fatty meal is taken. The degree of contraction should be represented in any model purporting to represent the system under all conditions. We consider two simplified systems one in the fasting state, and the second after administration of meal with a high fat content We assume in the former that the sphincter is completely closed, and all bile flows into the gall bladder, while in the latter case all bile will flow into the duodenum. Flow diagrams are shown in Figure (3.9) and (3.10). We now obtain analytic expressions for the intensities in each compartment.

The same mathematical model may be used for both the fasting and non fasting state by substitution of the parameters relating to the gall bladder in the former case to those relating to the duodenum in the latter, namely the transport time from the liver, and the radioactive intensity.

Comparison of the system for the transport of isotope in the kidneys with the present system shows that the majority of the analysis is directly applicable here. The system equation giving the time evolution of q_0 and q_1, the intensities in the vascular and extra vascular space, is given by:

$$\frac{d}{dt}\begin{bmatrix} q_0 \\ q_1 \end{bmatrix} = \begin{bmatrix} -(r_0 + r_2 + r_3)/V_0 & r_1/V_1 \\ r_0/V_0 & -r_1/V_1 \end{bmatrix} \begin{bmatrix} q_0 \\ q_1 \end{bmatrix}$$

The volume flows entering the Liver and Kidneys are given by

$$\frac{d}{dt} q_L = r_2 q_0$$

$$\frac{d}{dt} q_K = r_3 q_0$$

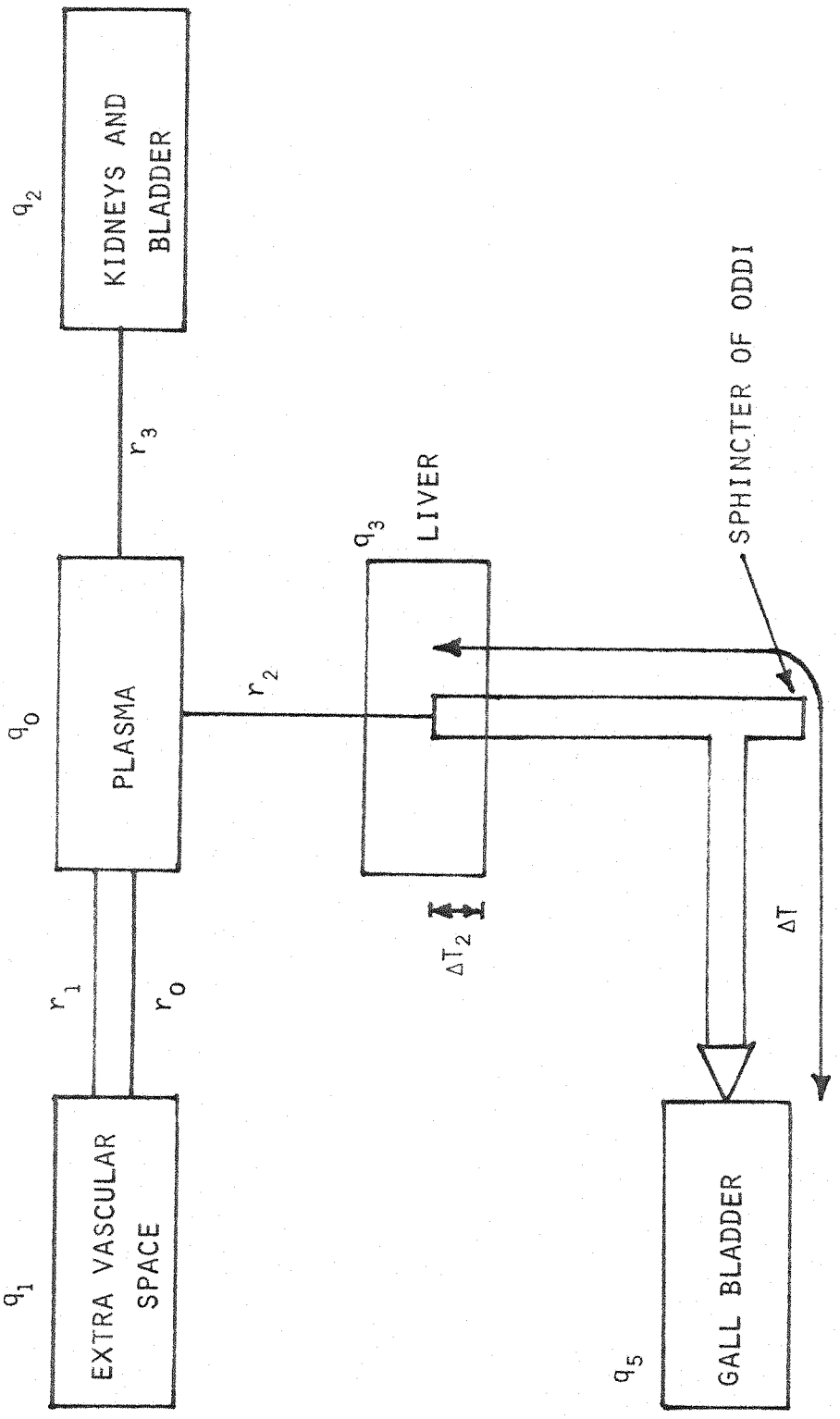

FIGURE 3.9 FLOW OF $^{99}Tc^{m}$ LABELLED ETHYL IDA IN THE FASTING STATE (SPHINCTER OF ODDI) CLOSED

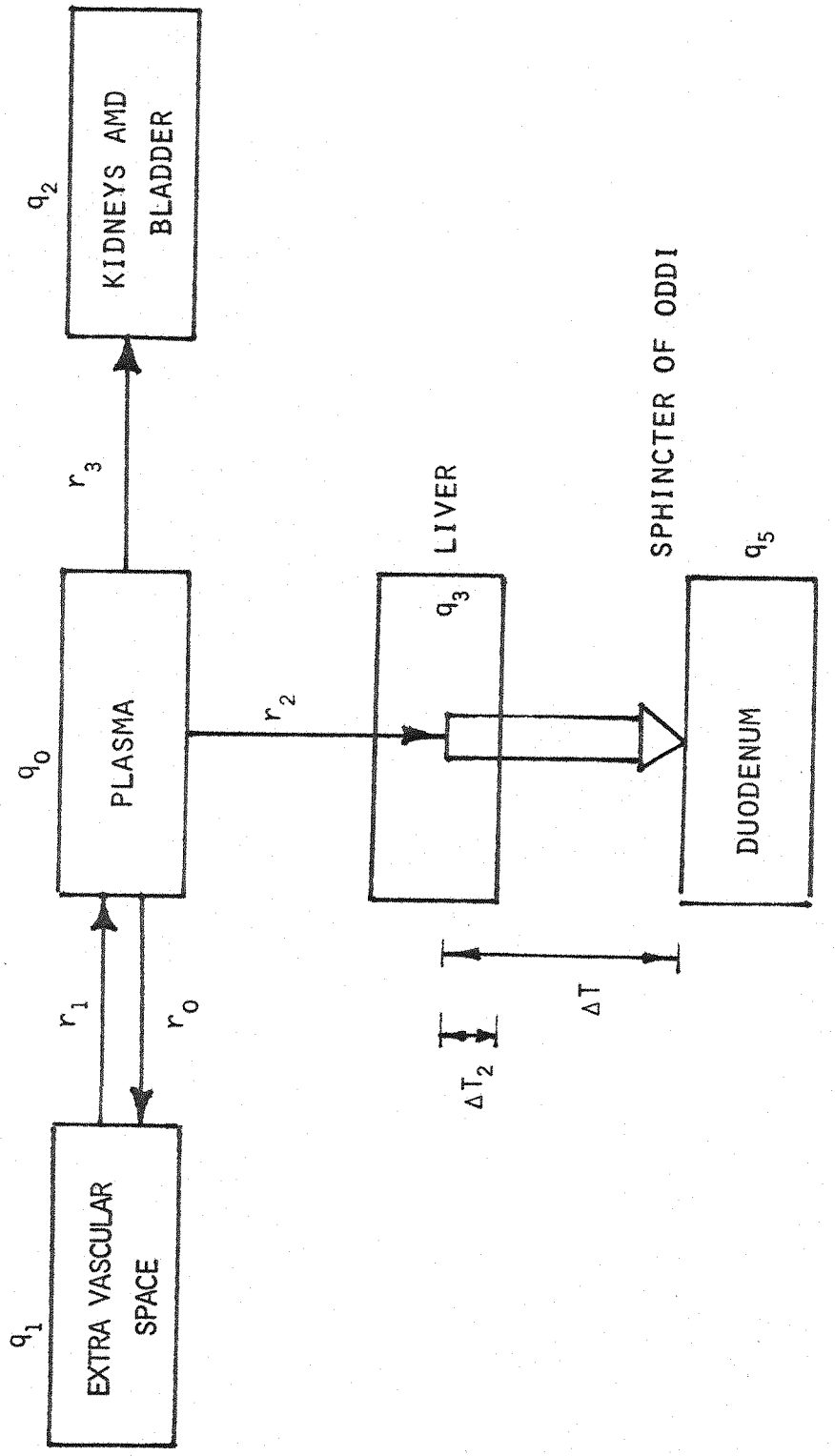

FIGURE 3.10 FLOW OF $^{99}Tc^{m}$ LABELLED ETHYL IDA AFTER ADMINISTRATION OF A HIGH FAT CONTENT MEAL (SPHINCTER OF ODDI OPEN)

From the analysis for the kidney we have equation 3,34, 3,35 and equation 3.42, 3.43

$$Q_o = \exp - \lambda_1 t + \frac{d\,Q}{\varepsilon} - 1$$

$$Q_1 = \exp - \lambda_2 t + \frac{d\,Q}{\varepsilon} - 1$$

$$q_o = r_1 [Q_o - d\,Q_1]$$

$$q_1 = \varepsilon [Q_1 - c [Q_o - d\,Q_1]]$$

where λ_1, λ_2, c, d, ε have been defined in the equations (3.26) and (3.29).

HIDA being extracted from the blood stream by the liver flowing on towards the gall bladder or duodenum is acted on by the same transport mechanism as DTPA when it is extracted from the blood stream by the kidneys, and flows on towards the bladder. Comparison of the two systems shows that we may use the results derived in the previous section directly. From equation (3.47) the intensity of ethyl IDA in the liver is given by

$$q_2 = \frac{r_1 r_2}{V_o} \left\{ \left[\frac{\exp \lambda_1 t - \exp \lambda_1 (t - \delta t_2)}{\lambda_1} + \frac{d\,Q\,\delta t_2}{\varepsilon} + \delta t_2 \right] \right.$$

$$\left. - d \left[\frac{\exp \lambda_2 t - \exp [\lambda_2 (t - \delta t_2)]}{\lambda_2} + \frac{d\,Q\,\delta t_2}{\varepsilon} + \delta t_2 \right] \right\}$$

With the same definities of λ_1, λ_2, c, d and ε as before, and V_o being the volume of the vascular space.

Since in this examination of biliary function the function of the kidneys is not being examined, their effect must be accounted for in

the most economical fashion. The best way to do this is to regard the two kidneys and the bladder as a single compartment and to it assign the total glomerular filtration rate. This treatment causes them to act in a manner similar to one of the kidneys when DMSA has been administered. We may again use this equation directly to give the intensity of ethyl IDA in the kidneys. From equation (3.34), (3.35) we obtain:

$$Q_3 = \frac{d\,Q}{\varepsilon}\left\{\frac{1}{\lambda_2} - \frac{r_1 r_3}{\lambda_1}\right\}$$

$$q_3 = d\,Q_3 + \frac{r_1 r_3}{\lambda_1}\,Q_0 - \frac{d}{\lambda_2}\,Q_1$$

Where

Q_0, Q_1, λ_1, λ_2, d, ε are as previously defined.

The remaining expression is that for the gall bladder or duodenum, depending upon whether the patient is in a fasting condition, or not. The expression for the intensity is given by the expression for the contribution of one kidney to the intensity in the bladder. For the case of DTPA we obtain from equation (3.49).

$$q_4 = \frac{r_1 r_2}{V_0}\left\{\left[\frac{\exp \lambda_1 t - \exp \lambda_1 \delta\tau}{\lambda_1} + \frac{d\,Q(t-\delta\tau)}{\varepsilon} - t - \delta\tau\right]\right.$$

$$\left. - d\left[\frac{\exp \lambda_2 t - \exp \lambda_2 \delta\tau}{\lambda_2} + \frac{d\,Q(t-\delta\tau)}{\varepsilon} - t - \delta\tau\right]\right\}$$

where τ is the delay from the liver to the gall bladder or the duodenum, and all other terms as before.

Conclusion

In this Chapter four major metabolistic flow mechanisms have been studied, and it has been shown that by the use of state space analysis expressions are derivable for the intensities of radioactivity in each organ in terms of the constant organ extraction, filtration or flow rates,and inter-organ time delays in the blood,bile,urine or other body fluids. These expressions allow the estimation of these constants to be posed using a Snyder estimation filter with a linear state equation together with non-linear measurements.

Possible methodologies are outlined for each case to allow the estimation to be performed, and are compared with present techniques.

CHAPTER 4

EVALUATION OF THE ESTIMATION ROUTINES

Introduction

The previous Chapters have shown how the parameters of the transport mechanisms of various radiopharmacuticals may be estimated using the radiation intensity measurements of a nuclear camera. The estimation must be made using a digital computer, hence in the first section of this Chapter the filtering equations of Chapter 2 are transformed to a form suitable for this treatment.

The estimation scheme for the liver spleen and bone marrow is examined in detail in this Chapter. The estimation scheme while similar to the single exponential, single parameter fit performed by Snyder '72 (Sny 4), estimates three parameters and brings to light techniques which are directly applicable to all the systems described in Chapter 3.

Time varying poisson processes, similar to those which would be produced by radiocolloid in the liver and spleen were simulated using the random number generating facility of a computer. The estimation technique to be tested (both the deterministic exponential fit and the stochastic filter) was then applied using the simulated process, and the estimated results compared to the values used to produce the simulated measurements. The comparison of the estimates to the known values gives an indication of the performance that the routine would give using real data.

1. Derivation of the Discrete Time Filter

The version of the continuous time system identification equations required in Chapter 3 and derived in Chapter 2 may be restated:

Given a process $r(t)$, generated by the equation

$$dr(t) = 0 \qquad 4.1$$

observed with measurements having a poisson rate vector $\lambda\,(r(t),t)$ where the vector $r(t)$ needs to be identified, then the best estimate, s, of r may be found using the equations

$$ds = \sum_{i=1}^{m} R(t)\,\frac{\partial \lambda^T}{\partial s}\,\gamma_i\,(\lambda^T(s)\,\gamma_i)^{-1}\,(dN(t) - \lambda(s)\,dt)\,\gamma_i$$

$$dR = \sum_{i=1}^{n} R(t)\,\frac{\partial^2 \ell n\lambda}{\partial s^2}\,R(t)\,\gamma_i^T\,dN(t)\,\sum_{i=1}^{m} R(t)\,\frac{\partial^2 \lambda}{\partial s^2}\,R(t)\,dt \qquad 4.2$$

These equations must be discretised before implementation on a digital computer. This may be done by replacing the differential dt by the measurement interval Δt, the differentials ds and dR by the differences $(S_{new} - S_{old})$ and $(R_{new} - R_{old})$, and the differential dN by the measurement ΔN obtained in the measurement interval Δt to obtain:

$$S_{new} = S_{old} + \sum_{i=1}^{m} R(t)\,\frac{\partial \lambda^T}{\partial s}\,\gamma_i\,(\lambda^T(s)\,\gamma_i)^{-1}(\Delta N(t) - \lambda(s)\Delta t)\,\gamma_i$$

$$R_{new} = R_{old} + \sum_{i=1}^{m} R(t)\,\frac{\partial^2 \lambda}{\partial s^2}\,R(t)\,\gamma_i^T\,dN - \sum_{i=1}^{m} R(t)\,\frac{\partial^2 \lambda}{\partial s^2}\,R(t)\,\Delta t \qquad 4.3$$

We note that the equations 4.2 were derived using the assumption that $dN = 0$ or γ_i † This assumption extends to the discrete case to give the restriction that ΔN must have no more than one contribution (event)

† Note γ_i defined as $[0 \ldots 1 \ldots 0]^T$ (1 in the ith position)

in each measurement, otherwise poor performance of the filter is obtained. This restriction sets a limit on the maximum time that may be taken for taking each measurement before updating the estimate. If variable time periods are permitted a new time period can be started whenever an event causes an element in the measurement vector to have more than one entry, however for simulation purposes it is shown that a fixed time period is necessary, and for real data aquisition a fixed time period is convenient. The correct apriori choice of the time period is of vital importance since it affects the computation time, the accuracy and stability of the filter.

2. Computer Simulation

The main prerequisite to test the performance of the estimation equation 4.3 is to produce simulated poisson processes, representing the measurements of rate λ (r,t) produced from a process with system equation $\dot{x} = A(r)\, x$. The problem is treated in three stages, first considering a process of uniform intensity, secondly of time varying intensity, and finally the desired result.

(a) Simulation of a Poisson Process of Uniform Intensity

A poisson process consists of a chain of events, each of which are independent and have an exponentially decaying probability distribution (Freeman (Fre)). A sample function of a poisson process is shown in figure 4.1.

Consider the likelihood of a particular event occurring at time t. If the time of the previous event was s, then the distribution function will have the form shown in Figure 4.2. Given the rate of the poisson process α, a random number in the range (0, 1) will correspond to a particular value of F(T), $F_p(t)$ and hence a collision time t_c. By reference to Figure 4.2 we may derive an expression for

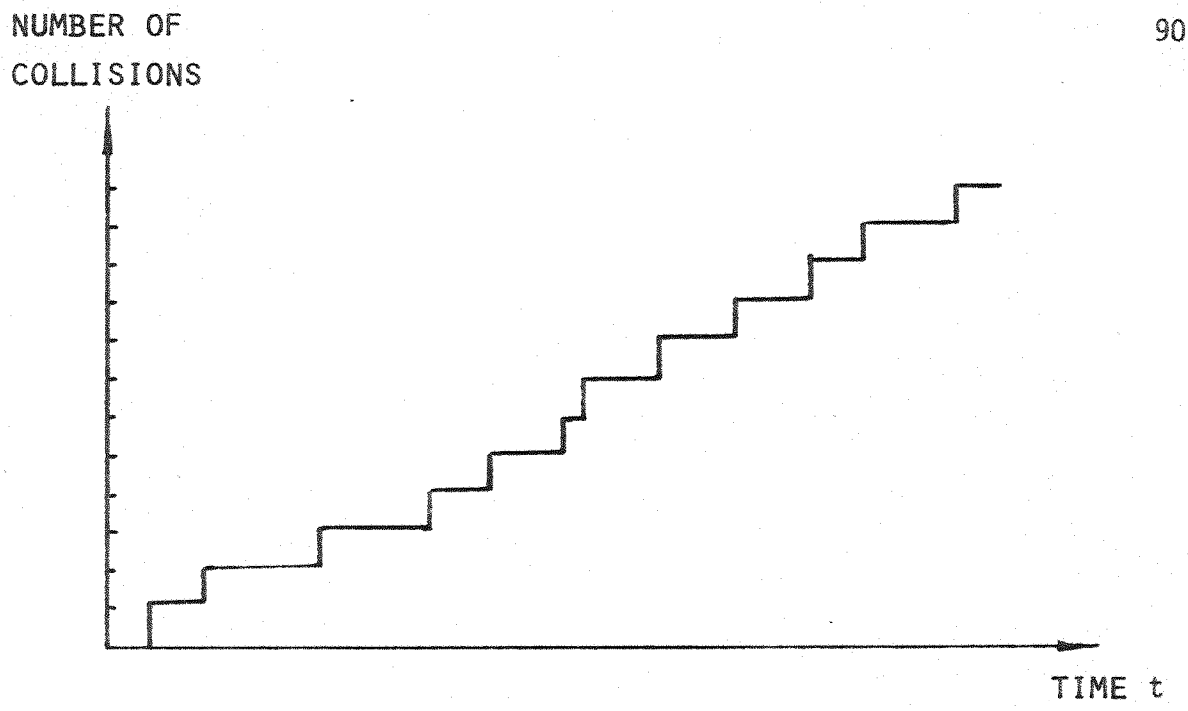

FIGURE 4.1 SAMPLE FUNCTION OF A POISSON PROCESS

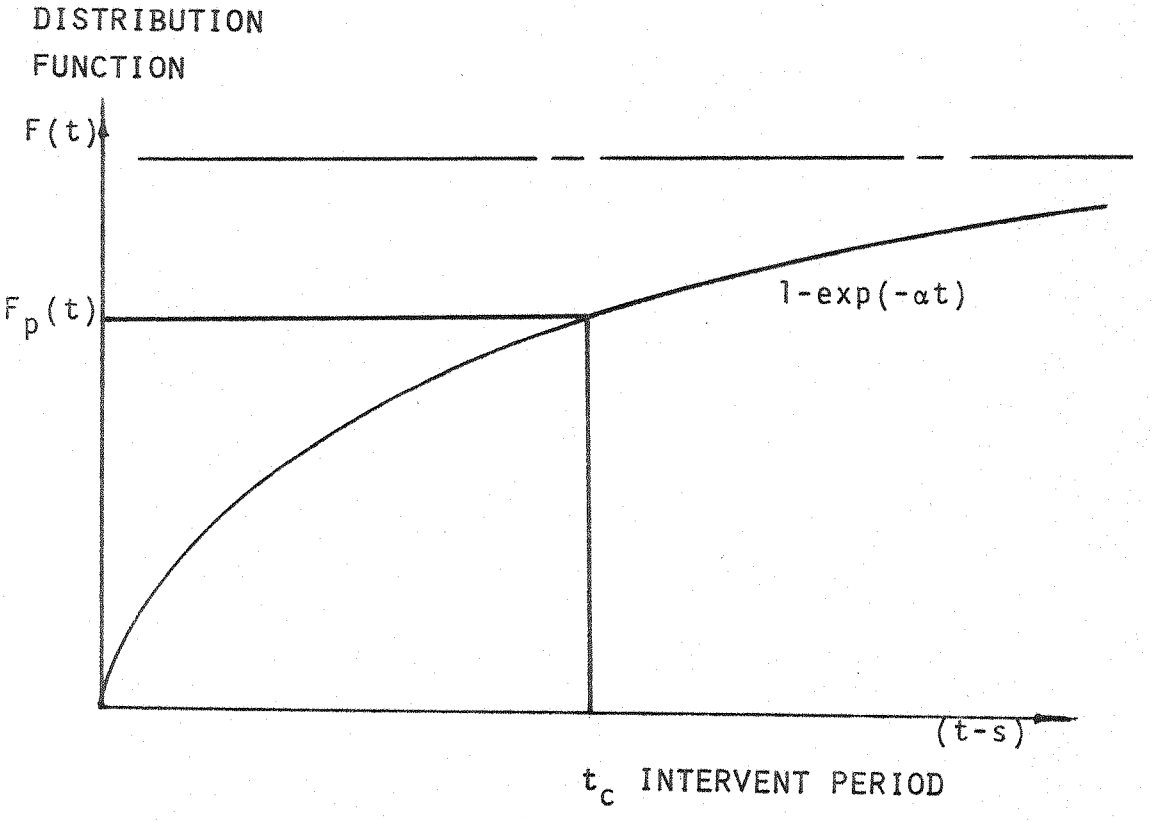

FIGURE 4.2 USE OF DISTRIBUTION FUNCTION TO DETERMINE THE INTEREVENT PERIOD (t-s).

the collision time:

$$\text{Random Number} = 1 - \exp(-\alpha t_c)$$

$$\therefore \quad t_c = -\frac{1}{\alpha}\left[\ell n\ (1 - \text{Random Number})\right]$$

Since (1 - Random Number) where 'Random Number' lies between 0 and 1 gives the same distribution as (Random Number), the typical collision time is given by

$$t_c = \frac{1}{\alpha}\left[\ell n\ (\text{Random Number})\right]$$

Since the time between collisions can be found the number of collisions between any two times can be calculated, thus enabling measurements to be genereted.

(b) Simulation of a Poisson Process of time varying intensity

A poisson process time varying intensity may be simulated by transformation of the time axis of a poisson process of uniform intensity the latter process being generated as shown in the previous subsection.

Consider a measurement process with rate $\lambda(t)$. The time variable t may be transformed to $u = \int_0^t \lambda_1(t)\,dt$ to obtain a poisson process of uniform measurement rate $\lambda_2(u)$, (Fre). This may be seen by noting that the number of events between 0 and t of λ_1 will be the same as the number between 0 and u of the transformed measurement rate λ_2, thus:

$$\int_0^t \lambda_1(t)\,dt = \int_0^u \lambda_2(u)\,du$$

and using the tranformation $u = \int_0^t \lambda_1(t)\,dt$

we obtain:

$$\int_0^t \lambda_1(t)\, dt \;=\; \int_0^{\int_0^t \lambda_1\, dt} \lambda_2(u)\, du$$

which has a solution $\lambda_2 = 1$ verified by substitution

$$\int_0^{\int_0^t \lambda_1(t)\, dt} \lambda_2\, du \;=\; \int_0^t \lambda_1(t)\, dt$$

thus the tranformation $u = \int_0^t \lambda_1(t)\, dt$ gives a uniform rate $\lambda_2(u)$

Points may be projected from the t axis onto the u axis, but not vice-versa since the transformation equation $u = \int_0^t \lambda_1(t)\, dt$ cannot always be inverted to give an expression for t in terms of u.

In any simulation the actual times of collision on the t axis may not be produced due to this limitation, however the number of events occurring between time t_1 and t_2 may be found by a two stage method by projection of the times t_1, t_2 onto the u axis to give an interval u_1, u_2, and then obtaining the number of events occurring on the u axis in this interval.

(c) Simulation of the Measurements of the Posson process $\lambda_1(x,t)$ where $\dot{x} = Ax$

The state equation $\dot{x} = Ax$ may be solved as shown in Chapter 1, equation (1.30), to give the expression

$$x = D \exp(D^{-1} A\, Dt)\, D^{-1} x(0)$$

where the notation is as in Chapter 1 and D and A are both functions of the unknown vector r whose values need to be estimated.

This solution may be inserted into the expression λ_1 to give an expression for the measurement rate in terms of r. We denote this

expression by λ_2 (r,t).

To generate the collisions the time axis is transformed as before using $u = \int_0^t \lambda_2 (r,t)\, dt$.

If λ_2 consists of measurements of the intensities, (it is a simple step to combine these), then we have

$$u = \int_0^t D \exp (D^{-1}A\, Dt)\, D^{-1}x(0)\, dt$$

D may be removed from inside the integral sign since it is independent of time to give

$$u = D \int_0^t \exp (D^{-1}ADt)\, dt\, D^{-1}x(0)$$

$$= D \int_0^t \exp Rt\, dt\, D^{-1}x(0)$$

where R is a diagonal matrix solely dependent apon r. (see section 2.3). Integrating we obtain

$$u = D\, R^{-1} \exp Rt \Big|_0^t D^{-1}x(0)$$

$$= D\, R^{-1} [\exp Rt - I]\, D^{-1}x(0)$$

We therefore have a different time axis for each measurement. The begining and end are projected onto each u_i axis (u is a vector), and the number of events occurring on each axis between the two respective points computed to give the required measurement vector.

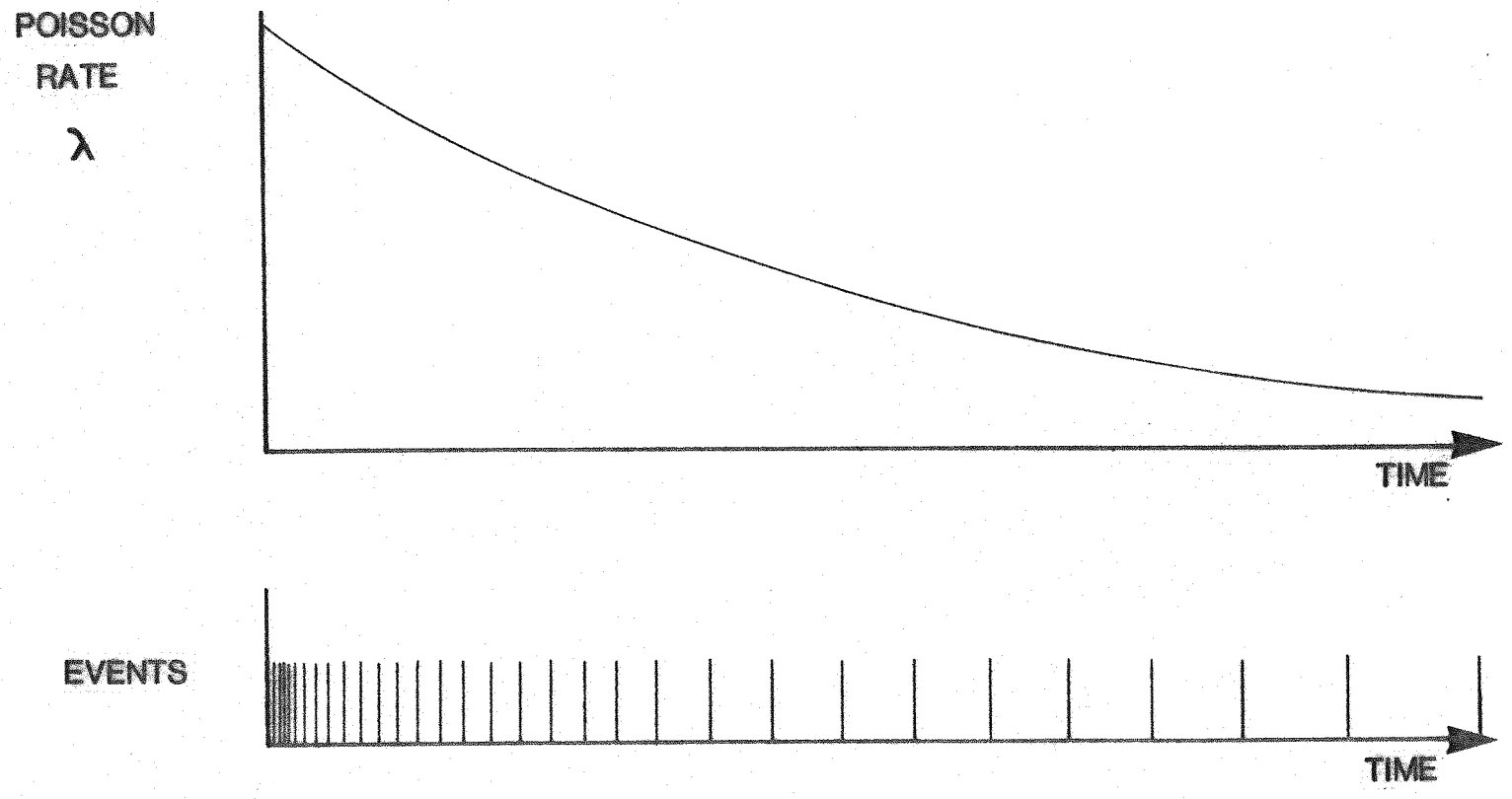

FIGURE 4.3 TYPICAL EXPONENTIALLY DECAYING POISSON PROCESS

Evaluation of the Discrete Time Filter through the Simulation and Estimation of the Extraction Rates to the Liver and Spleen

It has been shown in the previous Chapter that the problem of the determination of the Liver and Spleen Extraction Rates may be reduced to the problem of the estimation of the rates r_1, r_2 and r_3 from the measurements of the intensities q_1, q_2 and q_3 in the four compartmental problem of Figure 4.4. This model was used to test the convergence of the discrete time filter. Three time varying processes were simulated as described in the previous section, corresponding to the measurements of the intensities of compartments 1-3. The known values of r_1, r_2 and r_3 used to produce the poisson processes were compared with the final estimates obtained after using the poisson processes as inputs to the estimation routine. A suitable algorithm for this procedure was derived, the main steps involved being

(1) Setting initial extraction rates, and isotope intensities

(2) Setting apriori estimates and covariances

(3) Setting discretisation periods

(4) Generation of pseudo measurements

(5) Improvement of the estimates using the discrete time filter

(6) Repeating from (4) as required

The algorithm was tested in Basic and the coding is given in Appendix G. The initial estimate and covariance of the state variables (the extraction rates) would normally correspond to or be derived from the most likely value and the expected range of each variable. In the simulation the expected ranges were made large, and initial estimates were chosen either above or below the true value to test for convergence.

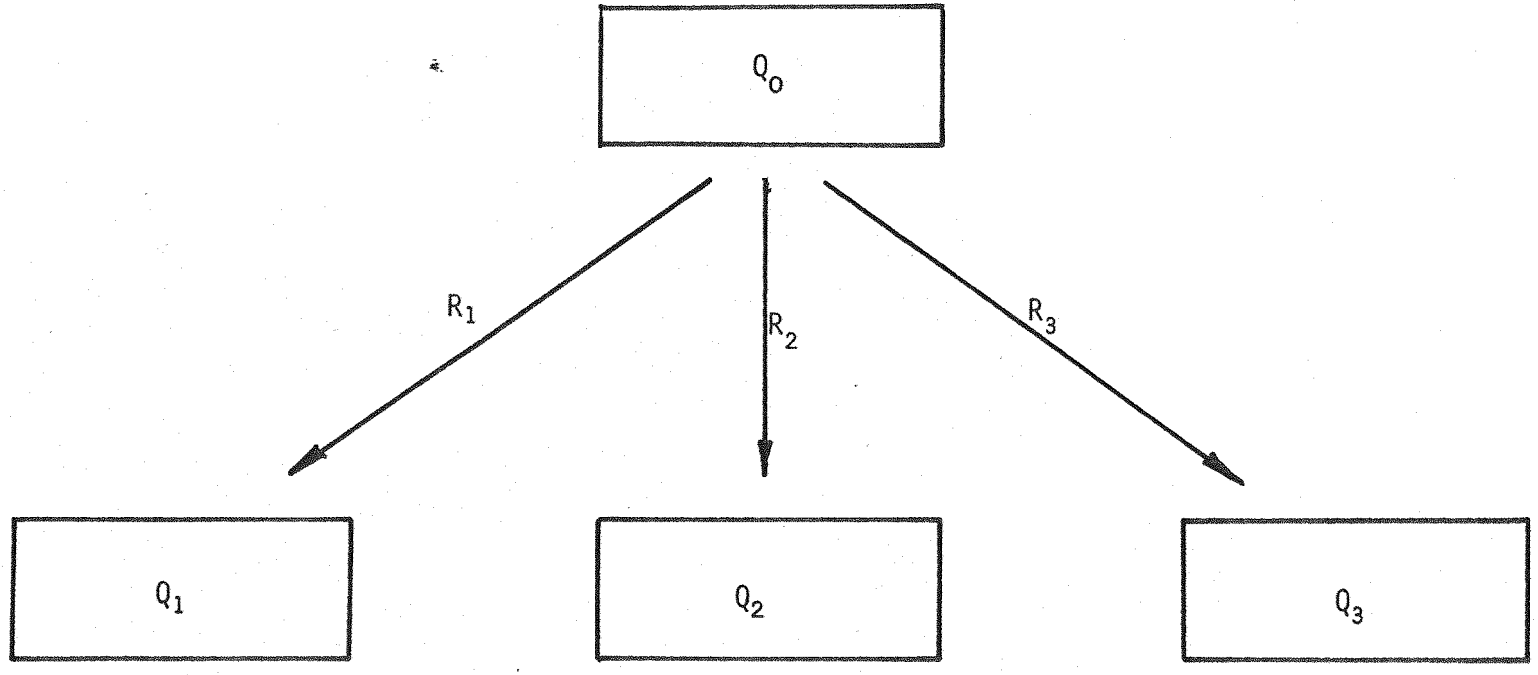

FIGURE 4.4 FOUR COMPARTMENTAL MODEL OF LIVER SPLEEN AND BONE MARROW SHOWING THE EXTRACTION RATES R_i AND INTENSITIES Q_i.

Differing intensities were simulated to give an indication of the minimum intensity required to give adequate results. The results were produced in the form of an estimate and a confidence interval, the latter being derived from the linear covariance. Since the confidence interval is not derived from the time covariance, care needs to be taken in its interpretation, and it was found in some cases to be smaller than the time value, giving an over optimistic confidence limit. As the initial isotope intensity was increased in the simulation the confidence limits were found to be more reliable, and the intervals proved to be a useful aid.

In order to increase the knowledge about and hence decrease the confidence interval of each parameter the measurements taken at any time must be dependent upon them. Analysis of the measurement rates in the liver spleen system shows that the intensity in each measurement compartment rises exponentially in the form q_i (1 - exp (-Rt)) to form a plateau of value q_i, Figure 4.5. It can be see that the period before the plateau gives information concerning the time constant R which has been shown to equal the sum of the extraction rates, or more exactly as given by equations (3.11), (3.12), (3.13) and (3.15). If by the time the plateau has been reached the estimated value of the sum of the extraction rates is still incorrect, this measurement will not improve appreciably with further measurements in the plateau region. Although individual parameters may improve slightly in accuracy due to the adjustment of ratios between differing parameters, information concerning this being contained in the plateau region, the total accuracy of the result will not improve dramatically in this region. The only procedure available to obtain a better estimate for the sum of the extraction rates is to use a higher count

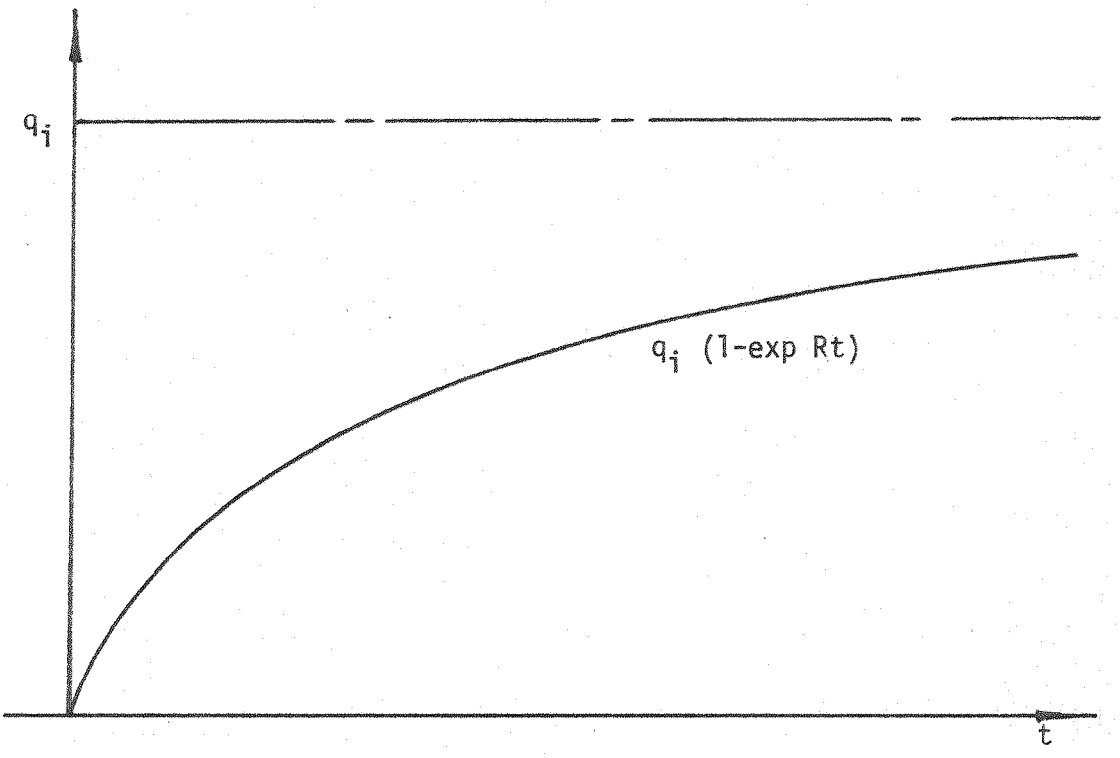

FIGURE 4.5 RISE IN INTENSITY OF RADIATION MEASURED OVER LIVER OR SPLEEN i=1 FOR LIVER i=2 FOR SPLEEN.

rate, the effect of this being shown in the results in Table 4.1 and Figures 4.6 - 4.10.

For the estimation routine to work well the number of counts from each measurement in each time interval has to be kept at one or zero. This number is dependent apon the time interval. For reasons discussed earlier a fixed time interval was chosen, hence one which fulfilled the most stringent requirement of the highest measurement rate throughout the whole period of measurement was chosen. The highest count rate occurred in the plateau region hence the reciprocal of the final expected intensity in counts per minute was taken as the discretisation period.

With a maximum extraction rate of r, with the sum of all extraction rates being R and an injected dose of Q we obtain:

$$\text{Final expected intensity in the compartment} = \frac{rQ}{R} \text{ counts/sec}$$

$$\therefore \quad \text{Discretisation Period} \leq \frac{R}{rQ} \text{ sec}$$

Results

The aim of the computation was twofold, firstly to use data obtained from dynamic scans using an Anger camera to show typical results that can be obtained using curve fitting techniques, secondly to evaluate and compare the performance of the stochastic filter using simulated measurements. Measurements typical of those that could be obtained from observations of a system of first order flow to three compartments, such as the liver spleen and bone marrow, were generated. In practice for the liver spleen bone marrow system only two measurements would be possible, of the liver and spleen making it impossible to estimate all parameters, but for completeness in the simulation all parameters were estimated. Since with simulated measurements the

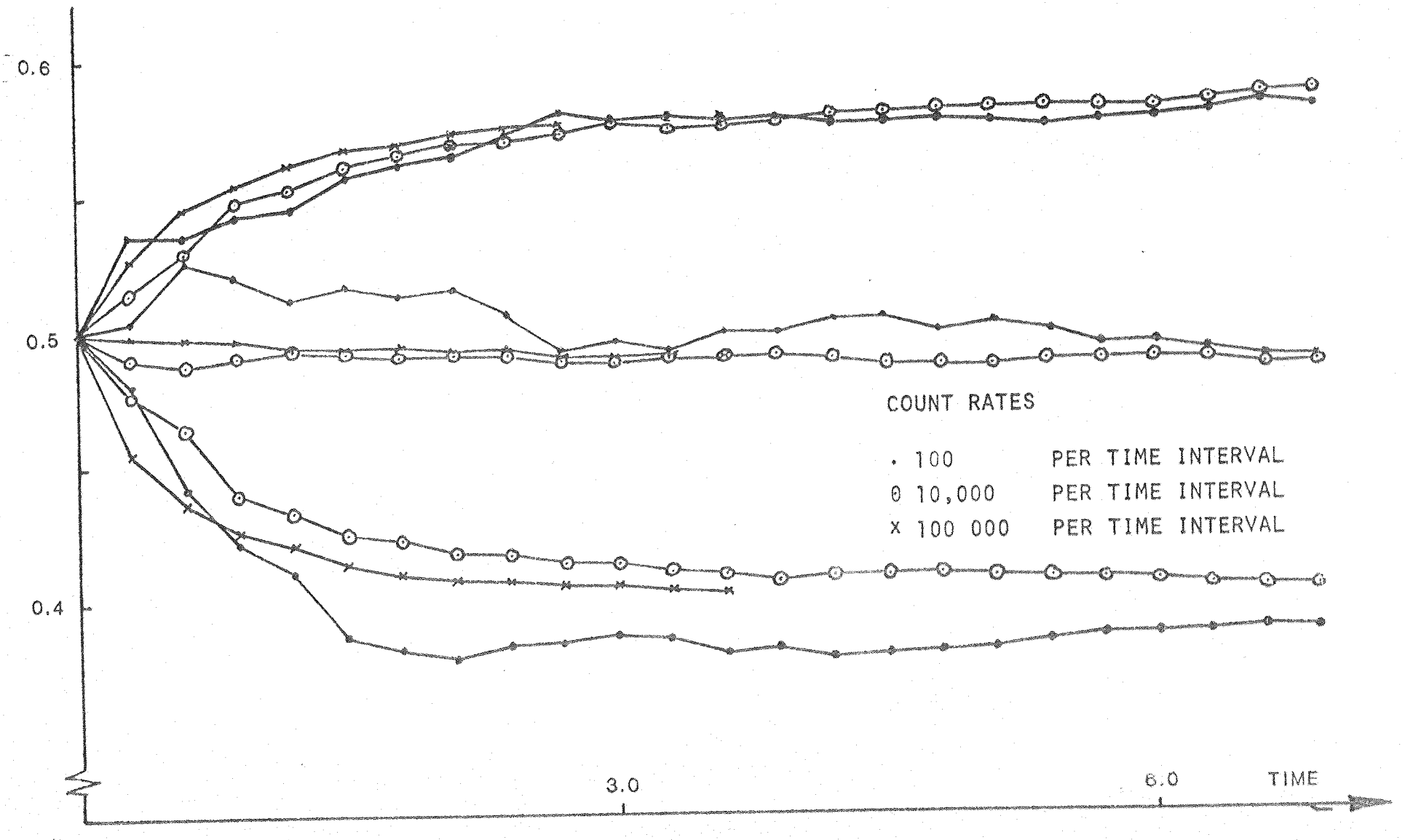

FIG 4.5 TIME EVOLUTION OF EXTRACTION RATES. TRUE VALUES 0.4, 0.5, 0.6

INITIAL ESTIMATES 0.5 - 0.2

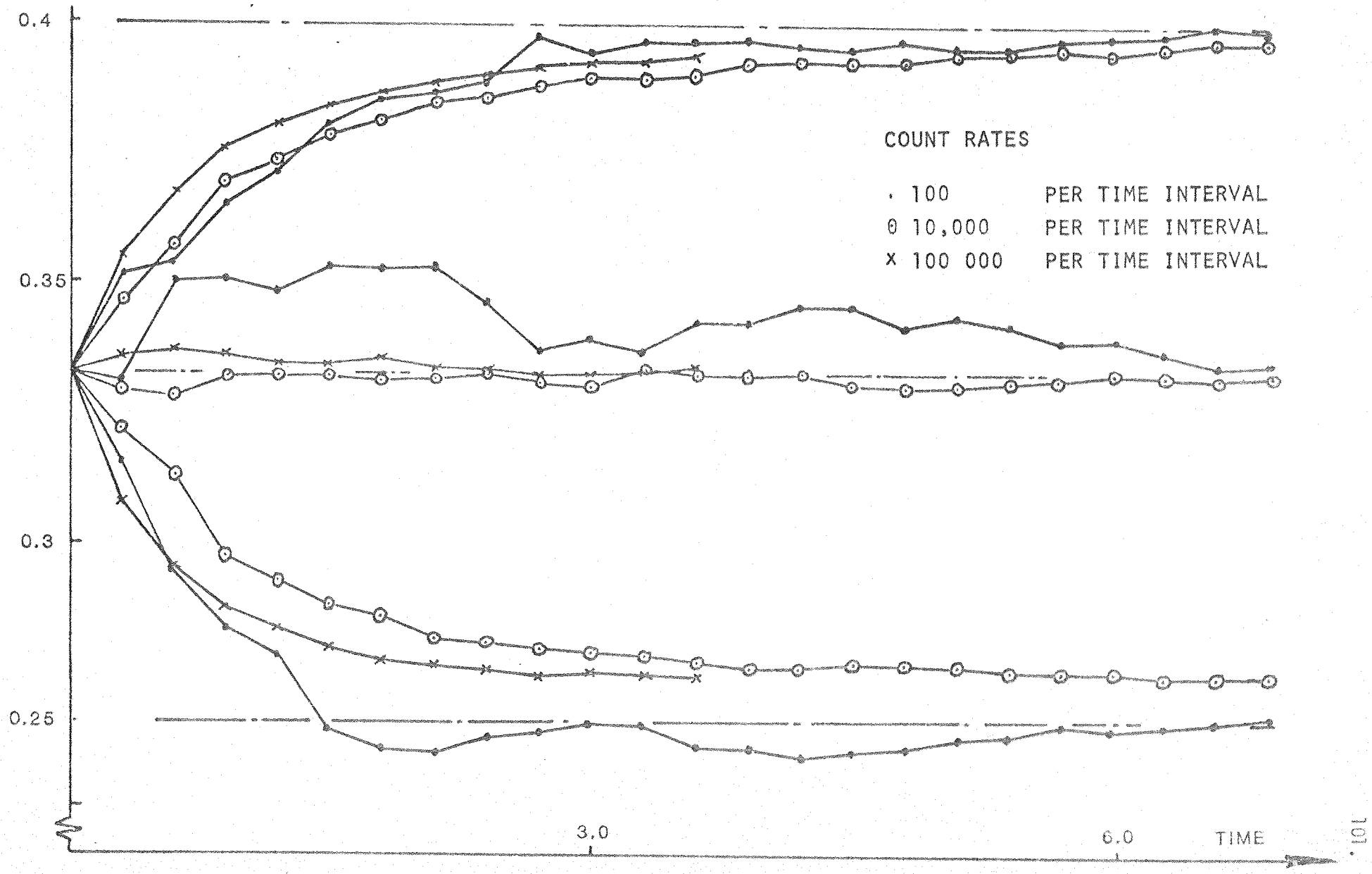

FIG 4.6 TIME EVOLUTION OF RATIO OF INDIVIDUAL TO TOTAL EXTRACTION RATE FOR TRUE RATES OF .4 , .5 , .6 AND TRUE RATIOS OF .266 , .333 , .400

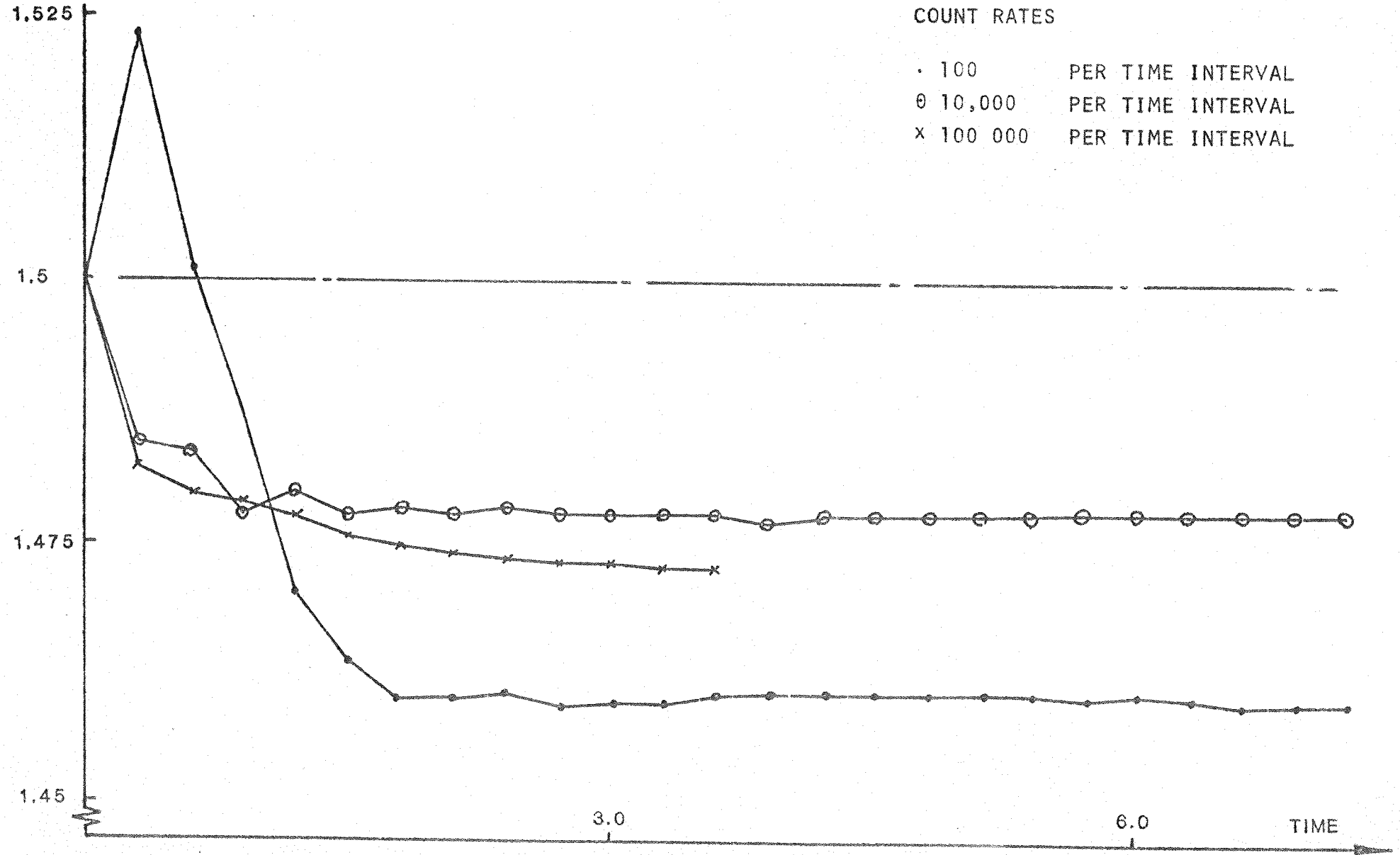

FIG 4.7 TIME EVOLUTION OF ESTIMATE OF TOTAL FLOW RATE TRUE VALUE 1.5

TRUE INDIVIDUAL RATES 0.4 , 0.5 , 0.6

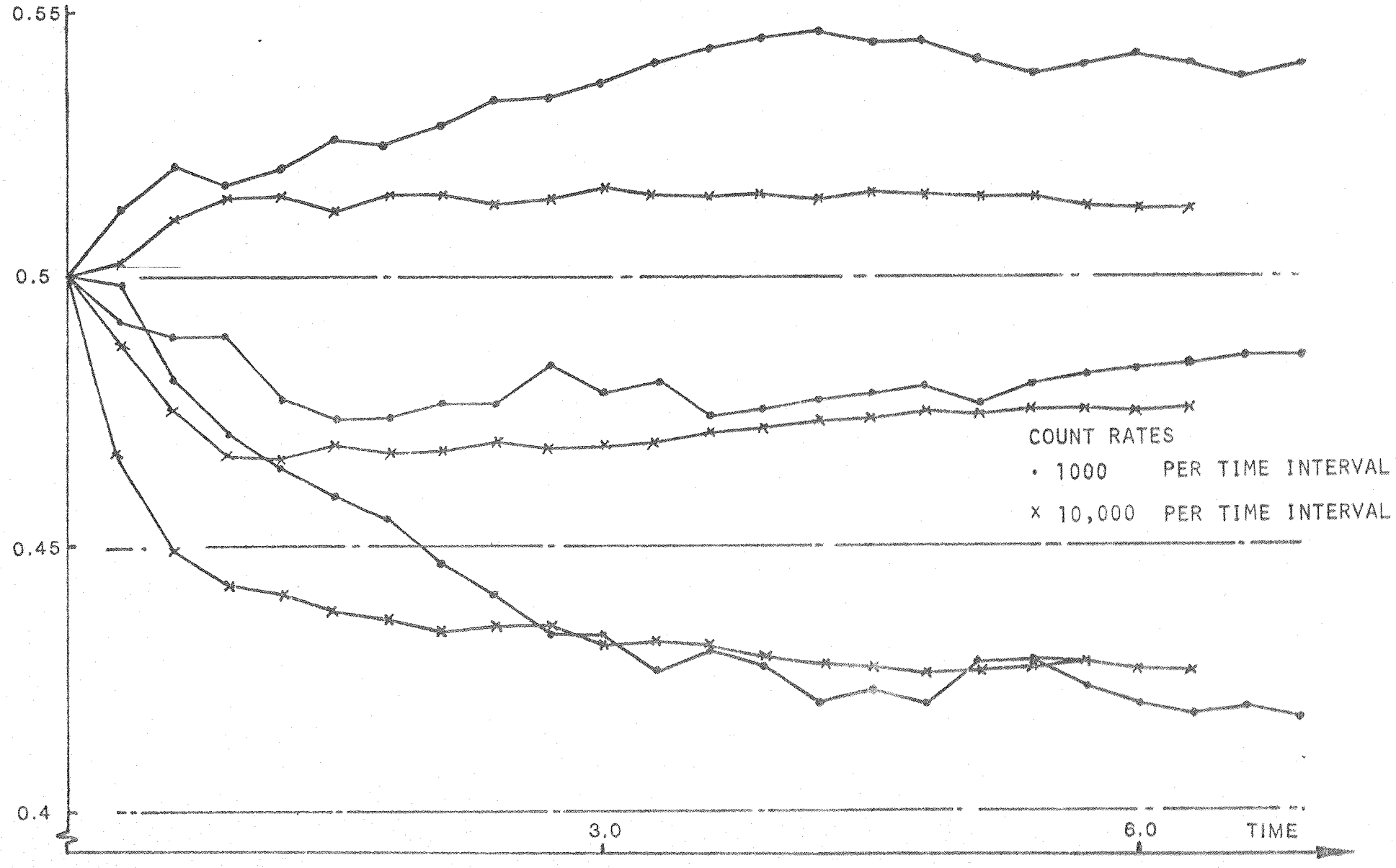

FIG 4.8 TIME EVOLUTION OF EXTRACTION RATES TRUE VALUES 0.4 , 0.45 , 0.5

INITIAL ESTIMATES 0.5 - 0.15

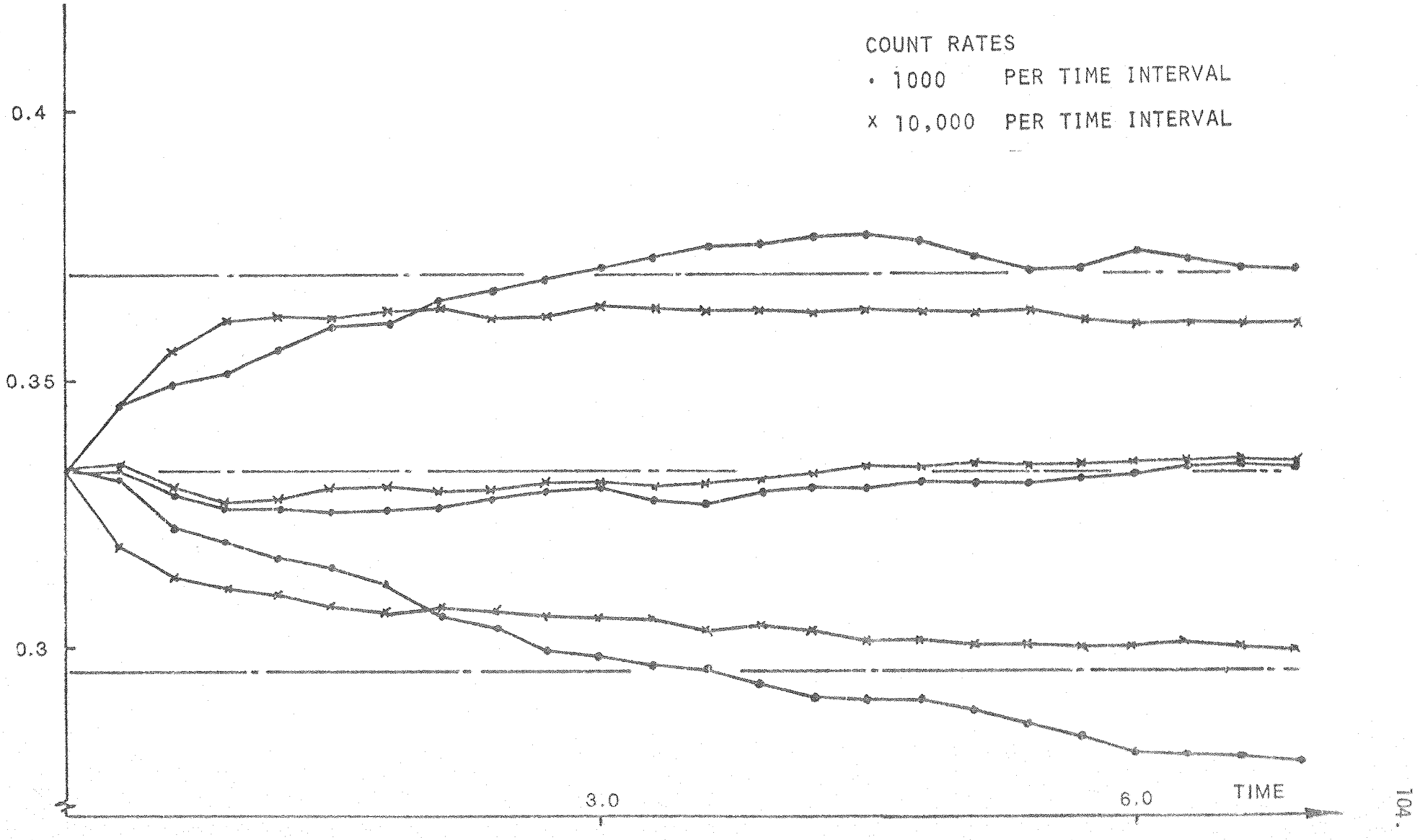

FIG 4.9 TIME EVOLUTION OF RATIO OF INDIVIDUAL TO TOTAL EXTRACTION RATE FOR TRUE RATES OF .4 , .45 , .5 AND TRUE RATIOS OF .296 , .333 , .370

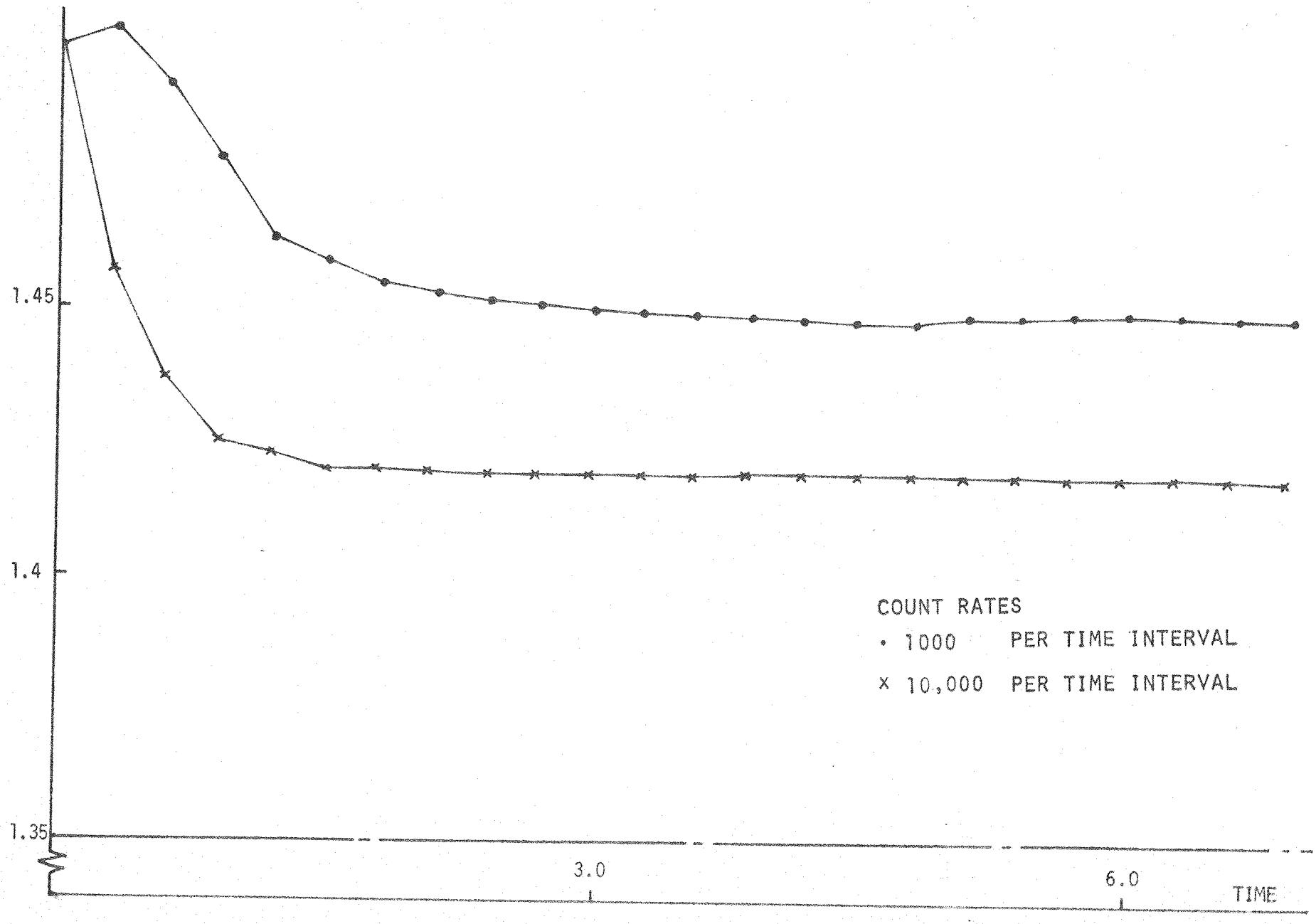

FIGURE 4.10 TIME EVOLUTION OF ESTIMATE OF TOTAL FLOW RATE TRUE VALUE 1.35

TRUE INDIVIDUAL RATES 0.4, 0.45, 0.5

true values of the model parameters are known, comparison of the estimates produced from the measurements can be made with true values to give a guide to the performance of the identification process. We first consider the curve fitting techniques.

Although some specialised curve fitting techniques which may be considered essentially as non sequential Kalman Filters can be used to give estimates of parameter errors, curve fitting routines in normal use give at most only the residue errors after curve fitting. They do not take into account apriori knowledge of the spread of parameter values and do not use the known statistics of the measurement noise in the production of the estimates of the states and errors in the estimates (covariance).

A curve fitting routine which gave no error estimates was used on patient data to produce estimates of the total flow rate. A listing of the program is given in Appendix F. The data was processed using a LINK system at Bristol Royal Infirmary to give customary pictorial representation of the data as shown in figures 4.12 to 4.14, then the curve fitting routines applied to give the total extraction rates. It should be noted that to obtain the correct measurement values so called 'blood background correction' needs to be applied. This is necessary since in the field of view of both the liver and spleen, plasma is present. This may be corrected for by subtraction of a certain fraction of general blood background, which may be observed at any region away from the liver spleen or bone, from the measurements over the liver and spleen. If this is done correctly then the liver and spleen curves will have equal total extraction rates as shown theoretically in Chapter 3. Results after processing the liver curve are shown in Table 4.2 and give an idea of typical values. Miller et al (Mil) gives further results using

the same method, showing the change of total extraction rate for differing diseases. The total extraction rates were of the order 0.15 min^{-1} giving a plateau after 15-20 minutes. The count rates observed were of the order 80,000 per minute over the liver region, giving a total count of the order 10^6 over the observation period up the the plateau.

To test the stochastic filter simulated measurements were used. The actual value of the simulated extraction rates were considered unimportant since scaling of the time axis can convert the measurement with nominal extraction rates to measurements of any desired extraction rate. The important parameter was considered to be the total number of counts in the measurements up to the plateau region. Very large counts equivalent to those experienced in real data were not simulated due to excessive computing time requirements with the facilities availiable, the total counts in the period of measurement up to the plateau being 10 to 100 times greater than those generated in the simulations. Despite this the results show the main trends experienced in the use of the filter and show the potentialities of the method.

The results verify the expected result that the total flow rate is only influenced by measurements taken before the plateau is reached, and that the results of the curve fitting techniques were more inaccurate than those obtained by the stochastic filter, but improved in accuracy as did those of the stochastic filter as the count rate was increased. The simulations showed that one would expect good correlation between the estimate and actual value of the total extractionrate for measurements with count rates of the order of 100 times greater than the maximum shown in Figure 4.10. This would correspond to total counts up to the plateau region in the order of 10^6, equivalent to the count density obtained using an Anger camera.

The ability of the filter to distinguish differing extraction rates can be tested in isolation to the estimation of the total extraction rate by estimating the ratio of the individual extraction rates to the total extraction rates. The time evolution of these ratio estimates are shown in Figures 4.6 and 4.9. The information can be estimated both from the data in the region up to the plateau and in the plateau region. Tolerable estimates were obtained with the highest count densities used, showing that good estimates would be obtained with real data from an Anger camera with a standard dose of 3-5 mCi. With the proposed Compton camera one would expect more accuracy in the estimate of total extraction rate with tighter confidence limits since the number of emissions which could be detected by the camera would be far higher due to the elimination of the lead collimator.

Count Rate 1000 per time unit

Actual Flow Rate	Stochastic Estimate Apriori	Final	Deterministic Estimate
Individual Rates			
.4	.5 ± .2	.389	
.5	.5 ± .2	.487	
.6	.5 ± .2	.582	
Total Rate			
1.5	1.5	1.451	2.14
Individual Rates			
.4	.5 ± .1	.419	
.45	.5 ± .1	.487	
.5	.5 ± .1	.541	
Total Rate			
1.35	1.5	1.447	1.985

Table 4.1a Comparison of Estimates due to Stochastic and Deterministic Algorithms, of the Extraction Rates of the Liver Spleen and Bone Marrow and of the Total Extraction Rate of all three organs

Count Rate 10,000 per time unit

Actual Flow Rate	Stochastic Estimate Apriori	Final	Deterministic Estimate
Individual Rates			
.4	.5 ± .15	.404	
.5	.5 ± .15	.488	
.6	.5 ± .15	.583	
Total Rate			
1.5	1.5	1.475	1.569
Individual Rates			
.4	.5 ± .15	.428	
.45	.5 ± .15	.477	
.5	.5 ± .15	.514	
Total Rate			
1.35	1.5	1.419	1.83

Count Rate 100,000 per time unit

Actual Flow Rate	Stochastic Estimate Apriori	Final	Deterministic Algorithm
Individual Rates			
.4	.5 ± .2	.403	
.5	.5 ± .2	.490	
.6	.5 ± .2	.578	
Total Rate			
1.5	1.5	1.471	1.81

Table 4.1b Comparison of Estimates due to Stochastic and Deterministic Algorithms

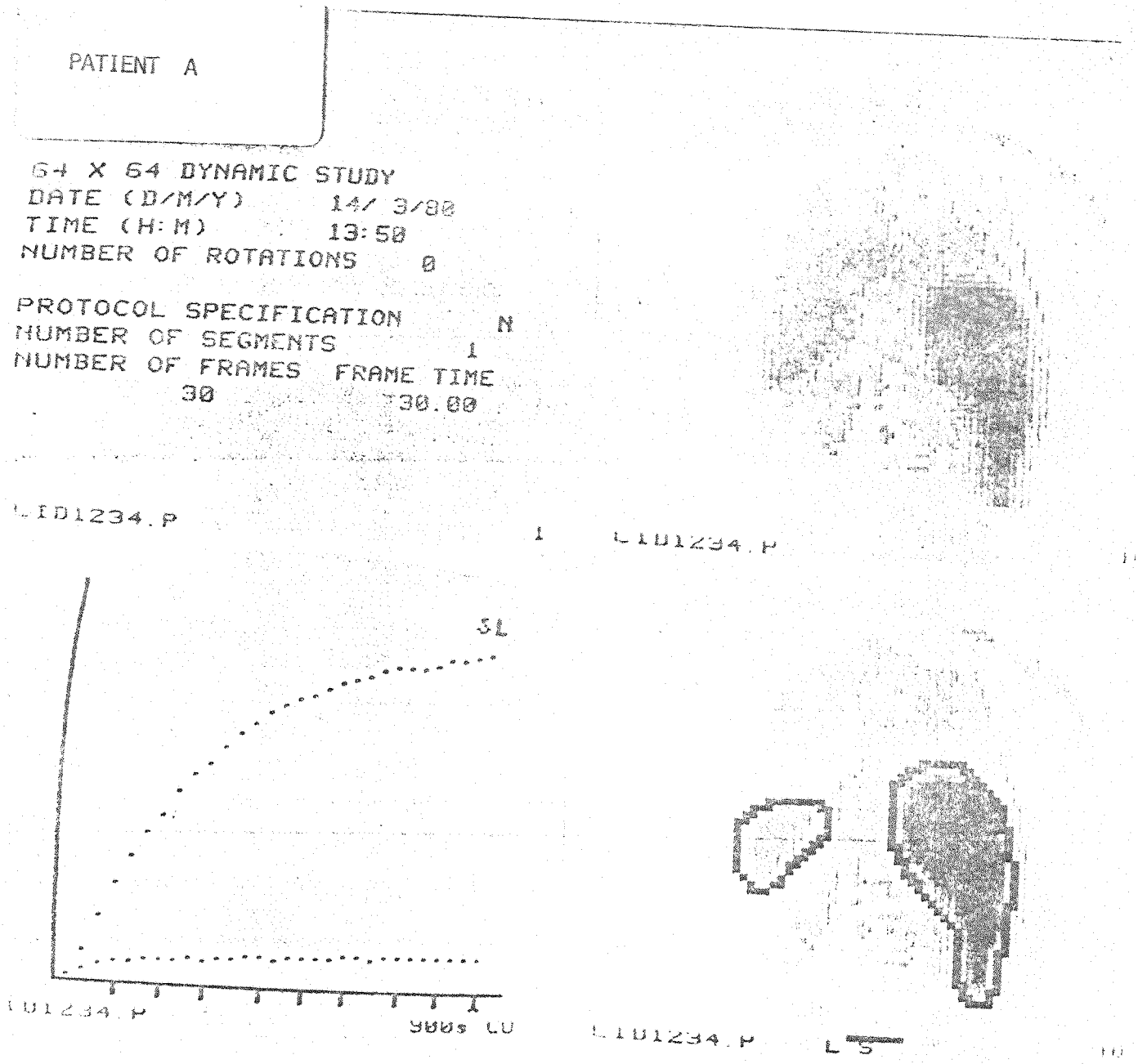

FIGURE 4.12 PICTORIAL RESULTS OF STUDY USING $^{99}Tc^{m}$ SULPHUR COLLOID : PATIENT A

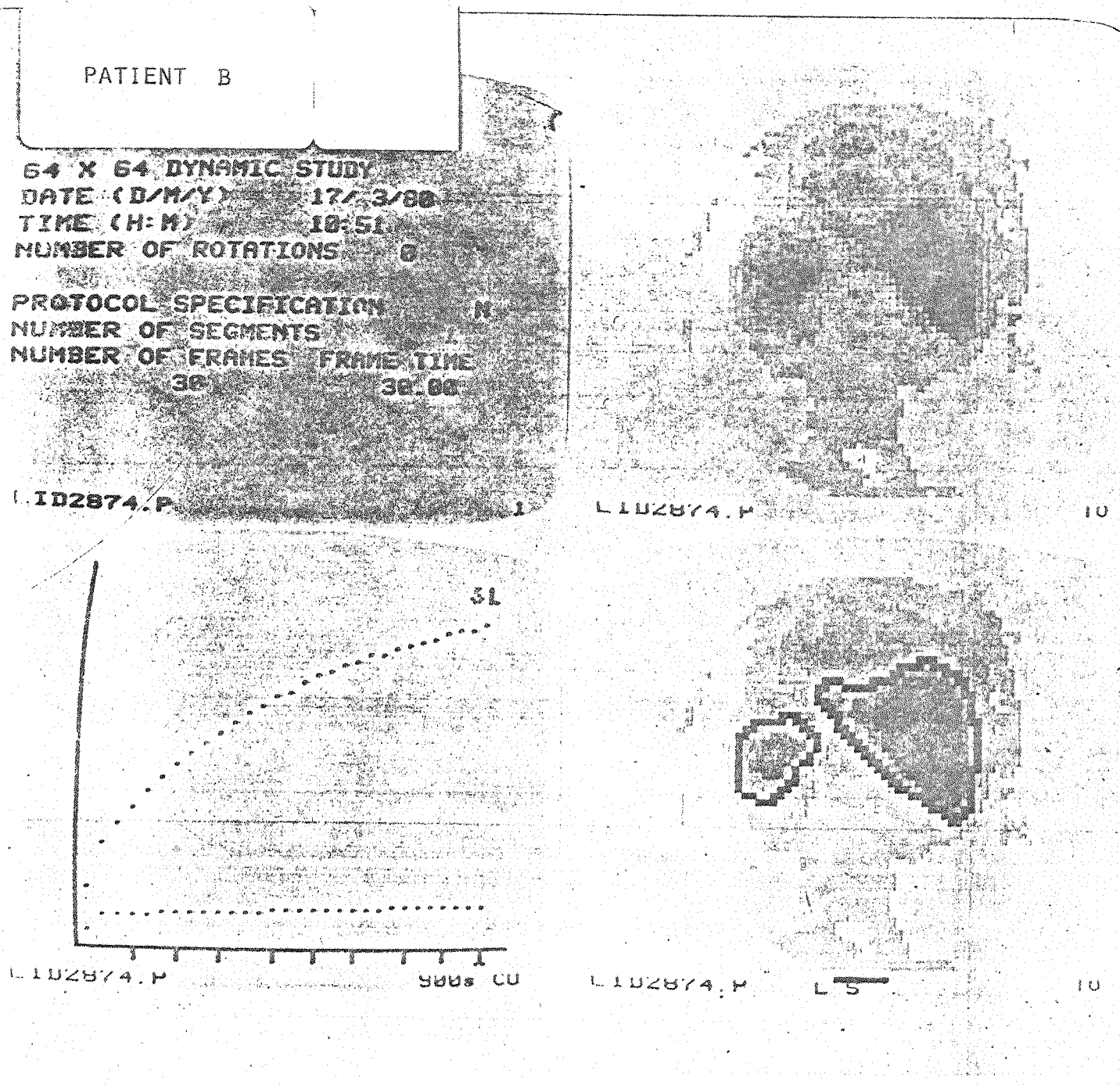

FIGURE 4.13 PICTORIAL RESULTS O STUDY USING $^{99}Tc^{m}$ SULPHUR COLLOID : PATIENT B

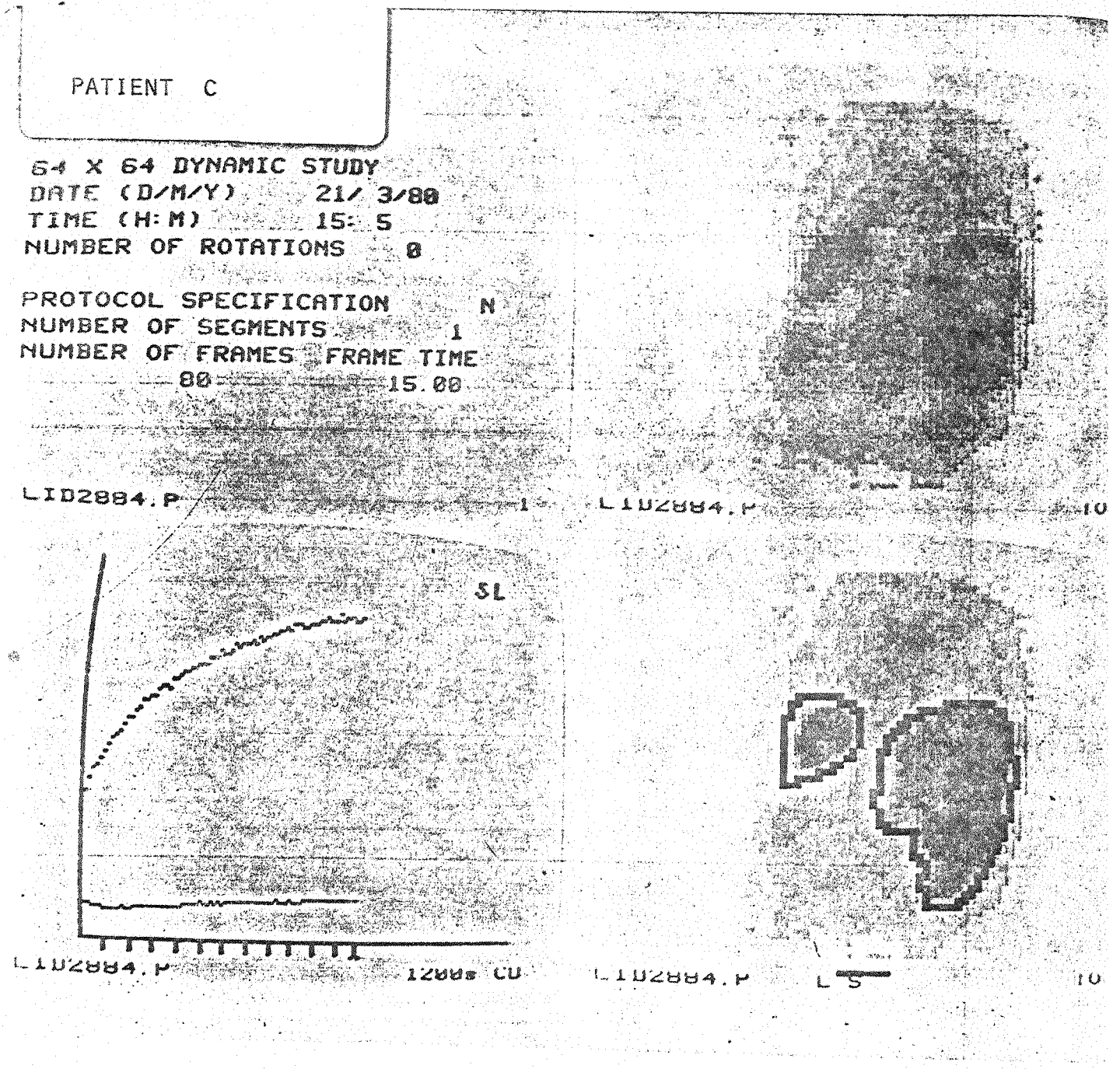

FIGURE 4.14 PICTORIAL RESULTS OF STUDY USING $^{99}Tc^{m}$ SULPHUR COLLOID : PATIENT C

Patient A	Total Extraction Rate	0.13 min^{-1}
Patient B	Total Extraction Rate	0.14 min^{-1}
Patient C	Total Extraction Rate	0.19 min^{-1}

Table 4.2 Comparison of Total Extraction Rates obtained using the Curve Fitting Method on Data Collected from Three Patients.

Conclusion and Further Work

An estimation scheme which takes full account of all apriori knowledge of the system and accounts for any system or measurement noise has been applied to the special case of estimation of the parameters affecting major systems of metabolistic flow in the body using radioactive tracers. The action of the body of four isotopes has been modelled, and the parameters of interest indicated. It has been shown how by the correct choice of the state variables of the estimation scheme, how these parameters may be identified.

The estimation scheme has been simulated using one of the metabolistic flow models. The results show that the parameters could be identified well with the number of counts normally availiable, and perhaps with far fewer counts allowing the possibility of a reduction of the radiation d se or the scanning time. It is therefore suggested that with this technique parameters could be identified using scanning times equivalent to those of static scans in everyday use.

Further reduction in scan times or improvement in the accuracy of results, of use especially in models with large numbers of parameters to estimate, could be made with improved equipment capable of responding to radiation not parallel to collimator holes, potentially possible with the use of a novel camera depending upon the Compton effect for its imaging ability. One outstanding difficulty of this camera is the computation time required to produce the image. Fast algorithms have been proposed to overcome this problem.

Difficulties besetting any quantitative technique in nuclear medicine is the need to compensate for absorbtion in tissue, air or other substances obstructing the path from the source to the radiation detector. One method for doing this is computerised tomography. This

after its success in the E.M.I. scanner is slowly being adopted by most medical systems to be used in conjunction with moving head Anger cameras. The computing time now offered is in most cases prohibitively slow, but with the introduction of new techniques if the computing time could be reduced to those approached by the most modern of X-ray scanners, then each scan could be regarded as a discrete measurement to be used by the estimation scheme proposed in this thesis, giving a technique which would give absolute metabolistic rates, be on-line, non-invasive thus providing a quick non-traumatic method of patient diagnosis. Using present devices the methods outlined by this thesis driven by measurements from an Anger camera, or indeed several hand held probes, would give information about metabolistic rates, which although difficult to express in absolute units can be compared with the results obtained from normal patients, and can certainly be used to diagnose and quantify the degree of malfunction of body organs.

REFERENCES

(Ale) ALEKSANDROVSKII, N.M. and DEITCH, A.M. : "Determination of Dynamic Characteristics of Non-linear Objects" review. Automn Remote Control, 29, 142-160, 1968.

(Ang 1) ANGER, H.O. : "A new Instrument for Mapping Gamma Ray Emitters" Biology and Medicine Quarterly Report, UCRL-3653, Jan. 1957.

(Ang 2) ANGER, H.O. : "A Survey of Radioisotope Cameras" ISA Transactions, 5, 311-334, 1966.

(Arn) ARNOLD, R.W., SUBRAMANIAN, G., McAFEE, J.C. et al : "Comparison of ^{99}Tc Complexes for Renal Imaging" J.Nucl.Med., 16, 357-367, 1975.

(Ast) ASTROM, K.J. and EYKOFF, P. : "System Identification - A Survey" Automatica, 7, 123-162 and Pergamon Press 1971.

(Ath 1) ATHANS, M., WISHNER, R.P. and BERTOLINI, A. : "Suboptimal State Estimation for Continuous Time Non-linear Systems from Discrete Noisy Measurements" IEEE, AC-13, No. 5, 504-514, October 1968.

(Ath 2) ATHANS, M. and FALB, P.L. : "Optimal Control" Mc Graw Hill, New York, 1966.

(Bal) BALAKRISHNAN, A.V. and PETVKA, V. : "Identification in Automatic Control Systems" Proc. Fourth IFAC Congress, Warsaw, Survey paper aso in Automatica 5, 817-829, 1969.

(Bek) BEKEY, G.A. : "Identification of Dynamic Systems by Digital Computers" Joint Automatic Control Conf. (Computer Control Workshop), 7-18, 1969.

(Bio) BIOZZI, G., BENACERRAF, HALPERN, B.N. et al : "Phagocytosis of Heat-denatured Human Serum Albumin labelled with ^{131}I and Application to the Measurement of Liver Blood Flow in Normal Man and in some Pathologic Conditions" J.Lab.Clin.Med., 51, 230-239, 1959.

(Bos) VAN DEN BOS, A. : "Estimation of Linear System Coefficients from Noisy Responses to Binary Multifrequency Test Signals" Second IFAC Symp. Identification and Process Parameter Estimation, Prague 7.2, 1970.

(Bre) BREIMAN, L. : "Probability Theory" Addison-Wesley, Reading, Mass, 1968.

(Bro) BROCKETT, R.W. and MESAROVIC, M.D. : "The Reproducibility of Multivariable Control Systems" J.M.A.A., 11, 548-563, 1965.

(Buc) BUCY, R.S. and JOSEPH, P.D. : "Filtering for Stochastic Processes with Applications to Guidance" Wiley, New York, 1968.

(Cha) CHANTER, C., GARNETT, E.S., PARSONS, V. and VEALL, N. : "Glomerular Filtration Rate Measurements in Man by the Single Injection Method using ^{51}Cr-EDTA. Clin. Sq. 35, 169-180, 1969.

(Chr) CHRISTIE, J.H., CRESTO, G., KOCK-WESTER, D. et. al. : "The Correlation of Clearance and Distribution of Colloidal Gold in the Liver as an Index of Hepatic Conditions" Radiology, 88, 334-340, 1967.

(Cla) CLARK, J.R. : "Estimation for Poisson Processes with Applications in Optical Communications" Ph.D. Thesis, MIT, 1971.

(Cot) COTTON, L.T. and RICHARDS, J. : "The Measurement of Venous Blood flow by the Measurement of Local Thermal Dilution" published in: Bain, W.H. (Ed) Blood Flow Through Organs and Tissues. E.S. Livingstone, Edinburgh and London, 1968.

(Cow) COWLES, A.C. BERGSTEDT, H.H. and GILLIES, A.J. : "Tissue Weights and Rates of Blood Flow in Man for the Prediction of Anaesthetic Uptake and Distribution" Anaesthesiology, 35 N. 5, 1971.

(Cra) CRAMER, H. and LEADBETTER, M.R. : "Stationary and Related Stochastic Processes" Wiley, New York, 1967.

(Cue) CUENOD, M. and SAGA, A. : "Comparison of some Methods used for Process Identification" IFAC Symp. Identification in Autom Control Systems, Prague, Survey paper. also in Automatica 4 235-269, 1968.

(Cul 1) CULVER, C.O. : "Optimal Estimation for Non-linear Stochastic Systems" Sc.D. Thesis, MIT, 1968.

(Cul 2) CULVER, C.O. : "Optimal Estimation for Non-linear Systems" AIAA Conference, Princeton, N.J., 1969, AIAA paper No. 69-852.

(Cum) CUMMING, I.G. : "Frequency of Input Signal in Identification" Second IFAC Symp. Identification and Process Parameter Estimation, Prague, paper 7.8, 1970.

(Den) DENARDO, S.J., BELL, G.B. et al : "Diagnosis of Cirrhosis and Hepatitis by Quantitative Heptic and other Reticuloendothelial Clearance Rates". J. Nucl. Med., 17, 449-459, 1976.

(Det) DETKO, J. : "Semiconductor Diode Matrix for Isotope Localisation" Phys. Med. Biol. 14,2, 245-253, 1968.

(Dob 1) DOBSON, E.L., WARNER, G.F., FINNEY, C.R. et al. : "The Measurement of Liver Circulation by means of the Colloid Dissapearance Rate". Circulation, 7, 670-695, 1953.

(Dob 2) DOBSON, E.L. and JAMES, H.B. : "The Behavior of Intravenously Injected Particulate Material : Its Rate of Dissapearance from the Blood Stream as a Measure of Liver Blood Flow" Acta. Med. Scand., 144, Supp. 273, 1952.

(Doo) DOOB, J.L. : "Stochastic Processes" Wiley, New York, 1953.

(Dos) DOSHI, R.B. : "Digital Image Processing and its Application to Compton Gamma Ray Camera" Ph.D. Thesis, University of Southampton, 1976.

(Dun) DUNCAN T.E. : "Probability Densities for Diffusion Processes with Applications to Non-linear Filtering Theory and Detection Theory" Ph.D. Thesis, Stanford University, 1967.

(Dyn) DYNKIN, E.B. : Markov Process, Vol. 1. Academic, New York 1965.

(Eve) EVERETT, D.B. : "A Proposed Gamma Ray Camera using the Compton Effect" Ph.D. Thesis, University of Southampton, 1975.

(Eve 2) EVERETT, D.B. and FLEMMING, J.S. : "An Investigation of the use of the Compton Effect in Gamma Ray Cameras" Joint project of Southampton University Control Group and the Wessex Regional Hospital Board Department of Nuclear Medicine.

(Eyk 1) EYKHOFF, P. : System Identification, Wiley Interscience, 1974

(Eyk 2) EYKHOFF, P. : "Process Parameter and State Estimation" IFAC. Symp. Identification in Autom. Control Systems, Prague, Survey Paper. Also in Automatica, 4, 205-233, 1966.

(Eyk 3) EYKHOFF, P, VAN der GRINTEN, P.M., KWAKERNAAK, H. and VELTMAN, B.P. : "Systems Modelling and Identification". Proc. Third IFAC Contress, London, Survey Paper, 1966.

(Eyk 4) EYKHOFF, P. : "Some Fundamental Aspects of Process - Parameter Estimation" IEEE Transactions Aut. Control., Ac.-8, 347-357, 1963.

(Fit) FITCH, W.R. : "The Generation and Time Domain Filtering of the Image of the Compton Effect Gamma Ray Camera" M.Phil Ph.D. Transfer Report. University of Southampton, December, 1977.

(Fle) FLEMING, J.S., : "Compton Effect Gamma Camera Detector System" Ph.D. Thesis, University of Southampton, 1975.

(Fre) FREEMAN, H. : Introduction to Statistical Inference, Addison Wesley, Massachusetts, 1963.

(Fro) FROST, P.A. : "Non-linear Estimation in Continuous Time Systems" Ph.D. Thesis, Stanford University, 1968.

(Gik) GIKHMAN, I.I. and SKOROKHOD, A.V. : "Introduction to the Theory of Ramdon Processes" Saunders, Philadelphia, 1969.

(God) GODFREY, K.R. : "The Application of Pseudo-Random Sequences to Industrial Processes and Nuclear Power Plant" Second IFAC Symp. Identification and Process Parameter Estimation, Prague, Paper 7.1, 1970.

(Gre) GRENADER, U. and ROSERBLATT, M. : "Statistical Analysis of Stationary Time Series" Wiley, New York, 1957.

(Hal) HALMOS, P. : "Measure Theory" Van Nostrand, Princeton, New Jersey, 1950.

(Hid) HIDA, T. : "Stationary Stochastic Processes" Princeton University Press, Princeton, New Jersey, 1970.

(Hil) HILSON, A.J.W., MOISEY, M.N., BROWN, C.B. et al : "Dynamic Renal Transplant Imaging with Tc - 99m DTPA (Sn) Supplanted by a Transplant Perfusion Index in the Management of Renal Transplants" : J.Nucl. Med., 19, 994-1000, 1978.

(Hir) HIRAMATSU, Y. R.E. O'MARA, McAFEE, J.C. et al : "Intrarenal Distribution of Diagnostic Agents" Invest Radiol, 5, 295-310, 1970.

(Hof) HOFKER, W.K. and D.P. OESTHOEK, D.P. : "The Checker Board Counter ; A semiconductor dE/dx Detector with Position Indicatio IEEE Trans. Nucl. Sci. NS-13/3, 208, 1966.

(Ito) ITO, K, : "Lectures on Stochastic Processes" Tata Institute of Fundamental Research, Bombay, India, 1961.

(Jas 1) JASWINSKI, A.H. : "Filtering for Non-linear Systems" IEEE, AC-11, 765-766, October 1966.

(Jas 2) JASWINSKI, A.H. : "Stochastic Processes and Filtering Theory" Academic, New York, 1970.

(Jen) JENKINS, G. and WATTS, D. : "Spectral Analysis and its Applications Holden Day, San Fransisco, 1968.

(Kal) KALMAN, R.E. : "A New Approach to Linear Filtering and Prediction Problems" J.Basic Engineering, 35-45, March 1960.

(Kar) KARRAN, S.J, EAGLES, C.J., FLEMING, J.S. and ACKERY, D.M. : "In Vivo Measurement of Liver Perfusion in the Normal and Partially Hepatectomized Rat using Tc-99m Sulphur Colloid" J. Nuclear Med, 20, 26-31, 1979.

(Kau) KAUFMAN, L., PEREZ-MEDEZ, V RINDI, A. etal : "Wire Spark Chambers for Clinical Imaging of Gamma Rays" Phys. Med. Biol., 16, 3, 417-426, 1971.

(Kaz) KAZEM, I. and GELINSKY, P. : "Nierenszintigraphie mit Ferro - ^{99}Tc - Komplex Teil II Gewebsverteilung und Biologishes Verhalten". Nucl. Med. (Stuttg.) 5, 409-420, 1966.

(Kus) KUSHNER, H.J. : "Introduction to Stochastic Control" Holt, Rinehart, New York, 1971.

(Kus 2) KUSHNER, H.J. : "On the Convergence of Lions Identification Method with Random Inputs" Report, Division of Applied Mathem, Brown University, R.I. 1969.

(Lan) LANDAU, I.D. : "An Approach to Synthesis of Model Reference Adaptive Control Systems" Report, Alsthon-Recherches. Also in IEEE Trans. Autom. Control 1970.

(Lee) LEE, R.C.K. : "Optimal Estimation, Identification and Control" MIT Press, Cambridge, Mass, 1964.

(Lie) LIEBELT, P.B. : "An Introduction to Optimal Estimation" Addison Wesley, 1967.

(Lin) LIN, T.H., KHENTIGAN, A. and WINCHELL, H.S. : "A ^{99m}Tc Chelate Substitute for Organoradiomercurial Renal Agents" J.Nucl.Med., 15, 34-35, 1974.

(Lio) LION, P.M. : "Rapid Identification of Linear and Non-linear Systems" Preprint, JACC, Washington, 1966.

(Lob) LOBERG, M.D., COOPER, M. HARVEY, F. et al : "Development of New Radiopharmacuticals Based on N-substitution of Iminodiacetic Acid" J.Nucl.Med., 17, 633-638, 1976.

(Loe) LOEVE, M. : "Probability Theory" Van Nostrand, Princeton, New Jersey, 1963.

(Man) MANN, H.B. and WALD, A. "On the Statistical Treatment of Linear Stochastic Difference Equations" Econometrica 11 Nos. 3 and 4, 1943.

(Man) MANN, H.B. and WALD, : "On the Statistical Treatment of Linear Stochastic Difference Equations". Econometrica 11, No. 3&4, 1943.

(Map) MAPLESON, W.W. : "Circulation Time Models of the Uptake of the Inhaled Anaethetics and Data for Quantifying them. Brit J. Anaesthesia, 43, 319, 1979.

(McG) MCGARTY, T.P. : "Stochastic Systems and State Estimation" Wiley, New York, 1974.

(McK) MCKEAN, H.P. : "Stochastic Integrals" Academic, New York, 1969.

(Med 1) MEDITCH, J.S. : "Orthogonal Projections and Discrete Linear Smoothing" j.SIAM Control, J, No.1. 74-89, 1967.

(Med 2) MEDITCH, J.S. : "Optimal Estimation and Control" McGraw Hill, New York, 1969.

(Mil) MILLER, J., DIFFEY, B.L. and FLEMING, J.S. : "Measurement of Colloid Clearance Rate as an Adjunct to Static Liver Imaging" Eur.J.Nucl.Med., 4, 1-5, 1979.

(Moo) MOODY, N.F. et al : "A Survey of Medical Gamma Ray Cameras" Proc. IEEE, 58,2, 217-242, 1970.

(Moy) MOYAL, J.E., : "Stochastic Processes and Statistical Physics" J. Royal Stat. Soc., Ser. B., 11, No.2, 150-210, 1949.

(Mun) MUNDSCHENK, H., HROMEC, A. and FISHER, J. : "Phagocytic Activity of the Liver as a Measure of Heptic Circulation - A Comparitive Study using ^{198}Au and ^{99}Tc - Sulphur Colloid" J. Nucl. Med., 12, 711-718, 1971.

(Nev) NEVEN, J. : "The Calculus of Probability", Holden Day, San Fransisco, 1965.

(Nik) NIKOFORUK, P.N. and GUPTA, M.M. : "A Bibliography of the Properties, Generation and Control Systems Applications of Shift Register Sequences", Int. J. Control, 9, 217-234, 1969.

(Oga) OGATA, K. : "State Space Analysis of Control Systems" Prentice Hall, Englewood Cliffs, New Jersey, 1967.

(Par) PARKER, R.P., GUNNERSEN, E.M. and WANKIN, J.L. : "Medical Radioisotope Scintigraphy" Vienna, IAEA, 1, 71-85, 1969.

(Pat 1) A Method of and Apparatus for Examination of a Body by Radiation such as X or Gamma Radiation, Patent Specification No. 1283915, 1972.

(Pol) POLAK, E. and WONG, E. : "Notes for a First Course on Linear Systems" Van Nostrand, New York, 1970.

(Paw) PAWULA, R.F. : "Generalisations and Extensions of the Fokker-Planck-Kolmogorov Equations". I.E.E.E., IT-13, 33-41, January, 1967.

(Paz) PAZDERA, J.S. and POTTINGER, H.L. : "Linear System Identification via Liapunov Design Techniques" Preprints J.ACC, 795-801, 1969.

(Pla) PLAYOUST, M.R., MCRAC, J. and BOWDEN, R.W. : "Inefficient Hepatic Extraction of Colloidal Gold : Resulting Inaccuracies in Determination of Hepatic Blood Flow" J.Lab. Clin. Med, 54, 728-738, 1959.

(Pop) POPOV, V.M. : "Absolute Stability of Non-linear Systems of Automatic Control" Automn. Remote Control, 22, 857-875, 1962.

(Pot) POTTS, T.F., ORNSTEIN, G.N. and CLYMER, A.B. : "The Automatic Determination of Human and Other Parameters" Proc. West. Joint Computer Conf., Los Angeles, 19, 645-660, 1961.

(Sag) SAGA, A.P. and MELSA, J.L. : "System Identification" Academic, London, 1971.

(Sap) SAPIRSTEIN, L.A., VINDT, D.G. MANDEL, M.J. and HANUSEC, G. : "Volumes of Distribution and Clearances of Intravenously Injected Creatmine in the Dog" Amer.J. Physiol., 181, 330-336, May 1955.

(Sch) SCHILLY, P., KLEINKNECT, K. STEFFEN, P. et al : "Construction and Performance of Large Multiwire Proportional Chambers" Nucl. Inst. Meth., 91,221-230, 1971.

(Sha) SHACKCLOTH, B. and BUTCHART, R.L. : "Synthesis of Model Reference Adaptive System by Liapunov's Second Method" IFAC Symp., Theory of Selfadaptive Control Systems, Teddington, 145-152, 1965.

(Sil) SILVERMAN, L.M. : "Inversion of Multivariable Linear Systems" I.E.E.E. Trans. Aut. Control AC-14, 270-276, 1969.

(Sko) SKOROKHOD, A.V. : "Studies in the Theory of Random Processes Addison Wesley, Reading, Mass., 1965.

(Sny 1) SNYDER, D.L. : "The State Variable Approach to Continuous Estimations" Ph.D. Thesis, M.I.T., Cambridge, Mass, 1966.

(Sny 2) SNYDER, D.L. : "The State Variable Approach to Analog Communication Theory" I.E.E.E. IT. 14, 1, 94-104, January, 1968.

(Sny 3) SNYDER, D.L. : "The State Variable Approach to Continuous Estimation with Application to Analog Communication Theory" MIT Press, Cambridge, Mass, 1969.

(Sny 4) SNYDER, D.L. : "Estimation of Stochastic Intensity Fuctions of Conditional Poisson Processes". Monography No. 128, Biomedical Computer Lab., Washington University, St. Louis, Mo., April 1970.

(Syn 5) SNYDER, D.L. : "Detection of Non-homogeneous Poisson Processes Having Stochastic Intensity Fuctions" Monograph No. 129, Biomedical Computer Lab., Washington University, St. Louis, Mo. April, 1970.

(Tap) TAPLIN, G.V. : "Dynamic Studies of Liver Function with Radioisotopes" In : Dynamic Studies with Radioisotopes in Medicine Unipub Inc., New York, 373-392, 1971.

(Ter) TER-PORGOSIAN, KASTNER, M.J., and VEST, T.B. : "Autofluorography of the Thyroid Gland by means of Image Amplification" Am. J. Roentgenol. Radio Therapy Nucl. Med, 81, 984, 1963.

(Tod) TODD, R.W. : "Proposed Gamma Ray Camera" Southampton University Control Group Report. 1974.

(Tre) TREVES, F. : "Basic Linear Partial Differential Equations Academic, New York, 1975.

(Uhl) UHLENBECK, G.E. and ORNSTEIN, I.S. : "On the Theory of Brownian Motion" Phys. Rev. 36, 823-841, September, 1930.

(Van) VAN TREES, H.L. : "Detection, Estimation and Modulation Theory" Vol. 1., Wiley, New York, 1965.

(Vet) VETTER, H., FALKNER, R. and NEURMAYR, A. : "The dissapearance rate of Colloidal Radiogold from the Circulation and its application to the Estimation of Liver Blood Flow in Normal and Cirrhotic Subjects" J. Clin. Invest., 33, 1594-1602, 1954.

(Wan) WANG, M.C. and UHLENBECK, G.E. : "On the Theory of the Brownian Motion" Rev. Modern. Phys., 17, Nos. 2 and 3, 323-342, April-July 1945.

(Whi) WHITTLE, P. : "Prediction and Regulation" Van Nostrand,Princeton, N.J. 1963.

(Wil) WILSON, G.A. and KEYES, J.W. : "The Significance of the Liver Spleen. Uptake Ratio in Liver Scanning" J. Nucl. Med., 15, 593-597, 1974.

(Wis) WISTOW, B.W., SUBRAMANIAN, G.,VAN HEERRTUM, R.L. et al : "An Evaluation of ^{99m}Tc labelled Hepatobiliary Agents" J. Nucl. Med. 18, 455-461, 1977.

(Wong) WONG, E. : "Stochastic Processes in Information and Dynamical Systems, McGraw Hill, New York, 1971.

(Wonh) WONHAM, W.M. : "Random Differential Equations in Control Theory" in A.T. Bharucha-Reid (ED) Probabalistic Methods in Applied Mathematics, Academic, New York, 131-212, 1970.

(Zad) ZADEH, L.A. : "From Circuit Theory to System Theory" Proc IRE., 50, 856-865, 1962.

(Zac) ZAKLAND, H., ALVAREZ, L.W., DERENZO, S.E. et al : "A Liquid Xerox Radioistope Camera" I.E.E.E. Trans Nuclear. Science. NS-19, 3, 206-213, June 1972.

(Zam) ZAMES, G. : "On the Input-Output Stability of Time Varying Non-Linear Feedback Systems, I.E.E.E. Trans Autom Control, 228-238, 1966.

APPENDIX A

THE COMPTON EFFECT

The Compton Effect occurs when a photon, a packet of electromagnetic radiation collides with a loosely bound electron. This commonly occurs in semiconductors where many electrons exist in energy bands, move throughout the whole structure and are not attached to individual atoms. In a Compton collision the photon is deflected and continues with reduced energy and hence with an increased wavelength. The electron is scattered with an energy equal to that lost by the photon. In this section we derive an expression for the angle through which the photon is deflected in terms of the initial energy of the photon, and the energy aquired by the electron.

Consider Figure A.1 which shows a photon scattered by a loosely bound electron. The total momentum of the photon is given by

$$p = h/\lambda$$

where

p = momentum of photon

h = Plancks Constant (6.636×10^{-3} Js)

λ = Wavelength of the radiation

Equating the momenta before and after impact in the directions parallel to and at right angles to the initial direction of the photon gives

$$\frac{h}{\lambda_1} = \frac{h}{\lambda_2} \cos \psi + mv \cos \theta$$

$$0 = \frac{h}{\lambda_2} \sin \psi - mv \sin \theta$$

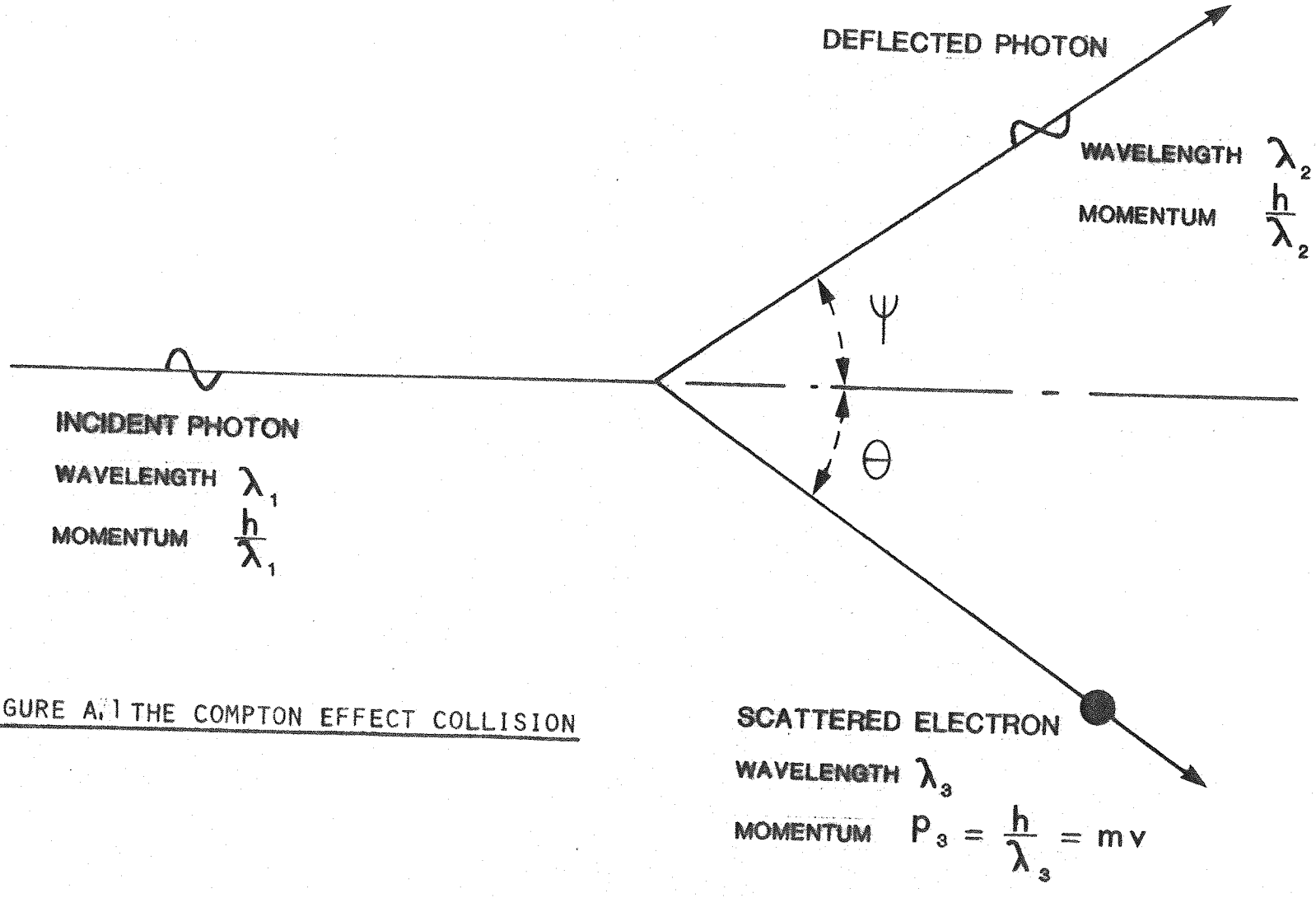

FIGURE A.1 THE COMPTON EFFECT COLLISION

hence we obtain

$$m^2v^2 = \frac{h}{\lambda_1^2} - \frac{2h^2}{\lambda_1\lambda_2}\cos\psi + \frac{h^2}{\lambda_2^2} \qquad (A.1)$$

Equating energy before and after impact we obtain

$$\frac{hc}{\lambda_1} + m_o c^2 = \frac{hc}{\lambda_2} + mc^2$$

$$\therefore \quad \frac{h}{\lambda_1} - \frac{h}{\lambda_2} + m_o c = mc \qquad (A.2)$$

The mass of an electron travelling with velocity v is given by

$$m = \frac{m_o}{(1 - (v/c)^2)^{\frac{1}{2}}}$$

hence

$$m^2v^2 = m^2c^2 - m_o^2c_o^2 \qquad (A.3)$$

Substituting equation (A.2) into equation (A.3) gives:

$$m^2v^2 = \left(\frac{h}{\lambda_1} - \frac{h}{\lambda_2} + m_o c \right)^2 + m_o^2c^2 \qquad (A.4)$$

Eliminating m^2v^2 between equation (A.1) and equation (A.4) gives

$$\frac{2h}{\lambda_1\lambda_2}\cos\psi = \frac{2h^2}{\lambda_1\lambda_2} 2 m_o c \left(\frac{h}{\lambda_2} - \frac{h}{\lambda_1} \right)$$

multiplying by

$$\frac{\lambda_1\lambda_2}{2h\, m_o\, c}$$

gives

$$\Delta\lambda \equiv \lambda_2 - \lambda_1 = \frac{h}{m_o c} (1 - \cos \psi) \qquad (A.5)$$

showing that the change in wavelength is independent of the initial wavelength.

If the energy of the incident photon is E_1 that of the emerging E_2 and the energy of the electron after the collision E_3, then, since the relationship between wavelength and energy is $\lambda = h\,c/E$ then equation (A.5) becomes

$$\frac{hc}{E_2} - \frac{hc}{E_1} = \frac{h}{m_o c} (1 - \cos \psi)$$

We know that energy is conserved in the collision

$$E_1 = E_2 + E_3$$

hence we may write

$$\frac{hc}{E_1 - E_3} - \frac{hc}{E_1} = \frac{h}{m_o c} (1 - \cos \psi) \qquad (A.6)$$

Thus the angle of deflection may be expressed in terms of the initial energy of the photon E_1 and the energy aquired by the electron in the collision

$$\psi = \cos^{-1} \left[1 - \frac{m_o c^2 E_3}{E_1 (E_1 - E_3)} \right] \qquad (A.7)$$

APPENDIX B

ANALYSIS OF NOISE PROCESSES

Introduction

Two processes which are commonly used to describe noise in both system and measurements are the Poisson and Wiener processes. These are both special forms of a class called stochastic processes. In this section mathematical descriptions of random and stochastic processes are given, and by the use of successive restrictions the Markov process, and then the Poisson and Wiener Processes are defined.

Definitions

To describe a random process the concept of a probability space is required.

Probability Space

The elements from which this can be constructed are:

(a) A certain or sure event Ω of probability 1

(b) A set of less sure events A_i

(c) A field in which the events A_i lie called a σ field

(d) A probability measure P

We now define the σ field and probability measure P and give a definition of the probability space, see reference (Haz) for a full description.

σ field A

A class of set $\{A_i\}$ is called a σ field A if

(1) $\Omega \in A$, $\phi \in A$ where ϕ is the null set and Ω is the sure event

(2) $A_i \cup A_j \in A$ if $A_i, A_j \in A$

(3) $A_i^{\,c} \in A$ if $A_i \in A$ where $A_i^{\,c}$ is the compliment of A_i

(4) $A_i \cap A_j \in A$ if $A_i, A_j \in A$

(5) $\bigcup_{i=1}^{\infty} A_i \in A$ for all $A_i \in A$

Probability measure P

The sets A_i are composed of points ω belonging to the sure event Ω. The probability measure P is defined as the assignment of quantitative values to each of these events or ω-sets.

Probability Space (Ω, A, P)

A probability space is defined as a space Ω containing a σ field A of sets A_i of points ω together with a probability measure P that is defined on all points in the sets A_i.

The events $\omega \in \Omega$ have properties which are isolated by mapping the events into the real line R. Let $x(\omega)$ represent any one of these properties (for example radioactive intensity). The quantity x is called random since it depends apon some point $\omega \in \Omega$, and is called a random process if it satisfies certain conditions.

Random Variable

Let (Ω, A, P) be a probability space and x a mapping of Ω into R where R is the real line. $x(\omega)$ is called a random variable if $x_0 \in R$ and the set $\{\omega : x(\omega) < x_0\}$ belongs to A where A is the σ field defined on Ω. Random variables are special classes of mappings from Ω into R such that the inverse image of the open interval in R are events.

Borel Field B

Given the random variable x mapping Ω into R , the inverse map of open intervals of R generates a σ field called a Borel field B. The sets belonging to the Borel field are called a Borel set, A random variable is a mapping whereby all inverse images of B are events that belong to the σ field A. i.e.

$$A = \{\omega: x(\omega) \in B, B \in B\} = A \quad (A \in A)$$

To define a stochastic process we need to generalise x to be a n-dimensional random process, mapping Ω into R^n, the n-dimensional Euclidean space. We define probabilities as

$$P\ (\{\omega: x(\omega) < \xi_1 \ldots x_n(\omega) < \xi_n\})$$

which is commonly written

$$P\ (x_1(\omega) < \xi_i \ldots x_n(\omega) < \xi_n)$$

We next cause the random process x to be a function of time $x(t,\omega)$. We thus obtain the definition

Stochastic process $x(t,\omega)$

A stochastic process is a finite real valued function $x(t,\omega)$ that is a mapping from Ω x T for some interval T into R^n such that for each fixed $t \in T$, $x(t,\omega)$ is a measureable function of the σ field A of events on Ω. Thus for each $t \in T$ the event

$$\{\omega: a_1 < x_1(t) < b_1 \ldots a_n < x_n(t) < b_n\}$$

belongs to the σ field A.

We thus assume that $\{x(t,\omega)\ ,\ \omega \in \Omega\}$ denotes an ensemble of measureable waveforms. It is conventional to denote the process

$x(t,\omega)$ by $x(t)$.

For a subset of stochastic processes called Markov processes it is possible to obtain a statistical description of the nature of the process, at all points $t = t_1 \ldots t_n$ belonging to a set $\{t_n\}$ dense on some interval T, this being called the joint distribution function.

A Markov process is one in which knowledge of the present state, depends solely apon the most recent past knowledge. We use the approach of Loeve (Loe) by the introduction of the concept of conditional expectation to define this process. Other approaches are given in (Dob 2), (Gik), (Bre).

Conditional Expectation $E(x|B)$

Let B be a sub σ field of A with sets $B_i \in B$. We define an indicator function I as an ω function such that

$$I = \begin{cases} 1 & \omega \in B_i \\ 0 & \omega \notin B_i \end{cases}$$

For a special class of stochastic processes called Markov processes it is possible to obtain a statistical description of the nature of the process at all points $t = t_1 \ldots t_n$ belonging to a set $\{t_n\}$ dense on some time interval T, this being called the joint distribution function. To give the definition of a Markov process we need the concepts of conditional expectation and conditional probability. These are developed rigorously in (Loe), outlined in (McG), and alternative techniques are given in (Dob), (Gik) and (Bre). Here we proceed using the concepts in their elementary form.

Markov Process

A Markov process $x(t)$, $t \in T$ is a process which satisfied the following conditions

For any integer $n \geq 1$, if $t_1 < t_2 < \ldots < t_n$ are parameter

values, the conditional probabilities $x(t_n)$ given $x(t_1) \ldots x(t_{n-1})$ are the same as those just given $x(t_{n-1})$. i.e.

$$P\ (x(t_n) \geq \lambda \mid x(t_1) \ldots x(t_n)) \;=\; P\ (x(t_n) \geq \lambda \mid x(t_{n-1})) \tag{B.1}$$

If the times are continuous intervals, then if $s < t$ and F_s is the sub σ field generated by $\{x(u);\ u<s\}$ then

$$P\ (x(t) \geq \lambda \mid F_s) \;=\; P\ (x(t) \geq \lambda \mid x(s)) \tag{B.2}$$

The probability distribution function $P(\ )$ is often differentiable. The derivative called the probability density function is often easier to manipulate and is defined as follows.

Probability Density Function $p(\ )$

Let the probability distribution function of the random vector $x \in R^n$ be given by

$$P\ (x_1(\omega) < u_1\ ;\ \ldots\ ;\ x_n(\omega) < u_n)$$

then the probability density of the random vector is given by

$$p_x(u) \;=\; \frac{\partial^n}{\partial u_1 \ldots \partial u_n}\ P\ (x(\omega) < u_1 \ldots x_n(\omega) < u_n) \tag{B.3}$$

where $u \in R^n$, and u_i are the components of the n x 1 vector u.

We may now derive an important equation governing the Markov Process.

Chapman Kolmogorov Equation

Let $p_x\ (u,t\ x_o,|t_o)$ be a probability density function on the Markov process $x(t)$.

We know that if $t_o < s < t$, and that if we transfer from state

x_o at time t_o to state u at time t via state v at time s then

$$p_x\,(u,t \mid x_o,\, t_o) \;=\; \int p_x\,(u,t \mid v,s;\, x_o,\, t_o)\; p_x\,(v,s \mid x_o,\, t_o)\; dv \tag{B.4}$$

From equation (B.1) for a Markov process

$$p_x\,(u,t \mid v,s\;;\; x_o\; t_o) \;=\; p_x\,(u,t \mid v,s) \tag{B.5}$$

Hence

$$p_x\,(u,t \mid x_o,\, t_o) \;=\; \int p_x\,(u,t \mid v,s)\; p_x\,(v,s \mid x_o,\, t_o)\; dv \tag{B.6}$$

The function $p_x\,(u,t \mid v,s)$ is called the transition probability density and shows how the Markov process progresses in time, and acts in a similar way to a transition matrix on a deterministic system, projecting the state of the system from one instant to the state at some other instant in time.

A complete statistical description at any time using the transition function is possible only if some initial density is known, since

$$p_x\,(u_1,t_1\;;\ldots;\; u_n,t_n) \;=$$

$$p_x\,(u_n,t_n \mid u_{n-1},\, t_{n-1}) \;\cdots\; p_x\,(u_2,t_2 \mid\; u_1,t_1)\; p_x\,(u_1,\, t_1) \tag{B.7}$$

A more detailed description of the Markov process is given in (Ito2).

We now restrict the discussion to independent increment processes. The two most important of these processes are the Wiener and Poisson processes. The Wiener process is a continuous process which when formally differentiated yields white noise. The Poisson process is a step process where the points of discontinuity are at

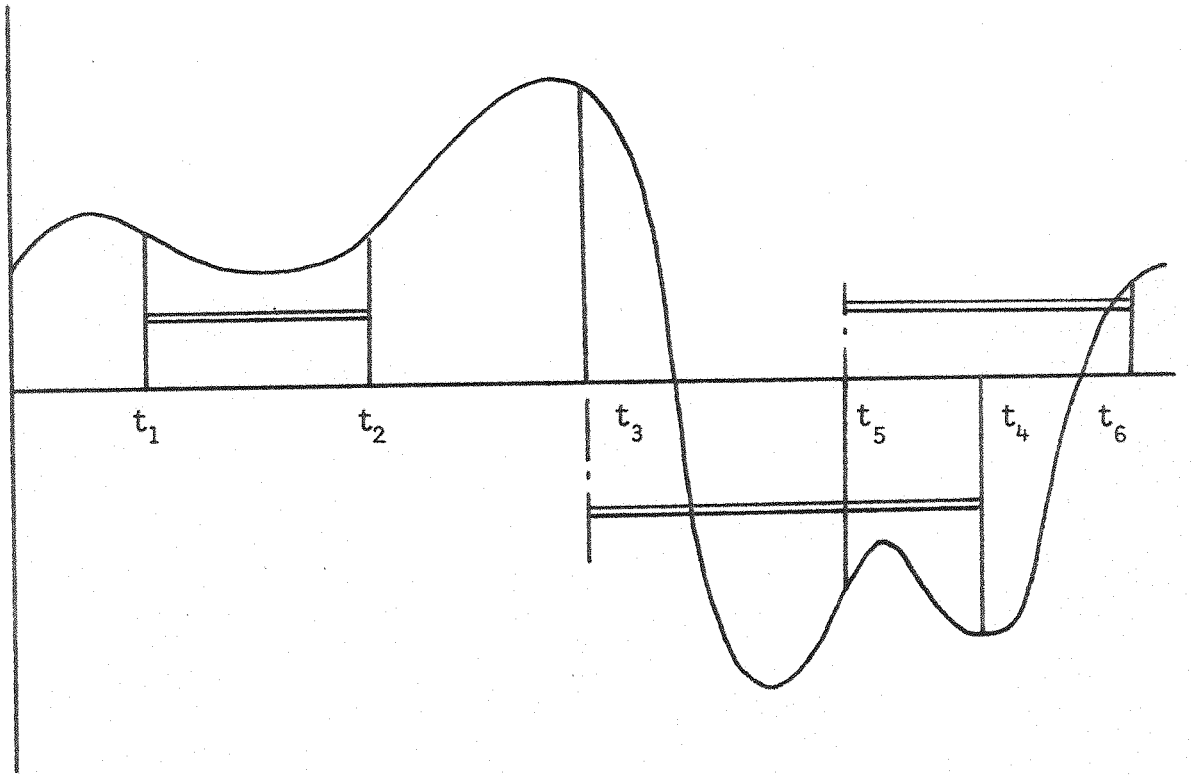

FIGURE B1 EXAMPLE OF AN INDEPENDENT INCREMENT PROCESS

countable. The theory given below is described in (McG) and in expanded forms in (Dob 2), (Ito2) and (McK 2). We now define the three types of processes.

Independent Increment Process

If the increments $x(t_i) - x(t_j)$; $x(t_n) - x(t_m)$ of the random process $x(t)$, $t \in T$ have conditional probabilities of the form

$$P\ (x(t_i) - x(t_j)\ \varepsilon\lambda \mid x(t_n) - x(t_m)\varepsilon\xi)$$

$$P\ (x(t_i) - x(t_j)\ \varepsilon\lambda) \qquad (B.8)$$

for any λ in R' and ξ a point in R', then $x(t)$ is an independent increment process.

This implies that the increments of the process over two non overlapping times are independent. Hence for three random variables $x(t_1) - x(t_2)$, $x(t_2) - x(t_3)$, $x(t_3) - x(t_4)$, and for any λ_1, λ_2 and λ_3.

$$P\ (x(t_1) - x(t_2)\ \varepsilon\lambda_1;\ x(t_2) - x\ (t_3)\ \varepsilon\lambda_2;\ x(t_3) - x(t_4)\ \varepsilon\lambda_3)$$

$$= P\ (x(t_1) - x(t_2)\ \varepsilon\lambda_1)\ P\ (x(t_2) - x(t_3)\ \varepsilon\lambda_2)\ P\ (x(t_3) - x(t_4)\ \varepsilon\lambda_3) \qquad (B.9)$$

Wiener Process

The Wiener process is defined from the independent increment process.

If $x(t,\omega)$; $t \varepsilon\ |0,\infty|$ is a scalar independent increment process such that $x(0,\omega) = 0$ for almost all ω, and for $t>s$

$$P\ (x(t) - x(s) < \lambda) = \frac{1}{\{2\pi\ (t-s)\}^{\frac{1}{2}}} \int_{-\infty}^{\lambda} \exp\left[\frac{-\xi^2}{2\ (t-s)}\right] d\xi \qquad (B.10)$$

that is the increments have a Gaussian Distribution, then $x(t,\omega)$ is a normalised Wiener process. When the variance is $\sigma^2 |t-s|$ then the process is not normalised.

A theorem with proof in (McG) and further discussion in (Ito 2), (Hid) gives a more concise description.

Let $x(t)$ be an independent increment process. If $x(t,\omega)$ is continuous in t for almost all ω then the distribution of the interval variable $x(I)$, $I = t_0,t$ is Gaussian.

Poisson Process

We again start from the independent increment process.

If $x(t,\omega)$, $t \in |0,\infty|$ is a scalar independent increment process such that

(1) $x(t,\omega)$ is a step function increasing with jumps of magnitude one, and vanishing at $t = 0$. $x(t,\omega) = 0$.

(2) for $t>s$ the probability that the number of jumps is k between times t and s is given by

$$P\,(x(t) - x(s) = k) = \exp(-\lambda\,|t-s|)\frac{(|t-s|)^k \lambda^k}{k!}$$

where $\lambda>0$ (B.11)

(3) The discontinuities are of the first kind, that is

$$x(t-0) \neq x(t) = x(t+0)$$

Then $x(t,\omega)$ is called a poisson process.

A more general description of the structure of Poisson Processes is given in (Paw). A theorem, proof of which is given in (McG) with further discussion in (Ito 2) and (Hid) derives a more concise description of the Poisson process.

Let $x(t)$ be a levy process i.e.

(1) $x(0) = 0$

(2) $x(t)$ is an independent increment process

(3) $x(t)$ has no independent increment discontinuities
i.e. $\lim_{t \to \infty} P(|x(t) - x(s)| > 0) = 0$

(4) the sample paths of $x(t)$ have discontinuities of the first kind.

If almost all sample functions are step functions with jumps of magnitude one, then $x(t)$ is a poisson variable.

This then completes an introduction to the Wiener and Poisson processes.

APPENDIX C

DERIVATION OF THE STATE ESTIMATION EQUATIONS

To obtain an estimate of the state of a system, the system must first be modelled, thus defining the parameters describing the system which are required to be known. Apriori knowledge and relavent measurements may then be used to give at any time the most likely value of the parameters describing the performance of the system, taking into account the disturbing influence of any noise inherent in the system or disturbing the measurements.

Here we describe a technique of modelling and estimation, for use particularly with a system observed by measurements containing Poisson noise, here having in mind the human metabolic system observed using radioactive tracers which are extracted by various organs, the radiation from which may be detected using various detectors, such as scintillation counters or eventually the Compton Effect camera.

The Model

Many continuous deterministic systems may be represented by an ordinary differential equation. These may be put into a state vector form (Oga)

$$\dot{x} = f(x,t)$$

This equation is generally driven by a random forcing function which we restrict to be an independent increment Markov process for analytical tractability. Several processes are possible but ones that have proved most useful are the Wiener and Poisson processes, (Appendix B). These processes when formally differentiated yield

stationary white noise. The derivative of the covariance function of a white noise process is infinite, and hence white noise is not realisable physically, however the process allows useful engineering results to be obtained (Kal 1), (McG). With this in mind we write the model with a random forcing function as a stochastic differential equation

$$dx(t) = f(x, t)\, dt + dn$$

Where n(t) is an independent increment process which implies that x(t) is Markov, and we limit this to the sum of a Wiener process which accounts for continuous fluctuations, and the poisson process which accounts for discontinuities.

We therefore assume that

$$dn(t) = dn_g(t) + dn_p(t)$$

Where $n_g(t)$ is an (n x 1) Wiener process and $n_p(t)$ an (n x 1) poisson process called a generalised poisson process.

We hence obtain the state equation

$$dx(t) = f(x,t)\, dt + dn_g + dn_p$$

the solution of which is given by

$$x(t) = x(a) + \int_a^t f(x,t)dt + \int_a^t dn_g + \int_a^t dn_p$$

The first integral is a standard Riemann Integral. The second and third may be interpreted in the Ito sense. In an Ito integral the second order terms must be retained since the second moments are of order dt not dt^2.

We now describe an Ito Integral.

Ito Integral

Let F_t be the σ field generated by a Wiener process $\{\omega(t) : s \leq t\}$. Let $\phi(t,F_t)$ be a step function such that

$$\phi\ (t,F_t) = \begin{cases} 0 & t < t_j \\ \phi_j\ (F_{t_j}) & t_j < t < t_j + 1 \\ 0 & t > t_j + 1 \end{cases}$$

then the Ito integral over an interval T such that $t \in T$ is defined as

$$\psi = \int_T \phi\ (t,F_t)\ d\omega(t) \triangleq \sum_{j=1}^{m} \phi_j\ (F_{t_j})(\omega(t_{j+1}) - \omega(t_j))$$

This is well defined since $\phi\ (t,F_t)$ is constant over any interval t_j, t_{j+1} and depends only apon F_{t_j} which depends only on $\omega(t)$ for $t < t_j$.

For any t_i, t_{i+1}

$$\int_{t_i}^{t_{i+1}} \phi\ (t,F_t)\ d\omega(t) = \phi_i\ (F_{t_i}) \int_{t_i}^{t+1} d\omega(t)$$

where the integral of the Wiener process is defined as

$$\int_{t_i}^{t_{i+1}} d\omega(t) \triangleq \omega(t_{i+1}) - \omega(t_i)$$

The definition of the Ito integral may be extended to the case where $\omega(t)$ is an independent increment process, but not a Wiener process, for example a poisson process Reference (Sko).

We wish to estimate the state x in the equation

$$dx(t) = f(x,t)\ dt + dn_g + dn_p.$$

To do this the estimation criteria must be examined in detail.

Let $dy\ (t,\omega)$ be a measurement given by

$$dy\ (t,\omega) = h(x(t),\ \omega)dt + dn\ (t,\omega)$$

where $n(t,\omega)$ is a Markov process. We must find the best method of estimating $x(t,\omega)$ at a given time t, given $y(s,\omega)$ from t_0 to t. A useful deterministic cost criterion is the expectation of some positive function of the error experienced by obtaining x from the data. Let $\hat{x}(t,\omega)$ be a function measurable with respect to the sub σ field generated by the measurements $y(s,\omega)$, $s \in [t_0,t]$ namely $O_{t_0,t}$ and let it be the estimate The error $\tilde{x}(t,\omega)$ is defined by

$$\tilde{x}(t,\omega) = x(t,\omega) - \hat{x}(t,\omega)$$

Let $f(\tilde{x})$ be a non negative function of $\tilde{x}$.
A quatitative cost function is $E(f(\tilde{x}))$

If

$$f(\tilde{x}) = |\tilde{x}|^P \quad \text{for } p \geq 1$$

then for all values of p, $p \neq 2$ then $f(\tilde{x})$ produces a Banach Space, but not a Hilbert space. We are therefore if we wish to be assured of the existence and uniqueness of a minimum error $\tilde{x}$ confined to the case where $p = 2$.

A suitable choice is therefore $E(|\tilde{x}|^2)$, the minimum mean square error (MMSE). It may be shown (McG) that by the use of set theoretic definitions of conditional expectation (Wo), the Radon-Nikodymtheorem (Nev), (Ha 2), martingales (Kus) and the martingale convergence theorem (Doo 2), (Won) that if the measurements $y(t,\omega)$ are given by

$$dy(s,\omega) = h(x(s,\omega),s)ds + dn(s,\omega)$$

for $s \in |t_0,t|$ as before, then the MMSE estimate is $E(x|O_{t_0,t})$ where

$$E(x|O_{t_0,t}) = \int u\, p_x(u,t|O_{t_0,t})\, du$$

the conditional probability density of the process x at time t, given

the minimum σ-field generated by the process $y(t,\omega)$. It is thus sufficient to obtain $p_x\ (u,t|\mathcal{O}_{t_o,t})$ to fully describe the process $\hat{x}(t,\omega)$, and the required estimate. We now show how this expression may be evaluated and how the required state estimate may be derived.

System Propagation Equations

We consider the Markov process

$$dx(t) = f(x,t)dt + dn_g + dn_p$$

as previously defined. We have shown in Appendix B that the probability denoting function is sufficient to describe the statistics of the process by means of the Chapman Kolmogorov Equations. The temporal evolution equations of the probability density function will describe the evolution of $x(t)$. We first define the characteristic function, the Fourier transform of the probability density function, which is more convenient to work with.

Characteristic Function

Let $p_x\ (u,t|x(s) = v)$ be the conditional probability density function of the random process x at time t, given that x at time s is equal to v.

The characteristic function $M_x\ (u,t|x(s))$ is defined by

$$M_x\ (u,t|x(s)) = E\ (\exp\ (j\ u^T\ x(t))|x(s) = v)$$

$$= \int_{R^n}\ \exp\ (ju^T\ \xi)\ p_x\ (\xi,t|x(s) = v)d\xi$$

where u and ξ are (n x 1) vectors, and the integration is over all R^n.

We now obtain the temporal evolution of $M_x\ (u,t|x(s))$ which is

equivalently the temporal evolution of $p_X(u,t|x(s))$. This evolution equation is called the Bartlett Moyal equation (Moy).

Bartlett Moyal Theorem

Let $M_X(u,t|x(s))$ be the characteristic function of the Markov process $x(t)$, $t \in T$ where t is some interval.

The Chapman-Kolmogorov equation (Appendix B) states

$$p_X(v, t + \Delta t|x(s) = \int p_X(v, t + \Delta t|r.t) \; p_X(r,t|x(s))dr$$

Using this in the definition of the characteristic function above we obtain

$$M_X(u, t + \Delta t|x(s)) =$$

$$\iint p_X(v,t + \Delta t|r,t)\, p_X(r,t|x(s) \exp(j\, u^T v)\, dv\, dr$$

$$= \int p_X(r,t|x(s)) \exp(j\, u^T r) \{\int p_X(v,t+ \Delta t|r) \exp(ju^Tv - ju^Tr)dv\}dr$$

$$= E\{\exp(j\, u^T x(t))\, E\{\exp(j\, u^T(x(t + \Delta t) - x(t))|x(t)\}|x(s)\}$$

Hence

$$M_X\{u, t + \Delta t|x(s)\} - M_X\{u, t|x(s)\} \cdot \frac{1}{\Delta t}$$

$$= E\{\exp(j\, u^T x(t) \cdot \frac{1}{\Delta t} E\{\exp(j\, u^T(x(t + \Delta t) - x(t))) - 1|x(t)\}|x(s)\}$$

(C.1

Now by definition

$$\frac{\partial M_X(u,t|x(s))}{\partial t} =$$

$$\lim_{\Delta t \to 0} \frac{1}{\Delta t} \{M_X(u, t + \Delta t|x(s)) - M_X(u, t|x(s))\}$$

Hence taking the limit as $\Delta t \to 0$ in equation (C.1) and defining the Ito differential of the Markov process $\psi(u,t, x(t))$, ((Fro) p.36), as

$$\lim_{\Delta t \to 0} \frac{1}{\Delta t} E\{(\exp\{ju^T(x(t+\Delta t) - x(t))\} - 1) | x(t)\} = \psi(u,t, x(t))$$

then we obtain

$$\frac{\partial M_x(u,t|x(s))}{\partial t} = E(\exp(ju^T x(t))\, \psi(u,t, x(t)|x(s))) \qquad (C.2)$$

Note that ψ is also called the infinitesimal generator of the Markov semigroup (Dyn),(Wong). We now wish to evaluate ψ and substitute it in the above equation.

From the definition of the Ito differential of the Markov process we obtain

$$\psi(u,t, x(t)) = \frac{E\{\exp(ju^T dx) - 1 | x(t)\}}{dt}$$

The n x 1 vector Markov process is generated by the equation

$$dx = f(x,t)\, dt + dn_g + dn_p$$

where dn_g is an (n x 1) Gaussian process with covariance matrix $Q(t)$ where

$$E\{dn_g(t)\, dn_g{}^T(t)\} = Q(t)\, dt$$

and dn_p is an (n x 1) generalised poisson process with rate vector $\Lambda(t)$ and jump probability $p_a(\alpha)$

Substituting in the definition for ψ we obtain

$$\psi(u,t, x(t)) = \frac{E\{\exp(ju^T dx) - 1 | x(t)\}}{dt}$$

$$= \frac{E\{\exp(ju^T f(x,t)\, dt + ju^T dn_g + ju^T dn_p) - 1 | x(t)\}}{dt}$$

$$= \frac{\exp\,(ju^T f(x,t)\,dt)\;E\;\{\exp\,(ju^T dn_g)\}\;E\;\{\exp\,(ju^T dn_p)\} - 1}{dt}$$

To evaluate this expression the characteristic functions of two independent noise processes must be evaluated.

Evaluation of $E\{\exp(ju^T dn_g)\} = M_{dn_g}(u,t)$

If $x(\omega)$ is an $(n \times 1)$ random vector, and is Gaussian, then the probability density of $x(\omega)$ is

$$p_x(u) = \frac{1}{(2\pi)^{n/2}\;|Q|^{\frac{1}{2}}}\;\exp\{-\tfrac{1}{2}\,(x-m)^T\,Q^{-1}(x-m)\}$$

where

Q is the $(n \times n)$ covariance matrix defined by

$$Q = E\{(x-m)(x-m)^T\}$$

where $m = E\{x\}$

Let $v = x-m$. The characteristic function of the process is then given by

$$Mx(u) = \int_{-\infty}^{\infty} \frac{\exp\{-\tfrac{1}{2}\,v^T Q^{-1}\,v\}}{(2\pi)^{n/2}\;|Q|^{\frac{1}{2}}}\;\exp\{juv\}\,dv = \exp\{-\tfrac{1}{2}\,u^T\,Q\,u\}$$

Hence

$$E\{\exp\,(ju^T dn_g)\} = \exp\{-\tfrac{1}{2}\,u^T\,Q\,u\,dt\}$$

Evaluation of $E\{\exp\,(j\,u^T dn_p)\}$

This is the characteristic function of the generalised poisson process. The probability of two or more jumps occurring in dt is $o(dt)$ hence

$$E\{\exp(ju^T dn_p)\} = 1 \cdot P\{\text{no jumps}\}$$

$$+ \sum_{i=1}^{n} E\{\exp(j u_i a_i)\} \cdot P\{\text{only one jump in } dn_i\}$$

But

$$P(\text{no jumps}) = \prod_{i=1}^{n} (1 - \Lambda_i\, dt)$$

$$= 1 - \sum_{i=1}^{n} \Lambda_i\, dt + o(dt)$$

and

$$P(\text{one jump only}) = \Lambda_i\, dt \prod_{j=1}^{n} (1 - \Lambda_j\, dt)$$

$$= \Lambda_i\, dt + o\, dt$$

where Λ is the rate of the poisson process dn_p.

Hence letting $M_{\alpha i}(u_i) = E\{\exp(j u_i \alpha_i)\}$, the characteristic function of the i^{th} jump we obtain

$$E\{\exp(ju^T dn_p)\} = 1 - \sum_{i=1}^{n} \Lambda_i\, dt\,(1 - M\{u_i\}) \qquad (C.5)$$

Substituting these two results into the equation for ψ, equation (C.3) we obtain

$$\psi(u,t,x(t)) = \frac{\exp\{ju^T f(x,t)\, dt\} \exp\{-\tfrac{1}{2} u^T Q\, u\, dt\}\{1-\Lambda_i(1-M(u_i))\, dt\}}{dt} \qquad (C.6)$$

Now $\exp\{j u^T f(x,t)dt\} = 1 + ju^T f(x,t)\, dt + o(dt)$

and $\exp\{-\tfrac{1}{2} u^T Q\, u\, dt\} = 1 - \tfrac{1}{2} u^T Q\, u\, dt + o(dt)$

Hence

$$\psi\ (u,t,\ x(t)) \ =$$

$$\frac{1 + ju^{T}f(x,t)dt - \frac{1}{2}\ u^{T}\ Q\ u\ dt - \Lambda_i\ (1-M\ \{u_i\})\ dt + o(dt)}{dt}$$

hence to o(dt)

$$\psi\ (u,t,\ x(t)) \ = \ j\ u^{T}f(x,t) - \tfrac{1}{2}\ u^{T}Q\ u - \Lambda_i\ (1-M\ \{u_i\}) \qquad (C.7)$$

Substituting equation (C.7) into equation (C.2) we obtain:

$$\frac{\partial M_x}{\partial t}\ (u,t,\ x(s)) \ = \ E\ \{\exp\ (j\ u^{T}x(t))$$

$$E\ \{\exp\ (j\ u^{T}x(t))\ (j\ u^{T}\ f(x,t) + \sum_{i=1}^{n}\ \Lambda_i\ (M_{\alpha i}\ \{u_i\}-1))$$

which when Inverse Fourier transformed yields

$$\frac{\partial p}{\partial t} \ = \ -\ \sum_{i=1}^{n}\ \frac{\partial\ (f_i p)}{\partial u_i} \ + \ \tfrac{1}{2}\ \sum_{i=1}^{n}\ \sum_{i=1}^{n}\ \frac{\partial^2 Q_{ij} p}{\partial u_i\ \partial_{uj}} \ + \ \sum_{i=1}^{n}\ \Lambda_i\ (-p+p*p_{ai}) \qquad (C.8)$$

where the covolution * is defined by

$$p\ *\ p_{a_i} \ = \ \int\ p_{a_i}\ \{u_i - v_i\} p_x\ \{u_1,\ \ldots\ v_i\ \ldots\ u_n,\ t|x(s)\}\ dv_i$$

Defining the forward operator $L^{\dagger}$ as

$$L^{\dagger} \ = \ -\ \sum_{i=1}\ \frac{\partial}{\partial u_i}\ (f_i) \ + \ \tfrac{1}{2}\ \sum_{i=1}^{n}\ \sum_{j=1}^{n}\ Q_{ij}\frac{\partial^2(.)}{\partial u_i\ \partial u_j} + \sum_{i=1}^{n}\ \Lambda_i(\ )*p_{a_i}-(\ ))$$

we obtain the equation

$$\frac{\partial p}{\partial t} = L^{\dagger}(p) \qquad (C.9)$$

where p is the transition probability density function for the process x. Although arguments on the existence and uniqueness of solutions are known, see (Dun), solutions, except in a very few cases are unknown.

The case where there is no poisson noise in the system equation, when dn_p is zero results in the last term of the $L^\dagger$ operator derived above being zero. The resulting equation is called the Fokker Planck equation, and is derived in references (Uhl), (Moy) and (Wan); examples being given in (Moy). No poisson noise exists in the system we consider.

The next stage is to use the measurements taken in the time interval t_o to t. These generate a sub σ field $O_{t_o,t}$.

We note that, see (Cla) for the proof that

$$O_{t_o,t+dt} = O_{t_o,t} \bigcup dN$$

where dN is an m x 1 measurement process, to obtain

$$p_x(u,t|O_{t_o,t+dt}) = p_x(u,t|O_{t_o,t}, dN) \qquad (C.10)$$

The measurements fall into two classes, the (m x 1) vector Gauissian measurement dy(t) given by

$$dy(t) = h(x(t),t) + d\omega(t)$$

Where $\omega(t)$ is a Wiener process with zero mean and covariance

$$E\left|d\omega(t)\, d\omega^T(t)\right| = R(t)dt$$

and the Poisson counting process dN(t) which is an (m x 1) vector process with arrival rate $\lambda(x(t),t)$ where $\lambda(x(t),t)$ is also an (m x 1) process. Here we consider only the effect of the poisson counting process, which is that observed when radiation intensity is measured. The case of Gaussian measurements is treated in (McG), (Sny 1), (Bre), (Men), (Lie) and others.

Let the (m x 1) vector measurement process dN(t) be a unit jump Poisson process with an (m x 1) rate vector which we denote by $\lambda(t)$, to distinguish if from the rate parameter $\Lambda(t)$ of the state equation.

d N(t) may take the values 0 or γ_i where

$$\gamma_i = (0, \ldots, 0, \underset{i}{1}, 0, \ldots, 0)^T$$

Thus the probability that dN_i and dN_j are both 1 with all others being 0 is o(dt).

Now the probability that the i^{th} event occurs is $\lambda_i(u,t)dt$. Hence for an arbitrary $\gamma_i \neq 0$

$$P\,(dN = \gamma_i | x(t) = u) = \lambda_i\,(u,t)dt \prod_{j\neq i}^{m} (1 - \lambda_j\,(u,t)dt)$$

$$= \lambda_i\,(u,t)$$

For the case dN(t) = 0

$$P\,(dN = 0|x(t) = u) = \prod_{i=1}^{m} (1 - \lambda_i\,(u,t)\,dt)$$

$$= 1 - \sum_{i=1}^{m} \lambda_i\,(u,t)\,dt$$

This may be written concisely using the vector γ where

$$\gamma = (\underset{1}{1}, 1, \ldots, \underset{m}{1}, 1)^T$$

as

$$P\,(dN = 0|x(t) = u) =$$

$$\lambda^T\,(u,t)\,dN\,dt + (1 - \lambda^T\,(u,t)\gamma dt)\,(1 - dN^T\gamma)$$

dN is a discrete random process, hence Bayes rule gives

$$p_X\,(u,t|O_{t_o,t},dN) = \frac{\{P\,dN|O_{t_o,t},x(t) = u\}}{P\{dN|O_{t_o,t}\}}\,p_X\,(u,t|O_{t_o,t})$$

where $P\,\{dN\,|O_{t_o,t}, x(t) = u\}$ is the probability that dN takes on its

prescribed value, given $O_{t_o,t}$ and $x(t)$.

The denominator may be written

$$P\{dN|O_{t_o,t}\} = \int P\{dN|O_{t_o,t},\ x(t) = v\}\phi_x\ (v,t|O_{t_o,t})dv$$

$$= E\{P\{dN|x(t)\}\}$$

Hence

$$\frac{p_x\ \{u,t|O_{t_o,t},dN\}}{p_x\{u,t|O_{t_o,t}\}} = \frac{\lambda^T(u,t)\ dNdt + (1-\lambda^T(u,t)\gamma dt)\ (1 - dN^T\gamma)}{E\{\lambda^T(x,t)\}\ dNdt + (1-E\{\lambda^T(x,t)\}\lambda dt)(1-dN^T\gamma)}$$

dN takes the values 0 or γ_i, hence:

$$= \frac{1 - \lambda^T(u,t)\gamma dt}{1 - E\{\lambda^T(x,t)\}\gamma dt}(1 - dN^T\gamma) + \sum \frac{\lambda^T(u,t)\gamma_i}{E\{\lambda^T(x,t)\}\gamma_i}\ dN^T\gamma_i$$

$$= 1 + \{\ \sum_{i=1}^{m}(E\{\lambda_i\ (x,t) - \lambda_i\ (u,t))\ \}(1 - dN^T\gamma)$$

$$- dN^T\gamma + \sum_{i=1}^{m}\ \frac{\lambda_i^{\ T}\ (u,t)}{E\{\lambda_i\ (x,t)\}}\ dN_i$$

$$= 1 + \sum_{i=1}^{m}\ \{\lambda_i\ (x,t) - E\ \{\lambda_i\ (x,t)\}\}\{E\{\lambda_i\ (x,t)\}\}$$

$$\{dN_i(t) - E\{\lambda_i(x,t)\}dt\}^T \qquad (C.11)$$

Hence p may be written in the form

$$p_x\ (u,t|O_{t_o,t+dt}) = p_x\ (u,t|O_{t_o,t})\ (1+q\ (dN,\ dt,\ u)) \qquad (C.12)$$

where

$$q\ (dN,\ dt,\ u) = \sum_{i=1}^{m}\ \{\lambda_i(u,t) - E\{\lambda_i\ (x,t)\}\}$$

$$\{E\{\lambda_i\ (x,t)\}\}^{-1}\ \{dN_i(t) - E\{\lambda_i\ (x,t)\}dt\} \qquad (C.13)$$

The characteristic function has been defined by

$$M_x\,(v, t+\Delta t | O_{t_o, t+\Delta t}) =$$

$$\int \exp\,(j\, v^T u)\; p_x\,(u,\, t+\Delta t | O_{t_o, t+\Delta t}) du$$

which may be manipulated to give

$$M_x\,(v,\, t+\Delta t | O_{t_o, t+dt}) =$$

$$\iint \exp\,(jv^T u)\; p_x\,(u,\, t+\Delta t | x(t) = s,\, O_{t_o, t})\; p_x\,(s, t | O_{t_o, t+\Delta t}) du ds$$

$$= \int \exp\,(jv^T s)\; p_x\,(s, t | O_{t_o, t+\Delta t}) \int \exp\,(jv^T (u-s))\; p_x\,(u, t+\Delta t | x(t)) du ds$$

$$= \int \exp\,(jv^T s)\; p_x\,(s, t | O_{t_o, t+\Delta t})\; E\{\exp\,(jv^T dx(t)) | x(t) = s\} ds$$

Substituting equation (C.12) gives

$$M_x\,(v, t+\Delta t | O_{t_o, t+\Delta t})$$

$$= \int \exp\,(jv^T s)\; p_x\,(u, t | O_{t_o, t})\; (1 + q\,(dN,\, \Delta t,\, u))$$

$$E\{\exp\,(jv^T dx(t)) | x(t) = s\} ds$$

Using the definition of characteristic function once more we can write

$$M_x\,(v,\, t+\Delta t | O_{t_o, t+\Delta t}) - M_x\,(v, t | O_{t_o, t})$$

$$= \int p_x\,(s, t | O_{t_o, t})\; \exp\,(jv^T s)\; E\{\exp\,(jv^T dx(t) - 1 | x(t) = s\} ds$$

$$+ \int p_x\,(s, t \mid O_{t_o, t})\; \exp\,(jv^T s) q\,(dN,\, dt,\, s)$$

$$E\{\exp\,(jv^T dx(t)) | x(t) = s\} ds \qquad (C.14)$$

taking the limit as $\Delta t \to 0$ changes the RHS of equation (C.14) to:

$$\lim_{\Delta t \to 0} \{M_x (v, t+\Delta t|0_{t_o,t+\Delta t}) - M_x (v,t|0_{t_o,t})\} =$$

$$\partial M_x (u,t|0_{t_o,t})$$

the Inverse Fourier transform of which is given by

$$\partial p_x (u,t|0_{t_o,t})$$

The same operations may be performed to the LHS of equation (C.14). Equation (C.1) shows that the first term of equation (C.14) may be written as

$$M_x \{u, t+\Delta t|x(s)\} - M_x u,t|x(s)\}$$

which when the limit as $\Delta t \to 0$ is taken, and the inverse Fourier transform performed yields the L^+ operator as shown by equation (C.9)

The second term of equation (C.14) contains the product of the expectation

$$E\{\exp (jv^T dx|x(t) = s\} = 1 + 0(dt)$$

and q (dN, dt, s). Since q (dN, dt, s) is already 0(dt) and the product of two 0(dt) terms is o(dt) the second term becomes

$$\int p_x (s,t|0_{t_o,t}) \exp (jv^T s)\, q\, (dN, dt, s)\, ds + o(dt)$$

taking the limit as $\Delta t \to 0$ and the inverse Fourier Transform we obtain $q(dN, dt, u)(p)$

Hence equation (C.14) yields after taking the limit as $\Delta t \to 0$ and taking the Inverse Fourier transform

$$\partial p = L^+(p)\, dt + q\, (dN, dt, u)(p)$$

where $p = p\, (u,t|0_{t_o,t})$

Substituting for q we obtain

$$\partial p = L^{\dagger} p + \sum_{i=1}^{m} \lambda_i \{x_i (u,t) - E\{\lambda_i (x,t)\}\}$$

$$\{E\{\lambda_i (x,t)\}\}^{-1} \{dN_i(t) - E\{\lambda_i (x,t)\}dt\}^{T} p \qquad (C.15)$$

Equation (C.15) is called Snyders equation, see (Sny 1-4). The corresponding equation for Gaussian Measurements is called the Kushner Stratonovich equation. Snyders equation may be used to give an estimate of the state variables.

Multiplying by the (nx1) state vector u and integrating the L.H.S. gives

$$\int u \partial p \, du = \partial \int up \, du = \partial \hat{x}(t)$$

where $\hat{x} = E(x)$

The $L^{\dagger}$ term is difficult to integrate. We simplify it by assuming that no Poisson noise disturbs the system. We hence treat a system disturbed by Gaussian noise, observed by measurements with poisson rates λ.

The forward operator $L^{\dagger}$ becomes

$$L^{\dagger}(.) = - \sum_{i=1}^{n} \frac{\partial}{\partial u_i}(f_i \cdot) + \tfrac{1}{2} \sum_{i=1}^{n} \sum_{j=1}^{n} Q_{ij} \frac{\partial^2 (.)}{\partial u_i \, \partial u_j} \qquad (C.16)$$

to integrate this term we use the following results

$$\int u_i \frac{\partial (f_i \, p)}{\partial u_i} du = \int f_i \, p \Big|_{-\infty}^{\infty} d_{u_i} - \int f_i \, p \, du = - \int f_i \, p \, dt \qquad (C.17)$$

$$\int u_j \frac{\partial (f_i \, p)}{\partial u_i} du = \int f(u,t) \, p \, du = E\{f(x,t) | 0_{t_o,t}\} \qquad (C.18)$$

$$\int u\, Q_{ij}\, \frac{\partial^2 p}{\partial u_i\, \partial u_i}\, du = 0 \qquad (C.19)$$

The last term in equation (C.15) gives

$$\int up \left\{ \sum_{i=1}^{m} \{\lambda(t) - \hat{\lambda}(t)\}^T \gamma_i \{\lambda^T(t)\gamma_i\}^{-1} \{dN(t) - \hat{\lambda}(t)\, dt\}^T \gamma_i \right\} du$$

$$= \sum_{i=1}^{m} E\{(x-\hat{x})\lambda^T(x)\}\gamma_i \{\hat{\lambda}^T \gamma_i\}^{-1} \{dN - \hat{\lambda}(t)\, dt\}^T \gamma_i \qquad (C.20)$$

Hence multiplying equation (C.15) by the (m x 1) state vector u and integrating, we obtain by the use of equations (C.16) to (C.20).

$$d\hat{x}(t) = E\{f(x,t)\} +$$

$$\sum_{i=1}^{m} E\{(x-\hat{x})\, \lambda^T(x)\}\gamma_i \{\hat{\lambda}^T \gamma_i\}^{-1} \{dN - \hat{\lambda}(t)\, dt\}^T \gamma_i \qquad (C.21)$$

where $\hat{\lambda} \triangleq E\{\lambda(t) | O_{t_o,t}\}$

The evaluation of this equation is analytically impossible, and approximations must be made. This may be achieved by assuming the non linearities may be expanded in multidimentional Taylor series. When this technique is applied to the case of Gaussian measurements, generalisation of the Kalman Bucy filter are produced. The continuous time version of this filter is given in the books of Meditch (Med 2) and Van Trees (Van 1-3). The results of the Kalman Filter were first derived using an approach similar to that used in deterministic control. The quadratic criterion deterministic control problem is the dual of the linear minimum mean square error problem, and the approach is discussed in the books of Meditch (Med 1) in Saga and Melsa (Sag), Jaswinski (Jas) and Breiman (Bre) among others. Here

we consider the case of poisson measurements. Several analyses have been performed noteably by Jaswinski (Jas 1), (Jas 2) and Culver (Cul 1), (Cul 2). Here the techniques of Ahens et al (Ath) are used. Snyder (Sn 1-3) derived and used the special case of linear state equations and non linear state equations which is the basis of the filtering schemes applied to the metabolistic flow problems described in the main text.

We proceed by expanding $f(x)$ and $\lambda(x)$ about their optimal points, that is letting

$$f(x) = f(\hat{x}) + (x-\hat{x})^T \frac{\partial f}{\partial \hat{x}} + \tfrac{1}{2} \sum_{i=1}^{m} \xi_i (x-\hat{x})^T \frac{\partial^2 f_i}{\partial \hat{x}^2} (x-\hat{x}) \qquad (C.22)$$

$$\lambda(x) = \lambda(\hat{x}) + (x-\hat{x})^T \frac{\partial \lambda}{\partial \hat{x}} + \tfrac{1}{2} \sum_{i=1}^{m} \xi_i (x-\hat{x})^T \frac{\partial^2 \lambda_i}{\partial \hat{x}^2} (x-\hat{x}) \qquad (C.23)$$

where $\xi_i = |0,0 \ldots 0,1,0 \ldots 0,0|^T$ (1 in position i, 0 in position n)

$$\frac{\partial \lambda}{\partial \hat{x}} = \left(\begin{array}{ccc} \frac{\partial \lambda_1}{\partial x_1} & \cdots & \frac{\partial \lambda_m}{\partial x_1} \\ \frac{\partial \lambda_1}{\partial x_n} & \cdots & \frac{\partial \lambda_m}{\partial x_n} \end{array} \right) \Bigg|_{x=\hat{x}}$$

$$\frac{\partial^2 \lambda_i}{\partial \hat{x}^2} = \left(\begin{array}{ccc} \frac{\partial^2 \lambda_i}{\partial x_1 \partial x_1} & \cdots & \frac{\partial^2 \lambda_i}{\partial x_1 \partial x_n} \\ \frac{\partial^2 \lambda_i}{\partial x_n \partial x_1} & & \frac{\partial^2 \lambda_i}{\partial x_n \partial x_n} \end{array} \right) \Bigg|_{x=\hat{x}}$$

and similar expressions exist for $\frac{\partial f}{\partial \hat{x}}$ and $\frac{\partial^2 f}{\partial \hat{x}^2}$

The use of equations (C.22) and (C.23) introduce some error into the estimates. The resulting estimates are termed linearised optimum estimates. It is convenient to denote the linearised state estimate by s, and the linearised covariance estimate by R.

Substituting equation (C.22) and (C.23) into equation (C.21) gives the linearised estimate.

$$ds(t) = f(s)\,dt + \sum_{i=1}^{m} E\{(x-\hat{x})\,(x-\hat{x})^T \frac{\partial \lambda^T}{\partial \hat{x}}\}$$

$$\gamma_i\,(\hat{\lambda}(s)^T\gamma_i)^{-1}(dN(t) - \hat{\lambda}(s)dt) \qquad (C.24)$$

The covariance matrix is defined by

$$P(t) = E\{(x(t) - \hat{x}(t)\,(x(t) - \hat{x}(t))^T | O_{t_o,t}\}$$

Hence we obtain

$$ds(t) = f(s)\,dt + \sum_{i=1}^{m} P(t)\,\frac{\partial \lambda}{\partial s}^T \gamma_i\,(\hat{\lambda}(s)^T\gamma_i)^{-1}$$

$$(dN(t) - \hat{\lambda}(s)dt) \qquad (C.25)$$

We now need to evaluate P(t). To do this we first use equation (C.25) to produce a subresult: To O(dt):

$$ds(t)\,ds(t)^T = \sum_{i=1}^{m}\sum_{j=1}^{n} P(t)\,\frac{\partial \lambda}{\partial s}^T \gamma_i\,(\hat{\lambda}^T(s)\gamma_i)^{-1}\gamma_i^T dN(t)$$

$$dN^T(t)\,\gamma_j\,(\hat{\lambda}(s)^T\gamma_j)^{-1}\gamma_j^{-1}\,\frac{\partial \lambda}{\partial s}^T P(t)$$

but

$$\gamma_i^T \, dN(t) \, dN^T(t) \, \gamma_j = dN_i(t) \, \delta_{ij}$$

Hence we obtain, denoting $\hat{\lambda}(s,t)$ by λ^*

$$\partial s(t) \, \partial s(t)^T = \sum_{i=1}^{m} P(t) \frac{\partial \lambda}{\partial s}^T \lambda_i^{*-1} \gamma_i \gamma_i^T \lambda^{*-1} \frac{\partial \lambda}{\partial s} P(t) \gamma_i^T dN(t)$$

but noting

$$\frac{\partial \lambda}{\partial s}^T \lambda_i^{-1} \gamma_i \, \gamma_i^T \, \lambda_i^{-1} \frac{\partial \lambda}{\partial s} = \frac{\partial \ell n \lambda_i}{\partial s}^T \frac{\partial \ell n \lambda_i}{\partial s}$$

and using the relationship

$$\frac{\partial^2 \ell n \lambda_i}{\partial s^2} = - \left(\frac{\partial \ell n \lambda_i}{\partial s} \right) \left(\frac{\partial \ell n \lambda_i}{\partial s} \right) + \frac{1}{\lambda_i} \left(\frac{\partial^2 \lambda_i}{\partial s^2} \right)$$

we obtain

$$\partial s(t) \, \partial^T s(t) = \sum_{i=1}^{m} P(t) \left\{ \frac{1}{\lambda_i} \frac{\partial^2 \lambda_i}{\partial s^2} - \frac{\partial^2 \ell n \lambda_i}{\partial s^2} \right\} P(t) \, \gamma_i^T dN(t) \tag{C.26}$$

P(t) may now be evaluated. From the definition of P(t) we obtain

$$P(t+dt) = E\{(u-\hat{x}(t+dt)) \, (u-\hat{x}(t+dt))^T | 0_{t_o, t+dt}\}$$

but

$$\hat{x}(t+dt) = \hat{x}(t) + d\hat{x}$$

hence

$$P(t+dt) = E\{(u-\hat{x}(t) - d\hat{x}) \, (u-\hat{x}(t) - d\hat{x})^T | 0_{t_o, t+dt}\}$$

$$= \int (u-\hat{x}(t))\ (u-\hat{x}(t))^T\ p_x\ (u,\ t+dt)\ du + d\hat{x}d\hat{x}^T$$

$$- \int (u-\hat{x}(t)d\hat{x}^T\ p_x\ (u,\ t+dt|0_{t_o,tdt})du$$

$$- \int d\hat{x}\ (u-\hat{x}(t))^T\ p_x\ (u,\ t+dt|0_{t_o,t+dt})du \qquad (C.27)$$

Noting that

$$\int (u-\hat{x}(t))\ dx^T\ p_x\ (u,t+dt|0_{t_o,t+dt})du$$

$$= \int (u-\hat{x}\ (t+dt) + d\hat{x})\ d\hat{x}^T\ p_x\ (u,\ t+dt|0_{t_o,t+dt})du$$

$$= \int (u-\hat{x}\ (t+dt))\ d\hat{x}^T\ p_x\ (u,\ t+dt|0_{t_o,t+dt})\ du + d\hat{x}\ d\hat{x}^T$$

$$= d\hat{x}\ d\hat{x}^T \text{ (since the estimate } \hat{x}\ (t+dt) \text{ is unbiased)}$$

equation (C.27) becomes

$$P\ (t+dt) = \int (u-\hat{x}(t))\ (u-\hat{x}(t))\ p_x\ (u,\ t+dt|0_{t_o,t+dt})\ du - d\hat{x}\ d\hat{x}^T \qquad (C.28)$$

From equation (C.15) we obtain

$$p_x\ (u,\ t+dt|0_{t_o,t+dt})$$

$$= p_x\ (u,t|0_{t_o,t}) + L^{\dagger}\ p_x\ (u,t|0_{t_o,t})\ dt + p_x\ (u,t|0_{t_o,t})m$$

where

$$m = \sum_{i=1}^{m} \{\lambda_i\ (u,t) - E\ \{\lambda_i\ (x,t)\}\}\ \{E\{\lambda_i\ (x,t)\}\}^{-1}$$

$$\{dN_i(t) - E\ \{\lambda_i\ (x,t)\}dt\}^T$$

Substituting this into equation (C.28) we obtain (C.29):

$$P\ (t+dt) + d\hat{x}\ d\hat{x}^T = \int (u-\hat{x}(t))\ (u-\hat{x}(t))^T\ p_x\ (u,t|0_{t_o,t})du$$

$$+ \int (u-\hat{x}(t)\ (u-\hat{x}(t))^T\ L^\dagger\ p_x\ (u,t)|0_{t_o,t})dt$$

$$+ \quad (u-\hat{x}(t))\ (u-\hat{x}(t))^T\ p_x\ (u,t|0_{t_o,t})\ m\ dt \qquad (C.29)$$

The first term of the R.H.S. of equation (C.29) equals P(t). To evaluate the second term consider the integral

$$\int (u_k - \hat{x}_k)\ (u_\ell - \hat{x}_\ell)\ L^\dagger p\ du$$

$$= \int (u_k - \hat{x}_k)\ (u_\ell - \hat{x}_\ell)\ \{ - \sum_{i=1}^{n} \frac{\partial(f_i p)}{\partial u_i} + \tfrac{1}{2} \sum_{i=1}^{n} \sum_{j=1}^{n} Q_{ij}\ \frac{\partial^2 p}{\partial u_i \partial u_j}\ \}du$$

which by integration by parts yields

$$= E\ \{(x_k - \hat{x}_k)\ f_\ell(x) \quad + E\ \{(x_\ell - \hat{x}_\ell)\ f_k(x) \quad + Q_{k\ell}$$

Hence using the expansion of equation (C.22):

$$f(x) \quad = \quad f(\hat{x}) + \frac{\partial f}{\partial \hat{x}}\ (x-\hat{x}) + \tfrac{1}{2} \sum_{i=1}^{n} \gamma_i\ (x-\hat{x})^T\ \frac{\partial^2 f}{\partial x^2}\ (x-\hat{x})$$

we obtain

$$\int (u-\hat{x})\ (u-\hat{x})^T\ L^\dagger\ p_x\ (u,t\,|0_{t_o,t})dt$$

$$= \frac{\partial f}{\partial \hat{x}}\ P(t) + P(t)\ \frac{\partial f^T}{\partial \hat{x}} \quad + Q$$

The third term is evaluated

$$\int (u-\hat{x})\ (u-\hat{x})\ p \sum_{i=1}^{m} \{\lambda(t) - \hat{\lambda}(t)\}\gamma_i\ (\lambda(t)\gamma_i)^{-1}$$

$$(dN(t) - \lambda(t)\ dt)^T\ \gamma_i\ du$$

$$= \int (u_k - \hat{x}_k)\,(u_\ell - \hat{x}_\ell)\, p$$

$$\sum_{i=1}^{n} \{\lambda(x) - \frac{\partial \lambda}{\partial \hat{x}}\,(x-\hat{x}) + \tfrac{1}{2} \sum_{i=1}^{m} \xi_i\,(x-\hat{x})^T \frac{\partial^2 \lambda}{\partial \hat{x}^2}\,(x-\hat{x}) - \hat{\lambda}(t)\}^T$$

$$(\lambda(t)\gamma_i)^{-1}(dN(t) - \lambda(t)dt)^T \gamma_i\, du$$

Noting that

$$\tfrac{1}{2} \int (u_k - \hat{x}_k)\,(u_\ell - \hat{x}_\ell)\, p \sum_{i=1}^{m} \xi_i\,(x-\hat{x})^T \frac{\partial^2 \lambda}{\partial \hat{x}^2}\,(x-\hat{x})\, du$$

$$= P \frac{\partial^2 \lambda}{\partial \hat{x}^2}\, P$$

We see that the third term equals

$$\sum_i P(t) \frac{\partial^2 \lambda}{\partial \hat{x}^2} P(t)\ \hat{\lambda}_i^{-1} \gamma_i^T\,(dN - \hat{\lambda}dt) \qquad (C.31)$$

Hence using equations (C.30) and (C.31) in equation (C.29) we obtain

$$P\,(t+dt) = P(t) + \frac{\partial f}{\partial \hat{x}}\, P(t) + P(t)\ \frac{\partial f}{\partial \hat{x}}^T + Q$$

$$+ \sum_i P(t) \frac{\partial^2 \lambda}{\partial \hat{x}} P(t)\, \lambda_i^{-1} \gamma_i^T\ (dN - \hat{\lambda}dt) - d\hat{x}\, d\hat{x}^T \qquad (C.32)$$

Evaluating this expression at the linearised optimum point, noting that

$$R(t) \triangleq P\,(s,t)$$

$$\lambda(t) \triangleq \lambda\,(s,t)$$

$$\partial P = P\,(t+dt) - P(t)$$

we obtain

$$dR(t) = \frac{\partial f}{\partial s} R(t) + R(t) \frac{\partial f^T}{\partial s} + Q$$

$$+ \sum R(t) \frac{\partial^2 \lambda}{\partial s^2} R(t) \hat{\lambda}^{-1} \gamma_i^T (dN - \lambda^* dt) - ds\, ds^T \qquad (C.33)$$

using equation (C.26) we obtain

$$dR(t) = \frac{\partial f}{\partial s} R(t)\, dt + R(t) \frac{\partial f}{\partial s}\, dt + Q(t)\, dt$$

$$- \sum_{i=1}^{m} R(t) \left\{ \frac{1}{\lambda_i} \left[\frac{\partial^2 \lambda_i}{\partial s^2} \right] - \frac{\partial^2 \ell n \lambda_i}{\partial s^2} \right\} R(t)\, \gamma_i^T dN(t) \qquad (C.34)$$

Equations (C.25) and (C.24) together form the estimation routines.

We summarise the results below.

Given a system disturbed by Gaussian noise, system equation

$$dx = f(t)\, dt + dn_g \qquad (C.35)$$

observed with measurements containing no Gaussian noise, with poisson rate vector λ (x,t), the first order linearised estimate s is given by the solution to the equations

$$ds = f(s)dt + \sum_{i=1}^{m} R(t) \frac{\partial \lambda}{\partial s} \gamma_i \, (\lambda^T(s)\gamma_i)^{-1} (dN(t) - \lambda(s)dt)$$

$$dR = \frac{\partial f}{\partial s} R dt + R \frac{\partial f^T}{\partial s}\, dt + Q(t)\, dt$$

$$+ \sum_{i=1}^{m} R(t) \frac{\partial^2 \ell n \lambda}{\partial s^2} R(t)\, \gamma_i\, dN(t) - \sum_{i=1}^{n} R(t) \frac{\partial^2 \lambda}{\partial s^2} R(t) dt \qquad (C.36)$$

In certain cases (Sny 4,5) (Eva 2), (Cla), simplifications occur in the filtering equations, though these are not normally as

great as those experienced in the case of linear Gaussian measurements. In the cases of metabolistic flow treated in the main text we may assume that no Gaussian noise occurs in the system, and that the state vector is constant. The equations obtained in this case for the state equation is

$$dx = 0$$

and for the estimates

$$ds = -R\frac{\partial\lambda}{\partial s}\,dt + R\frac{\partial \ell n\lambda}{\partial s}\,dN$$

$$dP = -\sum_{i=1}^{m} R\frac{\partial^2\lambda}{\partial s^2}\,Rdt + \sum_{i=1}^{m} R\frac{\partial^2 \ell n\lambda}{\partial s^2}\,RdN$$

In the case of a scalar exponentially varying measurement, drastic simplifications are obtained. With the problems treated in the text no other general simplifications occur, and each is treated on its own merits.

APPENDIX D

ANALYTIC SOLUTION OF THE EQUATION $\dot{x} = Ax$ OF DIMENSION 2

The equation $\dot{x} = Ax$ has a solution

$$x = \exp(At)\, x(0)$$

This solution is in general difficult to evaluate, if however the matrix A is diagonal then the evaluation is trivial. For most cases of non-diagonal forms,† by suitable change of variable, the matrix A may be diagonalised, the resulting equation solved, and the solution to the original equation obtained. The equation of dimension 2 is treated in this Appendix, and the general technique shown in Appendix E for a particular case of an equation of dimension 3.

Consider the equation $\dot{x} = Ax$, which for a matrix A of dimension (2x2) may be written

$$\frac{d}{dt}\begin{pmatrix} q_1 \\ q_2 \end{pmatrix} = \begin{pmatrix} \alpha & \beta \\ \gamma & \delta \end{pmatrix}\begin{pmatrix} q_1 \\ q_2 \end{pmatrix} \qquad (D.1)$$

This may be manipulated to give

$$\frac{d}{dt}\begin{pmatrix} q_1/\beta \\ q_2/\sqrt{\beta\gamma} \end{pmatrix} = \begin{pmatrix} \alpha & \sqrt{\beta\gamma} \\ \sqrt{\beta\gamma} & \delta \end{pmatrix}\begin{pmatrix} q_1/\beta \\ q_2/\sqrt{\beta\alpha} \end{pmatrix} \qquad (D.2)$$

We have two cases. If $\beta\gamma>0$ then let $\varepsilon = \sqrt{\beta\gamma}$ to obtain (D.3)

† For cases of non repeated eigenvalues.

$$\frac{d}{dt}\begin{bmatrix} q_1/\beta \\ q_2/\varepsilon \end{bmatrix} = \begin{bmatrix} \alpha & \varepsilon \\ \varepsilon & \delta \end{bmatrix}\begin{bmatrix} q_1/\beta \\ q_2/\varepsilon \end{bmatrix} \qquad (D.3)$$

If $\beta\gamma<0$ then let $j\varepsilon=\sqrt{\beta\varepsilon}$, $\varepsilon = \sqrt{|\beta\gamma|}$ to give

$$\frac{d}{dt}\begin{bmatrix} q_1/\beta \\ q_2/j\varepsilon \end{bmatrix} = \begin{bmatrix} \alpha & j\varepsilon \\ j\varepsilon & \delta \end{bmatrix}\begin{bmatrix} q_1/\beta \\ q_2/j\varepsilon \end{bmatrix}$$

$$\begin{bmatrix} q_1/\beta \\ q_2/\varepsilon \end{bmatrix} \quad \begin{bmatrix} \alpha & \varepsilon \\ -\varepsilon & \delta \end{bmatrix}\begin{bmatrix} q_1/\beta \\ q_2/\varepsilon \end{bmatrix} \qquad (D.4)$$

If $\beta\gamma=0$ then $\beta = 0$ or $\gamma = 0$ and the matrix may be transformed into diagonal form by straightforward row subtraction.

The next stage is to transform either of the resulting equations (D.3) or (D.4) to a diagonal form.

Treating the symmetric matric (D.3), with the definitions

$$q_1^* = q_1/\beta \qquad q_2^* = q_2/\varepsilon \quad \text{we obtain}$$

$$\frac{d}{dt}\begin{bmatrix} q_1^* \\ q_2^* + cq_1^* \end{bmatrix} = \begin{bmatrix} \alpha & \varepsilon \\ \varepsilon + c\alpha & \delta + c\varepsilon \end{bmatrix}\begin{bmatrix} q_1^* \\ q_2^* \end{bmatrix} \qquad (D.5)$$

$$\frac{d}{dt}\begin{bmatrix} q_1^* \\ q_2^* + cq_1^* \end{bmatrix} = \begin{bmatrix} \alpha - c\varepsilon & \varepsilon \\ \varepsilon + c\alpha - c(\delta + c\varepsilon) & \delta + c\varepsilon \end{bmatrix}\begin{bmatrix} q_1^* \\ q_2^* + cq_1^* \end{bmatrix}$$

(D.6)

With the restriction

$$\varepsilon + c\alpha - c(\delta + c\varepsilon) = 0$$

i.e. with the definition $c \triangleq \dfrac{\delta - \alpha \pm \sqrt{(\delta-\alpha)^2 + 4\varepsilon^2}}{-2\alpha}$

$$= \frac{\alpha - \delta \pm \sqrt{(\delta-\alpha)^2 + 4\varepsilon^2}}{2\alpha} \qquad (D.7)$$

We obtain an upper diagonal matrix

$$\frac{d}{dt}\begin{pmatrix} q_1^* \\ q_2^* + cq^* \end{pmatrix} = \begin{pmatrix} \alpha - c\varepsilon & \varepsilon \\ \phi & \delta + c\varepsilon \end{pmatrix}\begin{pmatrix} q_1^* \\ q_2^* + cq_1^* \end{pmatrix} \qquad (D.8)$$

this may now be converted to a diagonal form

$$\frac{d}{dt}\begin{pmatrix} q_1^* + d(q_2^* + cq_1^*) \\ q_2^* + cq_1^* \end{pmatrix} = \begin{pmatrix} \alpha - c\varepsilon & \varepsilon + d(\delta+c\varepsilon) - d(\alpha - c\varepsilon) \\ \phi & \delta + c\varepsilon \end{pmatrix} = \begin{pmatrix} q_1^* + d(q_2^* + cq_1^*) \\ q_2^* + cq_1^* \end{pmatrix} \qquad (D.9)$$

d is a variable, hence we may make the restriction $\varepsilon + d(\delta+c\varepsilon) - d(\alpha-c\varepsilon) = 0$, defining d and forming a diagonal matrix equation

$$\frac{d}{dt}\begin{pmatrix} Q_1 \\ Q_2 \end{pmatrix} = \begin{pmatrix} \alpha - c\varepsilon & \phi \\ \phi & \delta + c\varepsilon \end{pmatrix}\begin{pmatrix} Q_1 \\ Q_2 \end{pmatrix} \qquad (D.10)$$

where $Q_1 = q_1^* + d(q_2^* + cq_1^*)$ (D.11)

$$Q_2 = q_2^* + cq_1^* \qquad (D.12)$$

$$c = \frac{\alpha - \delta \pm \sqrt{(\alpha-\delta)^2 + 4\varepsilon^2}}{2\alpha} \tag{D.13}$$

$$d = \frac{\varepsilon}{\alpha - \delta - 2c\varepsilon} \tag{D.14}$$

The skew symmetric matrix of equation (D.4) may be converted to diagonal form in a similar manner. With the definitions $q_1^* = {}^{q_1}/_{\beta}$ $q_2^* = {}^{q_2}/_{\varepsilon}$, equation (D.4) becomes

$$\frac{d}{dt}\begin{pmatrix} q_1^* \\ q_2^* + cq_1^* \end{pmatrix} = \begin{pmatrix} \alpha & \varepsilon \\ -\varepsilon + c\alpha & \delta + c\varepsilon \end{pmatrix}\begin{pmatrix} q_1^* \\ q_2^* \end{pmatrix} \tag{D.15}$$

$$\frac{d}{dt}\begin{pmatrix} q_1^* \\ q_2^* + cq_1^* \end{pmatrix} = \begin{pmatrix} \alpha - c\varepsilon & \varepsilon \\ -\varepsilon + c\alpha - c(\delta + c\varepsilon) & \delta + c\varepsilon \end{pmatrix}\begin{pmatrix} q_1^* \\ q_2^* + cq_1^* \end{pmatrix} \tag{D.16}$$

With the restriction $-\varepsilon + c\alpha - c(\delta + c\varepsilon) = 0$, defining c, we obtain an upper diagonal matrix

$$\frac{d}{dt}\begin{pmatrix} q_1^* \\ q_2^* + cq_1^* \end{pmatrix} = \begin{pmatrix} \alpha - c\varepsilon & \varepsilon \\ 0 & \delta + c\varepsilon \end{pmatrix}\begin{pmatrix} q_1^* \\ q_2^* + cq_1^* \end{pmatrix} \tag{D.17}$$

Noting that equation (D.17) is of the same form as equation (D.8) we obtain the diagonal form corresponding to equation (D.10) namely

$$\frac{d}{dt}\begin{pmatrix} Q_1 \\ Q_2 \end{pmatrix} = \begin{pmatrix} \alpha - c\varepsilon & 0 \\ 0 & \delta + c\varepsilon \end{pmatrix}\begin{pmatrix} Q_1 \\ Q_2 \end{pmatrix} \tag{D.18}$$

where $$Q_1 = q_1^* + d\,(q_2^* + cq_1^*) \tag{D.19}$$

$$Q_2 = q_2^* + cq_1^* \tag{D.20}$$

$$c = \frac{\alpha - \delta \pm \sqrt{(\alpha - \delta)^2 - 4\varepsilon^2}}{2\varepsilon} \tag{D.21}$$

$$d = \frac{\varepsilon}{\alpha - \delta - 2c\varepsilon} \tag{D.22}$$

Due to the similarities in the two cases they may be combined. We hence obtain the summary. Given a matrix equation of dimension 2 of the form

$$\frac{d}{dt}\begin{pmatrix} q_1 \\ q_2 \end{pmatrix} = \begin{pmatrix} a_{11} & a_{21} \\ a_{12} & a_{22} \end{pmatrix}\begin{pmatrix} q_1 \\ q_2 \end{pmatrix} \tag{D.23}$$

then we may write

$$\frac{d}{dt}\begin{pmatrix} Q_1 \\ Q_2 \end{pmatrix} = \begin{pmatrix} \lambda_1 & 0 \\ 0 & \lambda_2 \end{pmatrix}\begin{pmatrix} Q_1 \\ Q_2 \end{pmatrix} \tag{D.24}$$

Where $$Q_1 = q_1^* + d\,(q_2^* + cq_1^*) \tag{D.25}$$

$$Q_2 = q_2^* + cq_1^* \tag{D.26}$$

$$q_1^* = q_1/a_{21} \tag{D.27}$$

$$q_2^* = q_2/\varepsilon \tag{D.28}$$

$$\varepsilon = \sqrt{|a_{12}\,a_{21}|} \tag{D.29}$$

$$c = \frac{a_{11} - a_{12} \pm \sqrt{(a_{22} - a_{11})^2 + 4\epsilon}}{2\epsilon} \qquad (D.30)$$

$$\lambda_1 = a_{11} - c\epsilon \qquad (D.31)$$

$$\lambda_2 = a_{22} + c\epsilon \qquad (D.32)$$

APPENDIX E

Diagonalisation of a Third order matrix to show the general technique of solution of an equation of the form $\dot{x} = Ax$.†

$$\frac{d}{dt}\begin{pmatrix} q_1 \\ q_2 \\ q_3 \end{pmatrix} = \begin{pmatrix} a_{11} & a_{12} & \\ a_{21} & a_{22} & a_{23} \\ & a_{32} & a_{33} \end{pmatrix} \begin{pmatrix} q_1 \\ q_2 \\ q_3 \end{pmatrix} \tag{E.1}$$

Using equations (D.23) to (D.32) we may change the first two variables to give

$$\frac{d}{dt}\begin{pmatrix} r_1 \\ r_2 \\ q_3 \end{pmatrix} = \begin{pmatrix} \lambda_1 & & \\ & \lambda_2 & a_{23} \\ a_{31}' & a_{32}' & a_{33} \end{pmatrix} \begin{pmatrix} r_1 \\ r_2 \\ q_3 \end{pmatrix} \tag{E.2}$$

where

$$a_{31}' = -c\varepsilon a_{32} \tag{E.3}$$

$$a_{32}' = \varepsilon a_{32} \tag{E.4}$$

which arise from the relationships

$$q_1 = a_{12} r_1 \tag{E.5}$$

$$q_2 = \varepsilon r_2 - \frac{c\varepsilon}{a_{12}} q_1 = \varepsilon r_2 - c\varepsilon r_1 \tag{E.6}$$

λ_1 and λ_2 are as given in equation (D.31) and (D.32)

Subtracting a multiple of the third variable from the second gives equation (E.7).

† For case with no repeated eigenvalues.

$$\frac{d}{dt}\begin{pmatrix} r_1 \\ r_2 \\ r_3 \end{pmatrix} = \begin{pmatrix} \lambda_1 & & \\ & \lambda_2 & a_{23} \\ & a_{32}' & \lambda_3 \end{pmatrix} \begin{pmatrix} r_1 \\ r_2 \\ r_3 \end{pmatrix} \tag{E.7}$$

where

$$r_3 = q_3 - \frac{a_{31}'}{\lambda_1} r_1 \tag{E.8}$$

$$\lambda_3 = a_{33} \tag{E.9}$$

Applying the result from Appendix D once more gives

$$\frac{d}{dt}\begin{pmatrix} Q_1 \\ Q_2 \\ Q_3 \end{pmatrix} = \begin{pmatrix} \mu_1 & & \\ & \mu_2 & \\ & & \mu_3 \end{pmatrix} \begin{pmatrix} Q_1 \\ Q_2 \\ Q_3 \end{pmatrix} \tag{E.10}$$

where

$$Q_1 = r_1 \tag{E.11a}$$

$$Q_2 = r_2/a_{23} \tag{E.11b}$$

$$Q_3 = r_3/\varepsilon_1 + c_1\, r_2/a_{23} \tag{E.11c}$$

$$\mu_1 = \lambda_1 \tag{E.12a}$$

$$\mu_2 = \lambda_2 + c_1\varepsilon_1 \tag{E.12b}$$

$$\mu_3 = \lambda_3 + c_1\varepsilon_1 \tag{E.12c}$$

$$\varepsilon_1 = \sqrt{|a_{23}\, a_{32}'|} \tag{E.13}$$

$$c_1 = \frac{\lambda_2 - a_{33} \pm \sqrt{(\lambda_2 - a_{33})^2 + 4\epsilon_1 {}^2 b_1}}{2\epsilon_1} \qquad \text{(E.14)}$$

$$b_1 = \text{sgn}\,(a_{23}\, a_{32}') \qquad \text{(E.15)}$$

The result of this section may be summarised:-

Given the system equation

$$\frac{d}{dt}\begin{pmatrix} q_1 \\ q_2 \\ q_3 \end{pmatrix} = \begin{pmatrix} a_{11} & a_{12} & \\ a_{21} & a_{22} & a_{23} \\ & a_{32} & a_{33} \end{pmatrix} \begin{pmatrix} q_1 \\ q_2 \\ q_3 \end{pmatrix} \qquad \text{(E.16)}$$

by change of variables we may form the diagonal matrix equation

$$\frac{d}{dt}\begin{pmatrix} Q_1 \\ Q2 \\ Q_3 \end{pmatrix} = \begin{pmatrix} \mu_1 & & 0 \\ & \mu_2 & \\ 0 & & \mu_3 \end{pmatrix} \begin{pmatrix} Q_1 \\ Q_2 \\ Q_3 \end{pmatrix} \qquad \text{(.17)}$$

where

$$Q_1 = q_1/a_{12} \qquad \text{(E.18a)}$$

$$Q_2 = \{q_2/\epsilon + cq_1/a_{12}\}/a_{23} \qquad \text{(E.18b)}$$

$$Q_3 = \{q_3 - a_{31}' q_1/\lambda_1\, a_{12}\}/\epsilon_1 + \{q_2/\epsilon + cq_1/a_{12}\}\, c_1/a_{23} \qquad \text{(E.18c)}$$

$$a_{31}' = -c\epsilon a_{32} \qquad \text{(E.18d)}$$

$$\lambda_1 = a_{11} - c\epsilon \qquad \text{(E.18e)}$$

$$\mu_1 = a_{11} - c\epsilon \qquad \text{(E.18f)}$$

$$\mu_2 = a_{22} + c\varepsilon - c_1\varepsilon_1 \tag{E.18g}$$

$$\mu_3 = a_{33} + c_1\varepsilon_1 \tag{E.18h}$$

$$\varepsilon = \sqrt{|a_{12}a_{21}|} \tag{E.18i}$$

$$\varepsilon_1 = \sqrt{|a_{23}a_{32}'|} = \sqrt{|a_{23}a_{32}\ \varepsilon|} \tag{E.18j}$$

$$c = \frac{a_{11} - a_{22} \pm \sqrt{(a_{11} - a_{22})^2 + 4\varepsilon^2 b}}{2\varepsilon} \tag{E.18k}$$

$$c_1 = \frac{a_{22} + c\varepsilon - a_{33} \pm \sqrt{(a_{22} + c\varepsilon - a_{33})^2 + 4\varepsilon_1^2 b_1}}{2\varepsilon_1} \tag{E.18ℓ}$$

$$b = \text{sgn}\,[a_{12}a_{21}] \tag{E.18m}$$

$$b_1 = \text{sgn}\,[a_{23}a_{32}\ \varepsilon]$$

$$= \text{sgn}\,[a_{23}a_{32}] \tag{E.18n}$$

APPENDIX F

DERIVATION OF THE INITIAL COVARIANCE OF A VARIABLE GIVEN THE INITIAL RANGE [a,b] ref.[Fre]

In this Appendix we derive the initial covariance of a variable x, given the initial apriori assumption that the probability that it has a certain value is uniform inside a certain range (a,b), and zero outside this range. Figure F.1 shows the uniform density function of the variable. Discontinuities exist at the end points at $x = a$ and $x = b$.

The density function is given by:

$$f(x) = \frac{1}{b-a}, \quad a<x<b, \quad f(x) = 0 \text{ elsewhere} \qquad (F.1)$$

The expected value (the mean) is given by:

$$E(x) \int_a^b xf(x)dx = \frac{x^2}{2(b-a)} \Big|_a^b = \frac{b^2-a^2}{2(b-a)} = \frac{a+b}{2} \qquad (F.2)$$

The covariance is given by

$$\sigma^2(x) = \int_a^b [x - E(x)]^2 f(x)dx$$

$$= \int_a^b \left(x - \frac{a+b}{2}\right)^2 \frac{1}{b-a} dx$$

$$= \frac{1}{3} \left(x - \frac{a+b}{2}\right)^3 \frac{1}{b-a} \Big|_a^b$$

$$= \frac{\left(\frac{b-a}{2}\right)^3 - \left(\frac{a-b}{2}\right)^3}{3\ (b-a)}$$

$$= \frac{(b-a)^2}{12} \qquad \text{(F.3)}$$

APPENDIX G

COMPUTER LISTINGS

```
C
C       CODE TO DETERMINE EXTRACTION RATES OF LIVER AND SPLEEN
C
        COMMON NR(16),NC(256),NA(256,16)
        DIMENSION A(240),S(240),CURVE(240)
C
        CALL OPEN (1,"RSWAP",2,IER,8192)
        CALL RDBLK (1,0,NA(1,1),32,IER)
        ICHK=0
        CALL CGP("L",A(1),NPT,JCR,NEL,1,240)
        ICHK=ICHK+1
40      CALL CGP("S",S(1),NPT,JCR,NEL,1,250)
        ICHK=ICHK+1
50      IF ( ICHK .LT. 2 ) GO TO 150
C
500     ACCEPT "TYPE 1 FOR LIVER, 2 FOR SPLEEN, 3
C                                          FOR SUM OF BOTH:",IFLAG
        IF ( IFLAG .EQ. 1 ) GO TO 1000
        IF ( IFLAG .EQ. 2 ) GO TO 1010
        IF ( IFLAG .EQ. 3 ) GO TO 1020
C
        GO TO 500
C
1000    DO 2000 I = 1,NPT
2000    CURVE(I)= A(I)
        GO TO 3000
C
1010    DO 2010 I = 1,NPT
2010    CURVE(I)= S(I)
        GO TO 3000
C
1020    DO 2020 I = 1,NPT
2020    CURVE(I)= A(I)+S(I)
        GO TO 3000
C
3000    CONTINUE
C
C       CORRECT FOR DECAY OF ISOTOPE
C       ----------------------------
C
        ACCEPT "ENTER TIME PERIOD BETWEEN FRAMES
C                                    IN SECS.  (INTEGER)",IFRAME
C
C       CONVERT TO MINUTES.
C
        T= FLOAT(IFRAME)/60.0
C
C       HALF LIFE OF TECHNECIUM IS 6 HOURS.
C
        T1= 6.0
C
        DO 5000 I=1,NPT
        CURVE(I) = EXP (0.693*I*T/T1/60.0)*CURVE(I)
5000    CONTINUE
C
C       FIT THE EXPONENTIAL
C
        ACCEPT "FIRST POINT OF FIT = ",IP
        ACCEPT "LAST POINT OF FIT = ",LP
C
        N=LP-IP+1
        SN= FLOAT(N)
```

```
C
      ACCEPT "IS PLATEAU TO BE COMPUTED YES=1 NO=0 ",K
      IF ( K .EQ. 0 ) GO TO 10
      ACCEPT "FIRST POINT OF PLATEAU = ",IPP
      ACCEPT "LAST POINT OF PLATEAU = ",LPP
C
      N = LPP - IPP + 1
      Y = FLOAT(N)
C
      DO 6000 I =IPP,LPP
6000  P = P + CURVE(I)
C
      P = P/Y
      TYPE "PLATEAU = ",P
      GO TO 6010
C
10    ACCEPT "TYPE THE PLATEAU (REAL NUMBER) ",P
C
6010  SX = 0.0
      SXS= 0.0
      SY = 0.0
      SXY= 0.0
C
      DO 7000 I =IP,LP
      CURVE(I)= ALOG (P - CURVE(I))
      X = FLOAT(I)
      SX = SX+X*F
      SXS= SXS+(X*F)**2
      SY = SY+CURVE(I)
7000  SXY= SXY+CURVE(I)*X*F
C
      XM=SX/SN
      YM = SY/SN
      B = (SXY-SN*XM*YM)/(SXS-SN*XM*XM)
      B = 0.0 - B
C
      TYPE "TOTAL EXTRACTION RATE (UNIT= PER MIN) = ",B
C
      T = 0.693/B*60.0
      TYPE "T1/2 IN SECS = ",T
C
C     STORE THE EXTRACTION RATE AND PLATEAU.
C     **************************************
C
      IF (IFLAG .EQ. 1) GO TO 9010
      IF (IFLAG .EQ. 2) GO TO 9020
      IF (IFLAG .EQ. 3) GO TO 9030
C
9010  P1=P
      B1=B
      GO TO 9500
C
9020  P2=P
      B2=B
      GO TO 9500
C
9030  P3=P
      B3=B
      GO TO 9500
C
9500  CONTINUE
```

```
C
      ACCEPT "HAVE ALL CURVES BEEN ENTERED ? TYPE 1 FOR YES
C
      IF ( JFLAG .EQ. 1 ) GO TO 9000        2 FOR NO ",JFLAG
C
      GO TO 500
C
9000  CONTINUE
C
C     CALCULATE INDIVIDUAL EXTRACTION RATES.
C     ======================================
C
C A>  SPLENIC EXTRACTION RATE
C
      E2 = P2*B3
      R2 = E2
C
C B>  LIVER EXTRACTION RATE
C
      E1 = P1*B3
      R1 = E1 / ( 3.0 - E2 )
C
      TYPE "EXTRACTION RATE OF SPLEEN PER MIN = ",R2
      TYPE "EXTRACTION RATE OF LIVER PER MIN  = ",R1
C
      GO TO 300
C
150   CALL TEXT ("CREATE CURVES (L) AND (S) ",1,1)
300   CALL WRBLK(1,0,NA(1),32,IER)
      CALL CLOSE (1,IER)
      CALL EXIT
      END
```

```
5 REM: PROGRAM TO PLOT ELLIPSES BY APPROXIMATE METHOD
10 SCALE 1,23,1,23
20 DISP "L=";L;
30 INPUT L
40 PRINT "L=";L;
50 DISP "INPUT1 IF GRAPH REQD";
60 INPUT S2
70 IF S2<1 THEN 120
80 FOR I1=1 TO 23
90 XAXIS I1
100 YAXIS I1
110 NEXT I1
120 DIM A[22,22]
130 MAT A=ZER[22,22]
140 GOTO 150
150 X1=Y1=Z1=0
160 X2=-1
170 Y2=-1
180 Z2=-10
190 X=X1-X2
200 Y=Y1-Y2
210 Z=Z1-Z2
220 C0=X*X+Y*Y
230 D0=C0+Z*Z
240 C=SQR(C0)
250 D=SQR(D0)
260 C1=X/C
270 S1=Y/C
280 C2=Z/D
290 T2=C/Z
300 DISP "TAN PHI=";
310 INPUT T3
320 PRINT "TANPHI=";T3;
330 T4=(T2+T3)/(1-T2*T3)
340 T5=(T2-T3)/(1+T2*T3)
350 DISP "HEIGHT OF SLICE H=";
360 INPUT H
370 PRINT "H=";H;
380 P=H*(T4+T5)/2
390 A=H*(T4-T5)/2
400 R=H*T3/C2
410 S0=H*T2-(H*T5)
420 S=A-S0
430 B=A*S/SQR((A-R)*(A+R))
440 K=B*B/(A*A)
450 J1=J2=(P+A)*C1+12
460 J3=J4=(P-A)*C1+12
470 K1=K2=(P+A)*S1+12
480 K3=K4=(P-A)*S1+12
490 I=0
500 IF J1>23 THEN 590
510 IF J1<1 THEN 590
520 IF K1>23 THEN 590
530 IF K1<1 THEN 590
540 A[INT(J1),INT(K1)]=A[INT(J1),INT(K1)]+1
```

```
550 PLOT J1,K1,-2
560 PEN
570 LABEL (*)A[INT(J1),INT(K1)]
580 GOTO 600
590 I=1
600 IF J3>23 THEN 680
610 IF J3<1 THEN 680
620 IF K3>23 THEN 680
630 IF K3<1 THEN 680
640 A[INT(J3),INT(K3)]=A[INT(J3),INT(K3)]+1
650 PLOT J3,K3
660 LABEL (*)A[INT(J3),INT(K3)]
670 GOTO 730
680 I=I+1
690 IF I=2 THEN 710
700 GOTO 730
710 PRINT "ELLIPSE ENDS OUT OF RANGE"
720 GOTO 1880
730 U=INT(A)*L
740 PRINT "U="U
750 Y2=0
760 Z2=1
770 V=1
780 Y2=Y2+K*(U+U+1)
790 PRINT "Y2="Y2;
800 IF Z2>Y2 THEN 1320
810 J1=J1-S1/L
820 J2=J2+S1/L
830 J3=J3-S1/L
840 J4=J4+S1/L
850 K1=K1+C1/L
860 K2=K2-C1/L
870 K3=K3+C1/L
880 K4=K4-C1/L
890 IF J1>23 THEN 970
900 IF J1<0 THEN 970
910 IF K1>23 THEN 970
920 IF K1<0 THEN 970
930 A[INT(J1),INT(K1)]=A[INT(J1),INT(K1)]+1
940 PLOT J1,K1
950 LABEL (*)A[INT(J1),INT(K1)]
960 GOTO 980
970 I=1
980 IF J2>23 THEN 1060
990 IF J2<1 THEN 1060
1000 IF K2>23 THEN 1060
1010 IF K2<1 THEN 1060
1020 A[INT(J2),INT(K2)]=A[INT(J2),INT(K2)]+1
1030 PLOT J2,K2
1040 LABEL (*)A[INT(J2),INT(K2)]
1050 GOTO 1070
1060 I=I+1
1070 IF J3>23 THEN 1150
1080 IF J3<1 THEN 1150
1090 IF K3>23 THEN 1150
1100 IF K3<1 THEN 1150
1110 A[INT(J3),INT(K3)]=A[INT(J3),INT(K3)]+1
1120 PLOT J3,K3
```

```
1130 LABEL (*)A[INT(J3),INT(K3)]
1140 GOTO 1160
1150 I=I+1
1160 IF J4>23 THEN 1240
1170 IF J4<1 THEN 1240
1180 IF K4>23 THEN 1240
1190 IF K4<1 THEN 1240
1200 A[INT(J4),INT(K4)]=A[INT(J4),INT(K4)]+1
1210 PLOT J4,K4
1220 LABEL (*)A[INT(J4),INT(K4)]
1230 GOTO 1290
1240 I=I+1
1250 IF I=4 THEN 1270
1260 GOTO 1290
1270 PRINT "ELLIPSE OUT OF RANGE"
1280 GOTO 1880
1290 Z2=Z2+V+V+1
1300 V=V+1
1310 GOTO 800
1320 U=U-1
1330 J1=J1-C1/L
1340 J2=J2-C1/L
1350 J3=J3+C1/L
1360 J4=J4+C1/L
1370 K1=K1-S1/L
1380 K2=K2-S1/L
1390 K3=K3+S1/L
1400 K4=K4+S1/L
1410 I=0
1420 IF J1>23 THEN 1500
1430 IF J1<0 THEN 1500
1440 IF K1>23 THEN 1500
1450 IF K1<0 THEN 1500
1460 A[INT(J1),INT(K1)]=A[INT(J1),INT(K1)]+1
1470 PLOT J1,K1
1480 LABEL (*)A[INT(J1),INT(K1)]
1490 GOTO 1510
1500 I=I+1
1510 IF J2>23 THEN 1590
1520 IF J2<1 THEN 1590
1530 IF K2>23 THEN 1590
1540 IF K2<1 THEN 1590
1550 A[INT(J2),INT(K2)]=A[INT(J2),INT(K2)]+1
1560 PLOT J2,K2
1570 LABEL (*)A[INT(J2),INT(K2)]
1580 GOTO 1600
1590 I=I+1
1600 IF J3>23 THEN 1680
1610 IF J3<1 THEN 1680
1620 IF K3>23 THEN 1680
1630 IF K3<1 THEN 1680
1640 A[INT(J3),INT(K3)]=A[INT(J3),INT(K3)]+1
1650 PLOT J3,K3
1660 LABEL (*)A[INT(J3),INT(K3)]
1670 GOTO 1690
1680 I=I+1
```

```
1690 IF J4>23 THEN 1770
1700 IF J4<1 THEN 1770
1710 IF K4>23 THEN 1770
1720 IF K4<1 THEN 1770
1730 A[INT(J4),INT(K4)]=A[INT(J4),INT(K4)]+1
1740 PLOT J4,K4
1750 LABEL (*)A[INT(J4),INT(K4)]
1760 GOTO 1790
1770 I=I+1
1780 IF I=4 THEN 1270
1790 Y2=Y2+K*(U+U+1)
1800 IF U>0 THEN 800
1810 FOR J=22 TO 1 STEP -1
1820 FOR I=1 TO 21
1830 WRITE (15,1870)A[I,J];
1840 NEXT I
1850 WRITE (15,1870)A[I,J]
1860 NEXT J
1870 FORMAT F2.0
1880 STOP
1890 END
```

```
0010 REM: PROGRAM CODE TO EVALUATE THE SYSTEM IDENTIFICATION
0020 REM: TECHNIQUE DESCRIBED IN CHAPTERS I & IV BY:
0030 REM: (1) SIMULATION OF POSSIBLE MEASUREMENTS OF
0040 REM:     RADIOACTIVE TRACER INJECTED INTO THE HEPATIC
0050 REM:     FLOW, GIVEN KNOWN RATES OF EXTRACTION OF THE
0060 REM:     TRACER FROM THE LIVER SPLEEN AND BONE MARROW.
0070 REM: (2) OBTAINING THE BEST ESTIMATE OF THE FLOW RATE FROM
0080 REM:     THESE SIMULATED MEASEUREMENTS USING THE STOCHASTIC
0090 REM:     SYSTEM IDENTIFICATION TECHNIQUE, USING SNYDER'S
0100 REM:     FILTER.
0110 REM: (3) COMPARISON OF THE KNOWN AND ESTIMATED RESULTS.
0120 REM
0130 TAB =10
0140 CLOSE
0150 LET A$="DATA"
0160 INPUT "DATA TO BE STORED IN DATA FILE NO ",B$
0170 LET C$=A$,B$
0180 OPEN FILE (3,0),C$
0190 OPEN FILE (0,3),"$LPT"
0200 INPUT "HARD COPY REQUIRED ? CR FOR YES",A$
0210 IF A$<>"" THEN GOTO 0240
0220 OPEN FILE (1,3),"$TTO1"
0230 GOTO 0250
0240 OPEN FILE (1,3),"$TTO"
0250 DIM A(500)
0260 DIM M(3),M1(5),M2(5),M3(5),Z9(3)
0270 DIM H1(3,3),H2(3,3),H3(3,3),O(3,3),P(3,3)
0280 DIM R1(6),R2(6),R3(6),S(3),U(3),G(3),A0(6),A1(6),E(3),S1(3),N(3)
0290 DIM U1(3)
0300 PRINT FILE (1),"DATA STORED IN FILE ";C$
0310 REM:SIMULATION OF THE ESTIMATION OF BLOOD FLOW RATES TO THE LIVER
0320 REM:SPLEEN AND BONE MARROW.
0330 REM
0340 REM: FLOW DIAGRAM
0350 REM
0360 REM:    LIVER <--- PLASMA ---> SPLEEN
0370 REM:                  I
0380 REM:                  V
0390 REM:           BONE MARROW
0400 REM
0410 REM:SET INITIAL VALUES
0420 REM: N0=LOOP NO  N1=LOOPS BETWEEN PRINTOUTS  N2=NEXT PRINTOUT NO.
0430 LET N0=0
0440 INPUT "ENTER NO OF ITERATIONS BETWEEN EACH PRINTOUT",N1
0450 INPUT "ENTER TOTAL NO OF PRINTOUTS REQD ",N5
0460 LET L9=N1
0470 LET N2=0
0480 REM: Q=TOTAL DOPANT INTENSITY
0490 INPUT "TOTAL DOPANT INTENSITY = ",Q
0500 PRINT FILE (1),"TOTAL DOPANT INTENSITY= ";Q
```

```
0510 REM: T1=CURRENT TIME
0520 REM: T2=DISCRETISATION PERIOD
0530 REM: T3=SIMULATION PERIOD
0540 REM: T4=UAXIS COLLISION INTERVAL
0550 REM: T5=UAXIS COLLISION POINTS
0560 REM: T6=TAXIS TIME + T2
0570 REM: T7=TAXIS TIME + 2*T2
0580 REM: T8=END OF TAXIS INTERVAL
0590 REM: T9=END OF FOLLOWING TAXIS INTERVAL
0600 LET T1=0
0610 INPUT "DISCRETISATION PERIOD = ",T2
0620 PRINT FILE (1),"DISCRETISATION PERIOD = ";T2
0630 REM: SET UP THE STATE TERMS
0640 REM: 1  * THE FIRST
0650 REM: 2  * DERIVATIVES OF
0660 REM: 3  * THE ESTIMATE
0670 REM: 4  * THE ESTIMATE
0680 REM: 5  * THE ACTUAL VALUE
0690 REM: 6  * THE 2ND DERIVATIVE
0700 REM: SET THE DIFFERENTIALS OF THE RATE VECTORS
0710 LET R1(1)=1
0720 LET R2(2)=1
0730 LET R3(3)=1
0740 REM: SET ACTUAL FLOW RATES
0750 INPUT "FIRST FLOW RATE ",R1(5)
0760 INPUT "SECOND FLOW RATE ",R2(5)
0770 INPUT "THIRD FLOW RATE ",R3(5)
0780 REM:SET ESTIMATES OF FLOWS
0790 INPUT "FIRST ESTIMATE",R1(4)
0800 INPUT "SECOND ESTIMATE ",R2(4)
0810 INPUT "THIRD ESTIMATE ",R3(4)
0820 INPUT "UNCERTAINTY OF KNOWLEDGE OF FLOW RATES +-",U1
0830 REM: STATE IS DEFINED AS ESTIMATE OF FLOW RATES
0840 LET S(1)=R1(4)
0850 LET S(2)=R2(4)
0860 LET S(3)=R3(4)
0870 PPRINT FILE (1),"ACTUAL FLOW RATES:";R1(5),R2(5),R3(5)
0880 PPRINT FILE (1),"ESTIMATE OF RATES:",R1(4),R2(4),R3(4)
0890 PRINT FILE (1),"UNCERTAINTY      :","+-",U1
0900 REM: SET INITIAL COVARIANCE
0910 REM: U=UNCERTAINTY OF KNOWLEDGE OF FLOW RATE
0920 MAT U=CON(3)
0930 MAT U=(U1)*U
0940 REM:CALCULATE INITIAL COVARIANCE MATRIX P
0950 FOR I=1 TO 3
0960   LET P(I,I)=U(I)↑2/12
0970 NEXT I
0980 REM:SET INITIAL COUNT REQUIREMENTS
0990 REM: G(I)=1 IF A COUNT GENERATION IS REQUIRED
1000 FOR I=1 TO 3
1010   LET G(I)=1
1020 NEXT I
1030 REM: PRINT THE RESULTS
1040 GOSUB 2530
1050 GOSUB 2590
```

```
1060 REM: MAIN ALGORITHM
1070 IF T2*N0>30 THEN STOP
1080 REM: (1) SET THE LIMITS OF THE TIME PERIODS ON THE U AXES
1090 GOSUB 1670
1100 REM: (2) DERIVE THE MEASUREMENT RATES AND THEIR DERIVATIVES
1110 GOSUB 1300
1120 REM: (3) GENERATE THE COUNT VECTOR
1130 GOSUB 1830
1140 REM: APPLY CORRECTION FOR COUNTS VIA FILTERING ALGORITHM
1150 LET D(1)=M(1)/M1(4)-T2
1160 LET D(2)=M(2)/M2(4)-T2
1170 LET D(3)=M(3)/M3(4)-T2
1180 GOSUB 2020
1190 REM: INCREMENT THE TIME PERIOD
1200 LET T1=T1+T2
1210 REM: PRINT RESULTS AND CHECK FOR END OF TEST PERIOD
1220 GOSUB 2590
1230 REM: REINITIALISE THE MEASUREMENT VECTOR
1240 GOSUB 2820
1250 GOTO 1060
1260 REM
1270 REM SUBROUTINES
1280 REM ***********
1290 REM
1300 REM: GENERATE THE MEASUREMENTS: ACTUAL, ESTIMATED AND REQUIRED DERI
1310 REM: OBTAIN THE ESTIMATED AND ACTUAL RATES
1320 REM: STORE IN VECTOR M, ELMENTS 4 AND 5 RESPECTIVELY
1330 FOR I=4 TO 5
1340   LET R0(I)=R1(I)+R2(I)+R3(I)
1350   LET A0(I)=1-EXP(-R0(I)*T6)
1360   LET A1(I)=Q*A0(I)/R0(I)
1370   LET M1(I)=R1(I)*A1(I)
1380   LET M2(I)=R2(I)*A1(I)
1390   LET M3(I)=R3(I)*A1(I)
1400 NEXT I
1410 REM: FIRST DERIVATIVES
1420 FOR I=1 TO 3
1430   LET R0(I)=1
1440   LET A0(I)=T6*(1-A0(4))
1450   LET A1(I)=(R0(4)*A0(I)-A0(4)*R0(I))/R0(4)↑2
1460   LET A1(I)=Q*A1(I)
1470   LET M1(I)=R1(I)*A1(4)+A1(I)*R1(4)
1480   LET M2(I)=R2(I)*A1(4)+A1(I)*R2(4)
1490   LET M3(I)=R3(I)*A1(4)+A1(I)*R3(4)
1500 NEXT I
1510 REM: SECOND DERIVATIVES
1520 REM: STORE IN H MATRICES
1530 FOR I=1 TO 3
1540   FOR J=1 TO 3
1550     LET R0(6)=0
1560     LET A0(6)=-T6*A0(I)
1570     LET A1(6)=R0(4)*A0(6)+A0(I)*R0(J)-R0(6)*A0(4)-R0(I)*A0(J)
1580     LET A1(6)=A1(6)-2*R0(4)*R0(J)*(R0(4)*A0(I)-A0(4)*R0(J))/R0(4)↑2
1590     LET A1(6)=Q*A1(6)
1600     LET H1(I,J)=R1(4)*A1(6)+R1(I)*A1(J)+R1(J)*A1(I)+R1(6)*A1(4)
1610     LET H2(I,J)=R2(4)*A1(6)+R2(I)*A1(J)+R2(J)*A1(I)+R2(6)*A1(4)
1620     LET H3(I,J)=R3(4)*A1(6)+R3(I)*A1(J)+R3(J)*A1(I)+R3(6)*A1(4)
1630   NEXT J
1640 NEXT I
1650 RETURN
```

```
1660 REM
1670 REM FIND THE TERMS WITH COLLISION TIMES ON THE U AXIS
1680 REM LESS THAN THE TIMES OF THE PROJECTION OF THE END
1690 REM OF THE CURRENT DISCRETISATION PERIOD ON THE U AXIS
1700 LET T6=T1+T2
1710 FOR I=1 TO 3
1720   ON I THEN GOTO 1730, 1750, 1770
1730   LET R9=R1(5)
1740   GOTO 1780
1750   LET R9=R2(5)
1760   GOTO 1780
1770   LET R9=R3(5)
1780   LET R0(5)=R1(5)+R2(5)+R3(5)
1790   LET T8(I)=Q*R9*(T6-(1-EXP(-R0(5)*T6))/R0(5))/R0(5)
1800 NEXT I
1810 RETURN
1820 REM
1830 REM: INCREMENT MEASUREMENT TERMS IF COLLISION HAS TAKEN PLACE
1840 REM: IN PRESENT TIME INTERVAL.
1850 FOR I=1 TO 3
1860   LET M(I)=0
1870   IF T5(I)=0 THEN GOTO 1920
1880   IF T5(I)>T8(I) THEN GOTO 1970
1890   REM: COLLISION HAS TAKEN PLACE IN PRESENT TIME INTERVAL.
1900   REM: INCREMENT COUNT.
1910   LET M(I)=M(I)+1
1920   REM: OBTAIN NEW U-AXIS POINT
1930   LET T4=-LOG(RND(1))
1940   LET T5(I)=T5(I)+T4
1950   REM: CHECK WHETHER POINT IS WITHIN CURRENT TIME INTERVAL
1960   GOTO 1880
1970 NEXT I
1980 REM: OBTAIN THE TOTAL COUNTS IN EACH MEASUREMENT.
1990 MAT Z9=Z9+M
2000 RETURN
2010 REM: ************************************************************
```

```
2020 REM: FILTERING ALGORITHM
2030 REM: FORM THE DIFFERENCE BETWEEN THE ACTUAL COUNT AND THE
2040 REM: ESTIMATED COUNT.
2050 REM: DIVIDE BY THE MEASUREMENT RATE.
2060 REM: (2) APPLY THE FILTERING EQUATION TO FORM THE NEW STATE VECTOR
2070 REM: PREMULTIPLY BY THE FIRST DIFFERENTIAL OF THE ESTIMATE OF THE
2080 REM: MEASUREMENT RATE
2090 LET E(1)=M1(1)*D(1)+M2(1)*D(2)+M3(1)*D(3)
2100 LET E(2)=M1(2)*D(1)+M2(2)*D(2)+M3(2)*D(3)
2110 LET E(3)=M1(3)*D(1)+M2(3)*D(2)+M3(3)*D(3)
2120 REM: (3) PREMULTIPLY BY THE COVARIANCE MATRIX P TO OBTAIN THE
2130 REM: REQUIRED CHANGE IN STATE
2140 REM: STORE IN S1
2150 MAT S1=P*E
2160 REM: PRODUCE THE NEW STATE VECTOR S
2170 MAT S=S+S1
2180 REM: (A) FORM THE OUTER PRODUCT OF THE DERIVATIVE OF THE
2190 REM: LOGARITHM OF THE MEASUREMENT RATES.
2200 MAT O=ZER(3,3)
2210 FOR I=1 TO 3
2220   LET O(I,I)=(M1(I)↑2*M(I)/M1(4)↑3+M2(I)↑2*M(I)/M2(4)↑3+M3(I)↑2*M(I)/M
3)/T2
2230 NEXT I
2240 REM
2250 REM: NOTE N(1),N(2),N(3) WILL BE ZERO OR ONE SINCE ONLY ONE
2260 REM: COLLISION TAKES PLACE PER TIME INTERVAL.
2270 REM: (B) MULTIPLY THE SECOND DERIVATIVE OF THE MEASUREMENT BY
2280 REM: THE ERROR TERM (DN/L-DT)=D.
2290 MAT H1=(D(1))*H1
2300 MAT H2=(D(2))*H2
2310 MAT H3=(D(3))*H3
2320 REM: SUM THE THREE MATRICES. STORE IN M1.
2330 MAT H1=H1+H2
2340 MAT H2=H1+H3
2350 REM: SUBTRACT THE OUTER PRODUCT TERM.
2360 MAT H1=H1-O
2370 GOTO 2400
2380 PRINT "MATRIX H1"
2390 MAT PRINT H1
2400 REM: PRE AND POST MULTIPLY BY THE COVARIANCE TO PRODUCE THE
2410 REM: CHANGE REQUIRED IN THE COVARIANCE.
2420 MAT H2=P*H1
2430 MAT H3=H2*P
2440 REM: PRODUCE THE NEW COVARIANCE MATRIX.
2450 MAT P1=P+H3
2460 MAT P2=INV(P1)
2470 LET D1=DET(P1)
2480 REM: STORE THE UPDATED VERSIONS OF THE STATE AND COVARIANCE.
2490 LET R1(4)=S(1)
2500 LET R2(4)=S(2)
2510 LET R3(4)=S(3)
2520 MAT P=P1
2530 REM: OBTAIN THE APPROXIMATE UNCERTAINTY OF THE ESTIMATE.
2540 LET U1(1)=SQR(12*P(1,1))
2550 LET U1(2)=SQR(12*P(2,2))
2560 LET U1(3)=SQR(12*P(3,3))
2570 RETURN
```

```
2580 REM
2590 REM: PRINT THE STATE VECTOR
2600 LET F=0
2610 MAT N=N+M
2620 IF N0<N2 THEN GOTO 2800
2630 IF N0=N2 THEN LET F=1
2640 PRINT FILE (F),"ITERATION";N0; TAB(20);"EVENT";M(1);M(2);M(3)
2650 PRINT FILE (F),"COUNTS IN CURRENT PERIOD ";N(1);N(2);N(3)
2660 PRINT FILE (F),"TOTAL COUNTS ";Z9(1);Z9(2);Z9(3)
2670 PRINT FILE (F),"CURRENT TIME=",T2*N0
2680 PRINT FILE (F),"STATE";S(1);"+-";U1(1);
2690 PRINT FILE (F),"STATE";S(2);"+-";U1(2)
2700 PRINT FILE (F),"STATE";S(3);"+-";U1(3)
2710 LET A=N(1)/T2/Q/N1
2720 LET B=N(2)/T2/Q/N1
2730 LET C=N(3)/T2/Q/N1
2740 LET L8=N0/L9+1
2750 WRITE FILE (3,L8),A,B,C
2760 PRINT FILE (F),A,B,C,L8
2770 IF L8>N5 THEN STOP
2780 MAT N=ZER
2790 LET N2=N0+N1
2800 LET N0=N0+1
2810 RETURN
2820 REM:INITIALISE THE MEASUREMENT VECTOR
2830 FOR I=1 TO 3
2840   LET M(I)=0
2850 NEXT I
2860 RETURN
2870 PRINT "D(1)=";D(1),"D(2)=";D(2),"D(3)=";D(3)
2880 RETURN
```

```
0310 REM: PROGRAM TO FORM AN ESTIMATE OF THE TOTAL EXTRACTION
0320 REM: RATES OF ORGANS BY CURVE FITTING TECHNIQUES.
0330 REM:  THE DATA PRODUCED BY THE SIMULATION ROUTINE IS USED
0340 REM: TO OBTAIN AN ESTIMATE OF THE ORGAN EXTRACTION RATES
0350 REM: USING DETERMINISTIC METHODS FOR COMPARISON WITH THE
0360 REM: ACTUAL VALUE, AND THE VALUE OBTAINED BY THE STOCHAS-
0370 REM: TIC TECHNIQUE.
0380 CLOSE
0390 INPUT "NO OF DATA POINTS",M9
0100 DIM A(M9),B(M9),C(M9)
0110 INPUT "DISCRETISATION PERIOD",T1
0120 LET T=T1
0130 INPUT "TYPE FILE NAME IN WHICH DATA IS STORED",A$
0140 OPEN FILE (0,0),A$
0150 FOR I=1 TO M9
0160   READ FILE (0,I),A(I),B(I),C(I)
0170   IF INT(I)=INT(I+1) THEN PRINT
0180 NEXT I
0190 INPUT "FIRST POINT OF FIT",P1
0200 INPUT "LAST POINT OF FIT",P2
0210 LET N=P2-P1+1
0220 INPUT "IS PLATEAU TO BE COMPUTED ? TYPE YES OR NO",A$
0230 IF A$="NO" THEN GOTO 0330
0240 INPUT "FIRST POINT OF PLATEAU",Q1
0250 INPUT "LAST POINT OF PLATEAU",Q2
0260 LET M=Q2-Q1+1
0270 FOR I=Q1 TO Q2
0280   LET P=P+A(I)
0290 NEXT I
0300 LET P=P/M
0310 PRINT "PLATEAU=",P
0320 GOTO 0340
0330 INPUT "PLATEAU ",P
0340 REM :FIT EXPONENTIAL.
0350 FOR I=P1 TO P2
0360   IF A(I)>P THEN LET A(I)=P-.0001
0370   LET A(I)=LOG(P-A(I))
0380   LET X=I
0390   LET S1=S1+X*T
0400   LET S2=S2+(X*T)↑2
0410   LET S3=S3+A(I)
0420   LET S4=S4+A(I)*X*T
0430 NEXT I
0440 LET X=S1/N
0450 LET Y=S3/N
0460 LET B=(S4-N*X*Y)/(S2-N*X*X)
0470 LET B=-B
0480 PRINT "TOTAL FLOW PER MIN =",B
0490 LET T=.693/B*60
0500 PRINT "T1/2 IN SECS=",T
```